ISSN: 1863-5598

ZKZ 64717
06–24

Bodo´s Power Systems®

Electronics in Motion and Conversion

June 2024

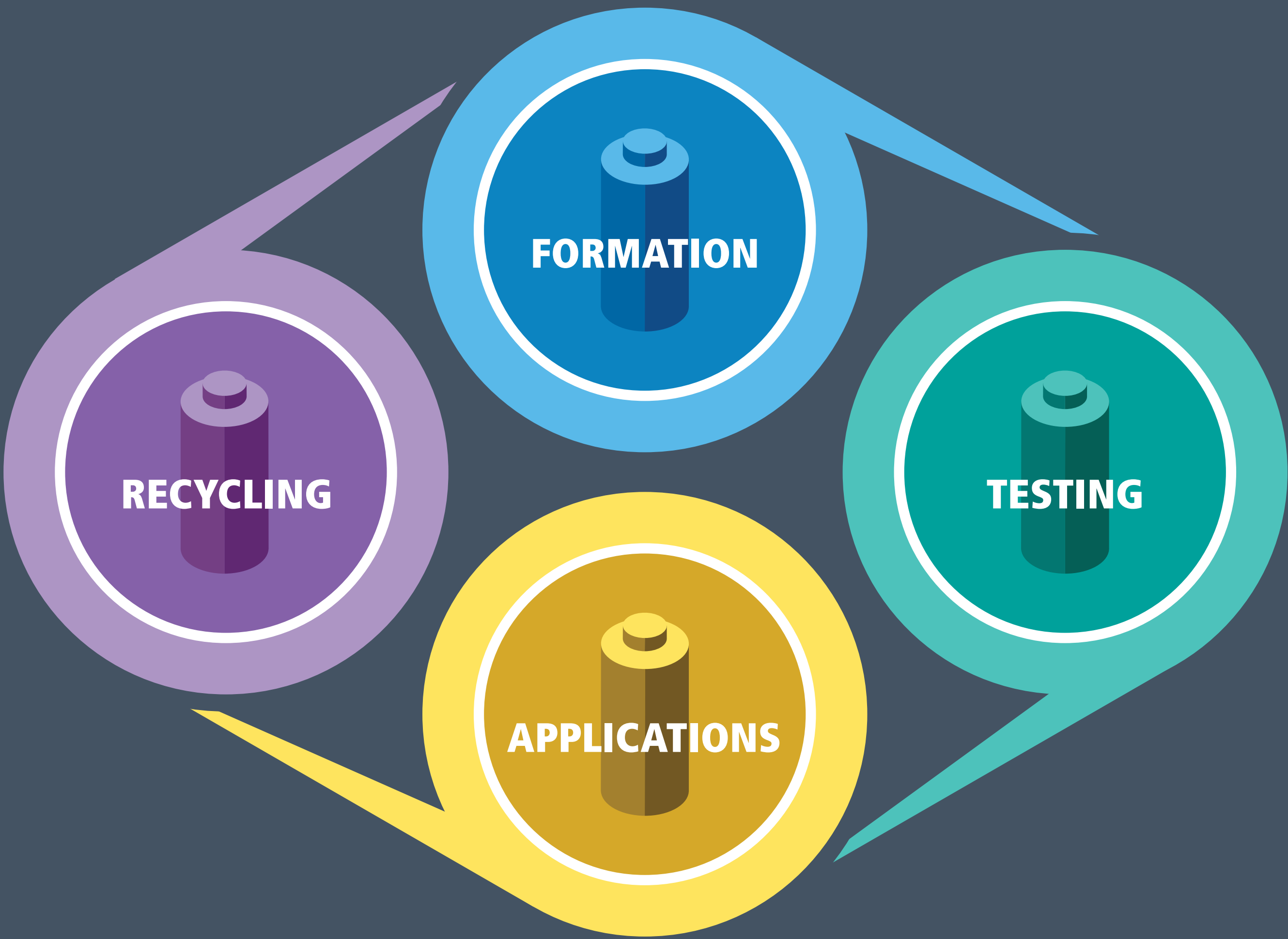

Fixed-ratio technology
High density power delivery
across the battery lifecycle

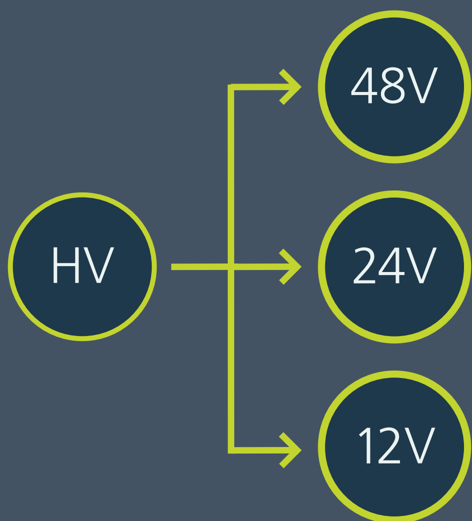

VICOR

PULSED INDUCTANCE MEASUREMENT

POWER CHOKE TESTER DPG10/20 SERIES

Inductance measurement from 0.1 A to 10 kA

KEY FEATURES

Measurement of the

- **Incremental inductance** $L_{inc}(i)$ and $L_{inc}(\int Udt)$
- **Secant inductance** $L_{sec}(i)$ and $L_{sec}(\int Udt)$
- **Flux linkage** $\psi(i)$
- **Magnetic co-energy** $W_{co}(i)$
- **Flux density** $B(i)$
- **DC resistance**

Also suitable for 3-phase inductors

WIDE RANGE OF MODELS

7 models available with maximum test current from 100A to 10000A and maximum pulse energy from 1350J to 15000J

KEY BENEFITS

- Very **easy and fast** measurement
- **Lightweight, small and affordable price-point** despite of the high measuring current up to 10000A
- **High sample rate and very wide pulse width range** => suitable for all core materials

APPLICATIONS

Suitable for all inductive components from **small SMD inductors** to **very large power reactors in the MVA range**

- **Development, research** and **quality inspection**
- **Routine tests** of small batch series and mass production

Technological leader in pulsed inductance measurement for 18 years

www.ed-k.de

ISSN: 1863-5598

ZKZ 64717
06–24

Bodo´s Power Systems®

Electronics in Motion and Conversion

June 2024

Enabling sustainable and efficient e-mobility power conversion systems

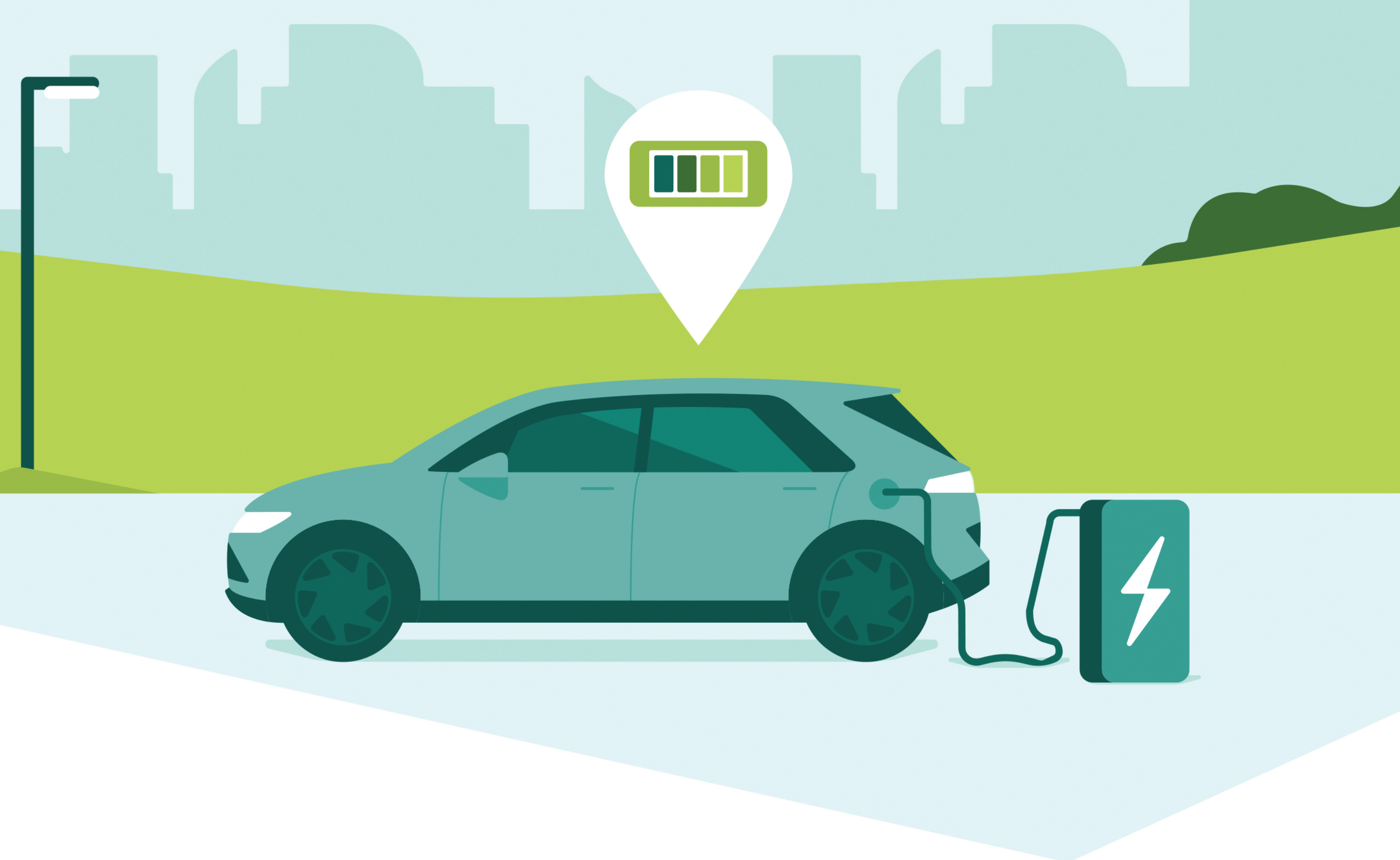

Trends in xEV power conversion

Webinar series | Watch now

Discover how our innovative silicon, SiC, and GaN power switches revolutionize the OBC market by addressing challenges in automotive charging.

Key takeaways:

- Overview of disruptive changes in xEV power conversion
- Introduction of CoolSiC™ Automotive MOSFETs 750 V
- How to select the right technology and package
- Demonstrators exemplifying key trends such as top-side cooling

Scan QR code to watch now

infineon


Electronic Concepts
Film Capacitor Innovation Without Limits
5PT Series
18.542mm
EC 5PT46
0.100 ±5%
400VDC
16.383mm
Smaller Than a Paperclip!
Specifically designed to meet
High Current Carrying Requirements Of Resonant Power Circuits
Cost Effective
Minimum inductance, lower impedance and ESR
Direct plug-in spade lugs
Contact ECI Today! sales@ecicaps.com | sales@ecicaps.ie
www.ecicaps.com

Content

Supporters & Friends

A Media
Katzbek 17a
24235 Laboe, Germany
Phone: +49 4343 42 17 90
Fax: +49 4343 42 17 89
info@bodospower.com
www.bodospower.com

Founder
Bodo Arlt, Dipl.-Ing. (FH)
bodo@bodospower.com

Editor in Chief
Alfred Vollmer, Dipl.-Ing.
alfred@bodospower.com

Correspondent Editor Bavaria
Roland R. Ackermann
roland@bodospower.com

Editor China
Min Xu – xumin@i2imedia.net

US Support
Rusty Dodge
rusty@eetech.com

Creative Direction & Production
Bianka Gehlert
b.gehlert@t-online.de

Publisher
Holger Moscheik
holger@bodospower.com

Free Subscription to qualified readers
Bodo´s Power Systems is available for the following subscription charges:
Annual charge (12 issues) is
150 € world wide · Single issue is 18 €
subscription@bodospower.com

Credit:
Background illustration cover and image p. 24: Mauri / stock.adobe.com

Printing by:
Westdeutsche Verlags- und Druckerei GmbH; 64546 Mörfelden-Walldorf
Germany

Freedom and Democracy

As an engineer I have lived in freedom. Looking back, I have been involved in power electronics for 65 years. My first years were as a little boy when I spent many hours working to get my Märklin model train running. Later as an engineer, I helped Mr. Lenz and Märklin with high-density MOSFETs, from Harris, for the digital drive of the locomotives. So, my memories show that I grew up in peace and had a good life.

For nearly four decades I have supported PCIM Europe. I remember Gerd and Christine working hard to get conference contributions and new companies to exhibit. It was fun for me, and I was pleased to offer my contribution as a board member. I am still here and enjoy travelling to PCIM. The asparagus season is always a motivation to travel to Nuremberg and hopefully June is not too late.

As is traditional, I will run my PCIM Podium focused on wide bandgap devices on Wednesday the 13th of June. The Podium will take place in Hall 7 on the Technology Stage with SiC from 11:20 to 12:15 and 13:15 to 14:15. The GaN podium will take place from 14:20 to 15:20. I am looking forward to seeing you there.

Working in power electronics is our job, but we are also human beings living on planet earth, and we should live in peace. Therefore, we must work hard to ban the aggressors and isolate them. War cannot be the way to manage our life on earth. Nature has enough big challenges to solve. Global warming can be limited by using semiconductors that reduce unwanted losses in systems.

At this point, I can only repeat what I said last year. All these memories and past stories about war, which were told by my parents, return while watching the news on TV. There are never winners after wars. I have grown up in peace but have missed Grandpas and Uncles because they served in the military and did not return home from World War one and two. War definitely destroys the resources needed to save our environment so that our children can have a safer world. We are all losers in the end, but mainly it will be the wider population who will suffer the most. It has an impact on all of us. My hope is that all of our children and grandchildren will grow up in peace and that war will not escalate to all areas of the world. Working to stop the war must be our most important task.

Politicians travel into war zones like tourists, and all is broadcasted on TV. The soldiers have families too, who also suffer. My wish is that the younger generation can grow up in peace. I am tired of seeing, on a daily basis, more destruction; I want to make the world a better world, and power semiconductors can at least contribute to reducing global warming, and wide bandgap devices are particularly promising in this respect.

At the end of the year, we will meet again in Munich for my WBG conference at the Munich Airport Hilton Dec. 3rd and 4th. After last year's great success, our program has experts from all around the world.

Bodo's magazine is delivered by postal service to all places in the world. It is the only magazine that spreads technical information on power electronics globally. We have EETech as a partner serving our clients in North America. If you speak the language, or just want to have a look, don't miss our Chinese version at bodospowerchina.com. An archive of my magazine with every single issue is available for free at my website bodospower.com.

My Green Power Tip for the Month:
Plan your travel wise and use the most efficient way of travel, visiting as many contacts as possible during your trip.

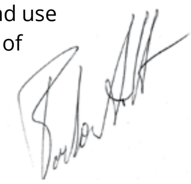

Events

PEMD 2024
Nottingham, UK June 10 – 13
https://pemd.theiet.org

GaN Marathon 2024
Verona, Italy June 10 – 12
www.ganmarathon.com

PCIM Europe 2024
Nuremberg, Germany June 11 – 13
www.pcim-exhibition.com

Sensor + Test 2024
Nuremberg, Germany
June 11 – 13
www.sensor-test.de

Speedam 2024
Ischia, Italy June 19 – 21
www.speedam.org

The smarter E Europe 2024
Munich, Germany June 19 – 21
www.thesmartere.de

CPE-PowerENG 2024
Gdynia, Poland June 24 – 26
https://cpe-powereng2024.umg.edu.pl

EnerHarv 2024
Perugia, Italy June 26 – 28
www.enerharv.com

electronica China 2024
Shanghai, Cina July 8 – 10
www.electronicachina.com.cn

New strategic Partnership

Finepower and Sanan Semiconductor signed a distribution contract in May 2024. "We are very pleased that with Finepower we have been able to gain a trustworthy partner with an extremely high level of technical understanding," said Michael Sleven, Vice President of Sanan Europe GmbH. And Reiko Winkler, General Manager of Finepower GmbH, commented “With Sanan we gained a perfect addition to our already strong power components portfolio. Silicon Carbide is the semiconductor material of the future for high voltage applications and Sanan offers the worldwide biggest

production capacity on an outstanding quality level, so we are very proud to work with them in this growing market.”

Finepower is a technical design-in distributor and engineering company, and Sanan is one of the very few companies in the world which offers the complete SiC production chain within their factories, including crystal growth, epitaxy, chip production. Even packaging of both discrete devices and modules is handled by Sanan. Michael Sleven describes Sanan as follows: “We have one of the biggest vertical inline factories for SiC in the world. Also, our GaN products are made on our own SiC substrates. So, we have every process step in our own hands.”. In China Sanan has been very active for quite a while, and now the company is expanding to Europe. Further details can be found in the VIP interview published in Bodo’s Power Systems in April 2024.

Finepower is an internationally active company with focus on modern power electronics applications. While its engineering team creates complete designs of high-end power electronic systems like onboard-chargers and DC/DC converters, the “distribution” business unit works with international partners to support customers with the best matching standard and customized components, such as power semiconductors, magnetic components, fans and heat sinks.

www.finepower.com
www.sanan-semiconductor.com

Innauguration of Plant in Malaysia

LEM chose to make such a substantial investment in the state of Penang/Malaysia by opening a new plant in this region. From employing around 70 people in April 2024, LEM expects to increase the headcount to more than 200 people by March 2025 and eventually more than 500, with sales from the factory expected to reach over € 200 millions. With plans in place already for an extension on the additional 5,000 m2 of land, the new 11,800 m2 factory features a state-of-the-art logistic system including automatic guided vehicles (AGVs) on the shopfloor which transport components from the warehouse to the high-tech production lines. LEM Malaysia is also the pilot for the roll-out of the company’s ERP system and will produce a substantial part of its energy through solar panels.

www.lem.com

Acquisition of Vertical GaN Developer

Power Integrations announced an agreement to acquire the assets of Odyssey Semiconductor Technologies, a developer of vertical gallium-nitride (GaN) transistor technology. The transaction is expected to close in July 2024, after which all key Odyssey employees are expected to join Power Integrations’ technology organization. The acquisition supports the company’s ongoing development roadmap for its proprietary PowiGaN technology, which is featured in many of the company’s product families including InnoSwitch ICs, HiperPFS-5 power-factor-correction ICs and the recently launched InnoMux-2 family of single-stage, multiple-output ICs. The company introduced 900- and 1250-V versions of PowiGaN technology and products in 2023. Commented Dr. Radu Barsan, Power Integrations’ vice president of technology: “We are executing on an ambitious roadmap that includes driving toward cost parity with silicon MOSFETs and expanding the voltage and power capabilities of PowiGaN. Our goal is to commercialize a cost-effective high-current and high-voltage GaN technology to support higher-power applications currently served by silicon carbide (SiC), at a much lower cost and higher performance enabled by the fundamental material advantages of GaN over SiC. The experience of the Odyssey team in high-current vertical GaN will augment and accelerate these efforts.”

www.power.com

Silicon Carbide Wafer Supply Agreement

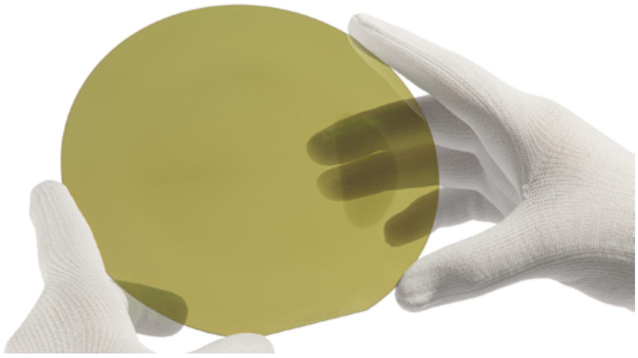

ROHM and STMicroelectronics announced the expansion of the existing multi-year, long-term 150 mm silicon carbide (SiC) substrate wafers supply agreement with SiCrystal, which is a ROHM group company. The multi-year agreement governs the supply of larger volumes of SiC substrate wafers manufactured in Nuremberg, Germany, for a minimum expected value of $230 million.

Geoff West, EVP and Chief Procurement Officer, STMicroelectronics, commented "This expanded agreement with SiCrystal will bring additional volumes of 150mm SiC substrate wafers to support our devices manufacturing capacity ramp-up for automotive and industrial customers worldwide. It helps strengthen our supply chain resilience for future growth, with a balanced mix of in-house and commercial supply across regions". "SiCrystal is a group company of ROHM, a leading company of SiC, and has been manufacturing SiC substrate wafers for many years. We are very pleased to extend this supply agreement with our longstanding customer ST. We will continue to support our partner to expand SiC business by ramping up 150mm SiC substrate wafer quantities continuously and by always providing reliable quality". said Dr. Robert Eckstein, President and CEO of SiCrystal, a ROHM group company.

www.rohm.com

Strategic Partnership to drive Zero-Emission Bus Transport in Europe

Daimler Buses and BMZ have entered into a strategic partnership for the development and supply of the next generation of e-bus batteries. Together with Daimler Buses, BMZ will further develop the existing battery technology specifically for the requirements of electrically powered buses. The new battery generation NMC4 – succeeding the current NMC3 technology – will combine high energy density, resulting in a longer range for e-buses, with an ultra-long cycle life. Customers of Daimler Buses will be able to use NMC4 batteries from the middle of the decade.

Daimler Buses is pursuing an e-roadmap across all segments: Electrically powered city buses have already been in series production since 2018; intercity e buses are to follow as of the middle of the decade and electrified coaches by 2030. With this, Daimler Buses aims to offer locally CO_2-neutral models based on batteries or hydrogen in every segment by 2030.

www.bmz-group.com

300 mm Wafer Fab dedicated for Power Semiconductors

Renesas has started operations at its Kofu Factory, located in Kai City, Yamanashi Prefecture, Japan. Renesas aims to boost its production capacity of power semiconductors in anticipation of the growing demand in electric vehicles (EVs). The Kofu Factory previously operated both 150 mm and 200 mm wafer fabrication lines until October 2014. Renesas made the decision to re-open the factory as a 300 mm wafer fab to support the growing demand for power semiconductors. The factory will start mass production of IGBTs and other products in 2025, doubling Renesas' current production capacity for power semiconductors.

www.renesas.com

Measurement Facility in Bengaluru/India

Rohde & Schwarz has inaugurated a facility center in Bengaluru's Manyata Tech Park, housing R&D, system integration as well as calibration and repair services. For Rohde & Schwarz, India is not merely a growth market but a vital component of its global strategy. The R&D team in Bengaluru is involved in developing next generation. The facility houses an ISO 9001 and ISO17025 (NABL) accredited calibration and repair service center, offering precision services to meet the rigorous quality standards of the industry. Furthermore, the facility will also encompass sales, applications, systems integration and a dedicated demo display area showcasing various test and measurement equipment and test solutions.

www.rohde-schwarz.com

Expanded Power Portfolio

Tektronix has acquired EA Elektro-Automatik (EA), a principal supplier of high-power electronic test solutions for energy storage, mobility, hydrogen, and renewable energy applications. The introduction of EA to the Tektronix team provides the company with expanded solutions, leveraging Tektronix's oscilloscopes and isolated probes, EA's power supplies and electronic loads, and Keithley's source meters and instrumentation. Combined, the Tektronix portfolio offers a set of capabilities for energy storage and power electronics design needs, from ultra-low to ultra-high power. With the addition of EA, Tektronix is well equipped to serve engineers who are electrifying our world. With emphasis on creating solutions for power electronics in the semiconductor, aerospace, and automotive industries, the Tektronix and EA product portfolio addresses issues in energy storage, mobility, and hydrogen fuel.

www.tek.com

Technology highlights missing Piece in the xEV Driving Equation

Allegro MicroSystems is pleased to announce, that GHSP, a global provider of mechanical and electromechanical systems and portfolio company of JSJ Corporation, is closely collaborating with and has adopted Allegro's gate driver and vehicle sensor technology for its eVibe vibration enhancement system.

In the rapidly evolving world of xEV technology, there is a new class of xEV enthusiasts who crave a more immersive motoring experience. GHSP's eVibe system transforms xEV driving by providing drivers with the noise and vibrations that mimic the familiar feel and sounds of a traditional internal combustion engine. "For more than a decade, Allegro has worked closely with market-leading automotive partners to develop

innovative solutions that help shift the future of driving, power and performance in electric vehicles," said Suman Narayan, Allegro's Senior Vice President, Products. "Our latest collaboration highlights a new, growing market segment and demand for Allegro's technology. We value GHSP's automotive expertise and look forward to our continued partnership as we develop solutions that drive innovation."

The impact of eVibe extends beyond just the driving experience. It represents a shift towards the future of xEV technology and the way owners engage with their vehicles. From mimicking an idle feel to simulated engine throttle and high-speed gear shifts via premium vibration indicators, GHSP's technology is providing drivers with a more immersive and connected drive. This innovation has the potential to reshape the xEV market, catering to a wider range of custom options and individual customer preferences, while also helping to further the adoption of electric vehicles.

www.allegromicro.com

SiC and more for Chinese EV Manufacturer

Infineon Technologies will provide silicon carbide (SiC) power modules HybridPACK™ Drive G2 CoolSiC™ and bare die products to Xiaomi EV for its recently announced SU7 until 2027. Infineon's CoolSiC-based power modules allow for higher operating temperatures, "resulting in best-in-class performance, driving dynamics and lifetime". Traction inverters based on the technology can, for example, further increase electric vehicle range. The HybridPACK Drive is Infineon's market-leading power module family for electric vehicles, with almost 8.5 million units sold since 2017.

Infineon provides two HybridPACK Drive G2 CoolSiC 1200 V modules for the Xiaomi SU7 Max. In addition, Infineon supplies Xiaomi EV with a broad range of products per car, including, for example, EiceDRIVER gate drivers and more than ten microcontrollers in various applications. The two companies also agreed to further cooperate on SiC automotive applications.

www.infineon.com

High Power next Core (HPnC)

with Fuji Electric's X series 7G IGBT and SiC

MAIN FEATURES
for traction & industrial applications

- **Latest chip technology**
  - Fuji Electric's X series IGBT and FWD with low losses
  - SiC – MOSFET: Super low switching loss energies
- **Available blocking voltages: 1700 V, 2300 V and 3300 V**
- **High reliability**
  - CTI>600 for higher anti-tracking
  - High thermal cycling capability with ultrasonic welded terminals
  - MgSiC base plate for traction version
  - Improvement of delta T_j power cycling capability by using 7G packaging technology
- **RoHS compliance**
  - Ultrasonic welded terminals
  - RoHS compliant solder material
- **Temperature detection**
  - Thermal sensor installed
- **Easy paralleling**
  - Minimized current imbalance
  - Easy scalability

Semiconductor Processing to Packaging Center to be built in New York State University

Semikron Danfoss now collaborates with SUNY Polytechnic Institute and other industry partners to build a Semiconductor Processing to Packaging Center that will focus on research, education and training. The facility will be established at the Semikron Danfoss office in Utica, located in the Quad C building on the SUNY Poly campus and will train 100-150 students per year in semiconductor processing, packaging and testing capabilities.

The center will be funded in part with the $4 million Empire State Development grant as well as a larger economic development package announced last fall. In addition to supplying space for two classrooms and a 5,000 square-foot clean room, Danfoss will provide multiple pieces of equipment used in the semiconductor manufacturing process. The Center will allow for both silicon device processing as well as SiC, GaN, AlN and their alloys, and Ga2O3 device processing for power electronics, optoelectronics and clean energy applications as well as their unique packaging needs.

It is anticipated that the students will be both traditional and non-traditional students, seeking either degrees or certificates. The goal of the Center is to increase graduates across advanced manufacturing disciplines by 10 percent in the next four years. The Center's curriculum will offer several workforce development training and upskilling pathways for industry partners and their employees as well as those seeking to gain entrance into the workforce.

www.semikron-danfoss.com

R&D Manager returns to the Team

Danisense welcomes back Petar Ljushev as R&D Manager. Petar Ljushev had already worked for Danisense for nearly four years previously between 2019 and 2022. He holds a PhD in the field of power electronics from the Technical University of Denmark (DTU), and has many years experience in industrial companies designing power electronics, large power resistors and resistor systems for demanding applications. In his new role at Danisense, he will be focusing on developing and launching new innovative current sense transducer products based on the company's successful and proven closed loop Flux Gate technology.

www.danisense.com

European and Korean Semiconductor Manufacturer cooperate on GaN and SiC

SweGaN, a European semiconductor manufacturer that develops and produces engineered high-performance Gallium Nitride on Silicon Carbide (GaN-on-SiC) epitaxial wafers, announces it has entered strategic partnership with South Korea based RFHIC Corporation. RFHIC is active in designing and manufacturing GaN RF & microwave semiconductors for communications and defense applications. The new, pivotal agreement encompasses an undisclosed equity investment from RFHIC. The two companies will focus on joint R&D and product development moving forward. Over the last decade, SweGaN has been developing and producing high-performance GaN-on-SiC epitaxial solutions for RF and power devices that can be used in various applications such 5G telecommunications infrastructure, defense radars, satellite communications, on-board chargers, and data centers.

This strategic investment by RFHIC shows the recognition of SweGaN's QuanFINE epitaxial solutions as a differentiator among GaN-on-SiC materials available on the market. In partnership with RFHIC, SweGaN gains additional resources to expedite market penetration and to achieve its business goals. RFHIC Corporation cites the partnership with SweGaN and investment strategy target strengthening RFHIC's gallium nitride semiconductor supply chain and further fortifying its competitiveness of RF and microwave products within the compound semiconductor arena. In the joint collaboration, SweGaN and RFHIC plan to address the increasing demand for GaN semiconductors and initiate new product developments for a variety of markets.

www.swegan.se

Call for Papers for Power Electronics Conference in 2025

After the EPE editions Grenoble 1987, Toulouse 2003, Lille 2013 and Lyon 2020, the 26th edition of the European Conference on Power Electronics and Applications will take place in Paris, France. The Power Electronics community will gather in Paris, from March 31st to April 4th, 2025, to exchange views on research progress and technological developments. Several tutorials as well as some technical visits will be planned and organized. In addition, the 40 years of EPE conferences will be celebrated. Now the organizer has started the call for papers for "the largest conference in its field, attracting experts from numerous countries to join in the discussions". With the objective to exchange and meet fellow professionals and academics, the EPE conference brings together researchers, engineers, etc. working at the forefront of power electronics technologies. The main topics will be electromobility, smart grids and renewable energy, energy storage systems, digitalization ("the powerful fusion of ai and IoT for sustainability"), sustainable and affordable power electronics as well as energy transition and societal change.

http://epe2025-paris.com

High Precision Current Logging. Ultra Compact

Increase Energy Efficiency for Electrical Systems

Optimizing the energy efficiency of electrical systems is an ongoing challenge. For this task, HIOKI has designed an innovative multi-channel current measurement solution specifically for development teams in the electrical and e-mobility industry. For the first time, even the smallest currents in an EV or other electrical systems can be measured and logged individually using ultra-compact, high-precision current sensors. Analyzing this data, engineers can draw conclusions on how to significantly improve energy efficiency.

Accurate current measurement of numerous consumers in electrical systems requires sensors with utmost precision. HIOKI's new AC/DC Zero-Flux current sensors offer a measurement range of 100 µA to 2 A for CT7812 and 100 mA to 20 A for CT7822. Both sensors measure with an impressive accuracy of ±0.3 percent. With this high precision and a minimum resolution of 0.1 mA, development engineers retrieve accurate consumption data even of low currents that enable them to significantly improve the energy consumption of their systems, enabling to extend the operating times or ranges of EVs.

Ultra-Compact Current Sensors for narrow spaces

HIOKI's new current sensors also impress with their ultra-compact design. A total length of only 7.65 cm and an innovative sliding mechanism enables connecting the current sensors to consumers effortlessly. Measuring even in confined spaces such as in engine compartments, enclosures, or electrical cabinets can be realized.

Effective Current Mapping with 55 Measurement Channels

For efficient current mapping, the new current modules LR8536 and U8556 provide in combination up to 55 current measurement channels. This allows for a simultaneous current consumer measurement with one set up even in complex electrical systems such as in EVs, trucks, construction vehicles, or agricultural machinery. The Data Logger LR8450-01 alternatively allows to log other signals such as temperature, strain, vibration, humidity, resistance, voltage, and CAN signals. With different parameter combinations the set up can be extended to max 330 channels, which provides a great solution for the engineer to judge the DUT considering all parameters at once.

Wireless Connection Now Possible

Another highlight of HIOKI's new multi-channel-current measurement solution is the flexibility of a wireless connection. The LR8450-01 is the first data logger using wireless modules that allow for a spatial separation of the current sensors from the data logger. This provides development teams with more flexibility for their set ups and a rapid assessment of the energy efficiency of electrical systems, especially in electromobility.

www.hioki.eu

Aligning Size, Cost and Efficiency Requirements

Onsemi is active in silicon, silicon carbide and gallium nitride power semiconductors. The company is one of the very few semiconductor manufacturers which control the entire supply chain in SiC from subtrate to the final product. We talked to Andrej Tomašik, General Manager onsemi Slovakia.

By Alfred Vollmer, Editor-in-Chief, Bodo's Power Systems

What are your most recent activities in Europe?
We recently established a new System Application Lab for EVs in Europe. This laboratory in Slovakia is reinforcing onsemi's commitment to the intelligent power management strategy and propelling further innovation and efficiency in this sector. The laboratory is specifically designed to foster the development of cutting-edge innovations, with a primary focus on electric vehicles. The capabilities integrated into this facility will enhance our collaboration with automotive manufacturers (OEMs), enabling us to deliver transformative silicon and silicon carbide solutions.

Andrej Tomašik, General Manager onsemi Slovakia

What are the core competences of onsemi – especially in terms of SiC and GaN?
Onsemi stands at the forefront of silicon carbide development. Our extensive array of power components provides customers with the flexibility to select the power topology that best aligns with the size, cost, and efficiency requirements of their designs. This includes the Elite SiC MOSFET family, which facilitates faster switching and more compact end-products, and the 1200 M3 SiC MOSFET, offering up to a 20% reduction in power loss compared to leading competitors. Additionally, our Elite SiC & Hybrid Elite SiC Modules exhibit lower thermal resistance than discrete devices. We offer comprehensive global applications support and possess the requisite application knowledge to meet design-in needs.

Why does onsemi manufacture its own substrate? What are the benefits?
We are progressing towards complete vertical integration, encompassing everything from substrate and epitaxy to the actual wafer fabrication and assembly operations, extending up to module production. This integration will facilitate the scaling and commercialization of our capabilities, allowing us to better serve our customers, exert greater control over the development and manufacturing processes, and enhance quality assurance.

What are the expected output volumes for the next five years in terms of Si, GaN and SiC?
The growth of electric vehicles (EVs), heightened safety focus, increasing demand for comfort, and environmental initiatives aimed at reducing waste and enhancing efficiency are pivotal factors shaping our company's strategy. Our emphasis on intelligent power and intelligent sensing portfolios is poised to create substantial growth opportunities. For context, in traditional combustion engine vehicles, our content value averages around $50, whereas in electric vehicles, it rises to an average of $750.

What is the importance of the automotive market for your company?
The automotive sector is a critical area of focus for onsemi, which is poised to play a significant role in the evolution of the automotive industry through advancements in vehicle electrification and safety. Automotive revenues constitute over 50% of onsemi's total revenue. Key domains include the development of EV auxiliary systems, traction inverters, HV-LV DC-DC converters, and on-board chargers in the realm of power management. Additionally, onsemi is committed to delivering high-quality, reliable image sensors that contribute to enhanced road safety. We have over 15 years of experience in automotive imaging and more than 500 million automotive sensors deployed in vehicles.

What are your most important power applications?
Our extensive portfolio fits applications across diverse markets, notably in the automotive sector, where SiC technology is leveraged to deliver scalable solutions for a broad array of OEM vehicle platforms. In the realm of advanced safety, onsemi provides an ADAS solution scalable to Level 5 autonomy, integrating intelligent power and sensing solutions to attain ASIL D functional safety. Our image sensors set the industry benchmark, offering vision capabilities 100 times more acute than the human eye.

Which trends do you see in which applications? Do you see a shift from SiC to GaN in some applications?
SiC and GaN technologies are increasingly favored for their superior performance over traditional silicon-based technologies. SiC is especially suitable for high-voltage applications, while GaN excels in low-voltage scenarios. Both technologies are anticipated to continue their upward trajectory in popularity and adoption in the forthcoming years.

www.onsemi.com

Fixed-ratio Converters unleash Innovation across the Battery Lifecycle

The ongoing adoption of electrification across many industries has been a boon for productivity and the environment, and battery production has been a core technological enabler for this trend. Driven in part by electric vehicles (EVs) and energy storage systems for renewable energy, the battery industry is among the fastest growing in the world.

By David Krakauer, VP of Global Marketing, Vicor

According to the International Energy Agency (IEA), global battery demand has increased tenfold from 43.8GWh/year annually in 2016 to 550.5GWh/year annually in 2022. Given the still-accelerating demand, every stage of the battery lifecycle merits examination. The battery lifecycle consists of four major stages: cell formation, battery testing, application use and battery recycling. A shortcoming in any one of these phases undermines the battery industry and the growth in electrification. Today, the battery lifecycle is constrained by limitations of existing power conversion technologies that threaten this growth. Vicor power-dense fixed-ratio converter technology brings a novel approach to achieving greater sustainability and cost-efficiency across all stages of the battery lifecycle.

Unlocking new possibilities with fixed-ratio converter technology

In high-voltage battery systems, DC-DC power conversion is a fundamental aspect of the power delivery architecture.

DC-DC conversion is commonly achieved with switched-mode power converters like a buck or boost topology or low drop-out regulators (LDOs). While these power converters can be effective , they limit the flexibility and performance of the power delivery network (PDN) with the rigidity of their outputs and their subpar conversion efficiencies. This is particularly true when working with high voltages associated with today's battery systems.

To overcome these shortcomings, Vicor has developed fixed-ratio converters that provide highly efficient, isolated conversion in a small package for high-voltage to low-voltage loads commonly referred to as safety extra-low voltage or SELV.

Analogous to a transformer in an AC-AC solution, a fixed-ratio converter performs DC-DC conversion with the output voltage being a fixed fraction of the DC input voltage (Figure 1). Similar to a transformer's step-down or step-up capabilities that are defined by the coil's turns ratio, a fixed-ratio converter's capabilities are defined by its K factor, which is expressed as a fraction relative to its voltage step-down capability (Figure 2).

Unlike traditional DC-DC converters that regulate the output voltage, a fixed-ratio converter provides no output regulation. These devices are also autonomous, requiring no feedback loop or external control mechanism.

Fixed-ratio converters offer several notable benefits over traditional converters.

Bidirectionality

Given that fixed-ratio converters operate independently of an external host or controller, these devices are inherently bidirectional. This means that, depending on the direction of the current flow, the same fixed ratio converter module will step the voltage either up or down. By achieving voltage boosting and bucking with one module, fixed-ratio converters unlock unprecedented flexibility and simplicity for PDN that rely on the bidirectional flow of current.

Flexibility and scalability

Fixed-ratio converters are exceptionally easy to parallel for higher power demands. Designers can easily add multiple fixed-ratio converter modules in parallel to scale a system to whatever output power demands are required. Similarly, designers can place multiple fixed-ratio converters in series to achieve unique voltage ratios based on their cascading K factors. In these cases, the converters need to be power-matched to ensure safe and reliable operation.

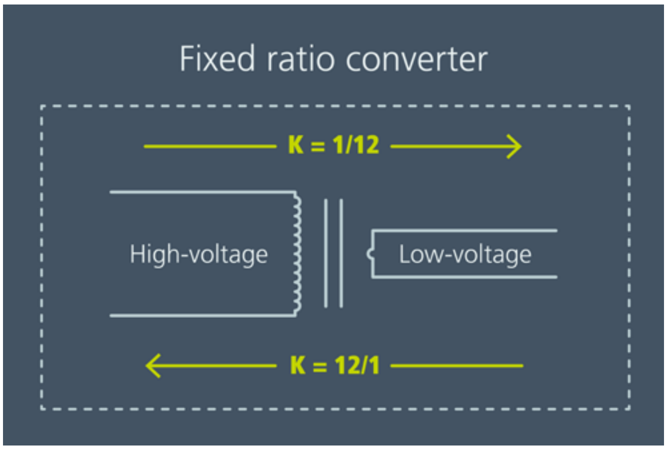

Figure 1: A bidirectional fixed-ratio converter operating as a step-down converter with K = 1/12 can also serve as a boost converter with a K of 12/1. This bidirectionality in a single module unlocks a number of unprecedented use cases for the battery industry.

BCM fixed-ratio converters

Input range	K Factor	Current	Power
36 – 60V	1/4, 1/6	130 to 150A	1,500 to 1,195W
38 – 55V	1/1, 2/3, 1/2, 1/3, 1/4, 1/5, 1/6, 1/8, 1/12, 1/16	6 to 70A	120 to 300W
200 – 330V	1/6	30A	270W
200 – 400V	1/8	30A	1,000W
240 – 330V	1/8	7A	235W
260 – 410V	1/8, 1/16, 1/32	17 to 125A	800 to 1,750W
330 – 365V	1/8, 1/28, 1/32	8 to 28A	300 to 325W
360 – 400V	1/8, 1/32	7 to 27A	300 to 325W
400 – 700V	1/16	40A	1,600W
500 – 800V	1/16	35A	1,600W

Figure 2: With support for a large range of different K-factor and output-power configurations, Vicor BCM fixed-ratio converters can meet the needs of most applications.

High efficiency in a small package
Finally, fixed-ratio converters are unmatched in power efficiency from a very small footprint. Whereas a conventional buck or boost converter achieves maximum power efficiencies in the low 90% range, fixed-ratio converters like the Vicor BCM® line demonstrate conversion efficiencies up to nearly 98%. This leads to more sustainable applications with decreased demand for thermal management overhead.

The importance of the power delivery network in cell formation
The first phase in the battery lifecycle is the cell formation stage.

In this phase, newly manufactured batteries must go through the formation cycling process, which consists of charging and discharging a cell for the first time. During this process, a cell is cycled repeatedly to build up gradually the cell's solid-electrolyte interphase (SEI) layer. The speed of this process is determined by cell chemistry, so cell formation latency is mostly a fixed-rate process.

Formation cycling in the battery requires an underlying power delivery network (PDN) that can support the repetitive charge and discharge cycles.

The standard PDN for such a system takes a three-phase AC input from the grid, rectifies it to high-voltage DC, and then uses multiple phases of DC-DC conversion to reach the nominal voltage required to charge a battery cell (e.g., 4.2V) (Figure 3). This final voltage required for battery charging will vary from plant to plant depending on the specific cell chemistry, but the several intermediary voltage drops from AC to a lower DC bus voltage, such as 12V, is standard across the industry.

Discrete component solutions are extremely difficult to design, require significant in-house power expertise, have a large BOM that presents cost and supply chain challenges, and increase time to market. Discrete solutions limit flexibility as they offer pre-defined output voltages. Where different cell chemistries require different voltages, it is more cost-effective for designers to create a flexible solution that they can modify based on cell chemistry. Discrete solutions don't allow for flexible cell formation systems that can be dynamically modified for compatibility with multiple cell types.

Cell formation demands system high throughput and efficiency
There are two major challenges with the existing PDNs in battery formation: throughput and efficiency.

From a throughput perspective the speed at which manufacturers can form a battery's SEI layer is inherently limited by cell chemistry. Hence, improving the cost-efficiency of the cell-formation process necessitates scalable systems that can form many batteries in parallel. However, with existing PDNs, the lack of a modular intermediary DC-DC phase limits the ability to easily scale a system without major design overhauls.

From an efficiency perspective, the constant charge and discharge of cells is very costly. To optimize efficiency, battery manufacturers reuse the energy spent during cell charging cycles by either storing it locally or sending it back to the grid on discharge cycles. This requires a PDN that supports the bidirectional flow of current and performs high-efficiency power conversion.

In both instances, fixed-ratio converters are an ideal solution. By integrating a fixed-ratio converter into the PDN, designers can redefine the architecture into three distinct phases: AC rectification, transformation to low voltage and constant-current conversion (bus converter).

In the constant-current conversion stage, designers can implement fixed-ratio converters to easily step down the higher DC level to a safer, lower level without the need for discrete solutions or single-module solutions. By simply integrating one or multiple fixed-ratio converters in parallel, designers can create a power delivery network that is modular and easily scales.

In this way, designers can make systems that cycle many batteries concurrently, enabling higher throughput, greater power density and improved efficiency. Additionally, this architecture allows designers to easily change the PDN to accommodate the required DC-DC conversion for a cell's unique nominal voltage. With a more flexible solution that requires no discrete components, designs reach the market faster and are less susceptible to failure.

For power conservation, the inherently bidirectional nature of a fixed-ratio converter is ideal in the cell-formation process. With fixed-ratio converters, cell manufacturers can easily switch between charge and discharge cycles, knowing that the fixed-ratio converter will automatically step up to a predefined higher voltage on discharge and similarly step it down on charging cycles. This unique feature improves process energy efficiency, enabling energy reuse during formation cycling.

Additionally, with a fixed-ratio converter efficiency of 97.9%, there is minimal power loss in the conversion cycle in either direction. Without fixed-ratio converters, such bidirectionality would necessitate multiple components (one for buck and one for boost). This would consume more power due to lower efficiencies and increase component count.

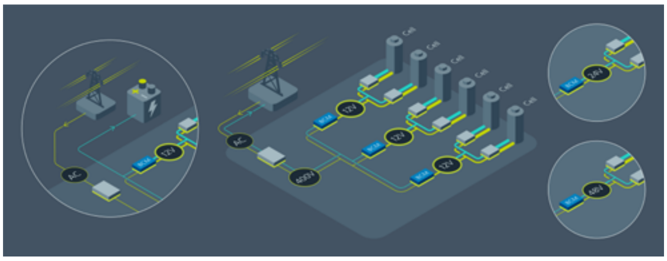

Figure 3: Battery manufacturers can use fixed-ratio converters to integrate bidirectionality and efficiency into cell formation power delivery networks.

Battery testing needs a flexible and scalable PDN
The next stage in the battery lifecycle is battery testing, where manufacturers combine battery cells into larger battery packs. Battery pack production is not constrained by the same chemistry-dependent time requirements related to the charging and discharging of cells, but it still faces similar throughput challenges.

For example, each cell must be properly tested and accurately measured so that multiple cells can be combined to form a larger battery pack. Then the larger battery pack also needs to be rigorously tested. This is not a value-add step, so the faster manufacturers complete this process, the lower the overall cost of the battery pack.

Flexibility and scalability in a PDN are needed to accommodate the wide variety of battery voltage and power levels, and high throughput is needed to test more batteries in the same physical space and in less time. Battery pack testers therefore need power delivery networks that are modular and scalable to the specific needs of their testing requirements and volumes. Like in the cell formation phase, the standard PDN of a battery testing facility entails the conversion of power from AC three-phase down to the cell's nominal voltage (Figure 4).

With fixed-ratio converters in the constant-current conversion stage of the PDN, battery test designers can avoid arduously designing the intermediary conversion stages. Instead, they can trust that their constant-current conversion is managed by the fixed-ratio converter. Designers can now focus on the final stage of the conversion process, where voltages need to match the cell's nominal voltage for testing. This simplified architecture enables the creation of modular and flexible systems that designers can readily modify for varied testing requirements.

Another important benefit of fixed-ratio converters is power density. With extremely high power efficiencies and small form factors, fixed-ratio converters can support kilowatts of power and hundreds of volts in industry-leading form factors. This helps support greater throughput testers by allowing for more testing equipment to fit within the same area constraints, hence creating the opportunity for testing more battery cells concurrently.

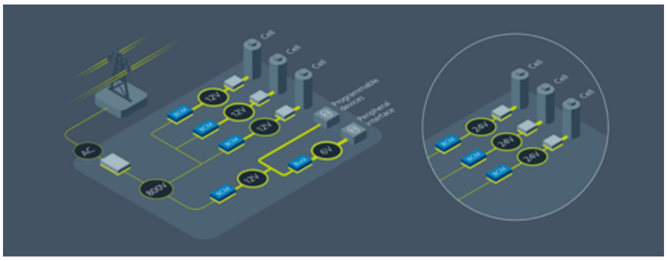

Figure 4: Fixed ratio converters unlock high levels of power density for battery-testing power delivery networks, enabling greater tester throughput by fitting more testing equipment into the same area.

Fixed-ratio converters reduce I^2R losses in battery applications

When the battery finally makes it out of the factory floor and into a real-world application, the challenges with PDN do not end.

In many emerging battery-powered applications, such as tethered robotics or ROVs, energy storage systems for renewables like solar and wind power and electric vehicles, there is a growing demand for extremely high-voltage power delivery (Figure 5). For example, electric vehicles are seeing a shift in architecture from 400V to 800V power delivery for the sake of greater power and efficiency.

For the same power, higher voltage levels allow for power delivery at lower currents. Therefore, one benefit of high-voltage power delivery is greater efficiency, as lower currents incur fewer I^2R losses. This enables more efficient applications that also require less overhead for thermal management.

Additionally, high-voltage power delivery decreases the wire gauge in vehicle wire harnesses. With lower current delivery requirements, designers can use smaller-diameter cables resulting in decreased system weight, material requirement and cost.

Naturally, the successful operation of such high-voltage systems relies on the ability to convert these high-voltages used in delivery to the lower voltages used at the load. At this point in the battery's lifecycle, fixed-ratio converters offer value by providing a simple and efficient means of DC power conversion.

Consider the example of a tethered robot. With a 1/16 K factor fixed-ratio converter, designers can take advantage of the 97.9% efficiency to step down voltages from the high voltage for power distribution (e.g., $800V_{DC}$) down to a lower voltage, like $48V_{DC}$. From the $48V_{DC}$, designers can use a conventional 90% efficient buck converter to reach the final 3.3V used for a microcontroller unit (MCU). Without a fixed-ratio converter, the entire conversion from 800V to 3.3V would occur at 90% efficiency, incurring significantly greater losses than the fixed-ratio converter architecture.

Thermal challenges in battery recycling

Once a battery has served its useful lifespan, the final stage in its lifecycle is recycling.

Battery recycling entails a high-power electrochemical process in which the raw materials and elements from the battery are chemically separated from the cell to be reclaimed and reused in the future. Like other industrial stages of the battery lifecycle, the PDN consists of converting three-phase AC input voltages to high-power DC, and then ultimately down to lower voltages to operate the recycling equipment (Figure 6).

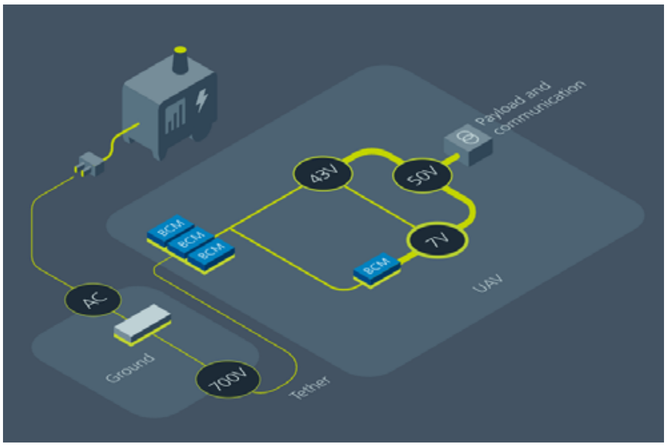

Figure 5: Applications like tethered robotics can use fixed-ratio converters to enable high-voltage power delivery without incurring significant power losses during conversion to lower voltages.

One challenge from the perspective of the PDN is that the battery recycling process creates a significant amount of heat. Therefore, the components within the PDN must be able to operate reliably at elevated temperatures. Similarly, power density becomes increasingly important in the design of the PDN, necessitating small form factors and high-efficiency power conversion.

Fixed-ratio converters offer an extremely power-dense solution to DC-DC conversion, capable of supporting kilowatts of power at hundreds of volts in extremely small form factors.

For example, the Vicor BCM6123 fixed-ratio bus converter boasts a power density of 2352W/in^3 (Figure 7). With this level of power density, designers can easily meet the temperature and performance requirements of battery recycling plants. And, as power requirements and demand continue to grow, the modular power architecture enabled through fixed-ratio converters allows for the system to scale up accordingly with minimal overhead needed.

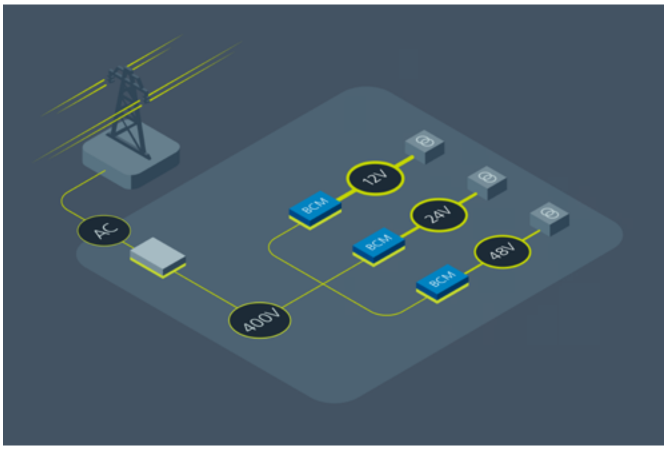

Figure 6: BCM fixed-ratio bus converters allow for reliable high power voltage conversion within the elevated temperature constraints of a battery recycling plant.

Bolstering the battery ecosystem with fixed-ratio converters

At each stage in the battery's lifecycle, there is a growing need for high-voltage power delivery networks that are efficient, power-dense and scalable. Success for the battery lifecycle necessitates success at each individual stage. Whether it's battery cell formation, testing, in-application use or recycling, the entire battery lifecycle benefits from fixed-ratio converters. As compared to traditional power conversion solutions, fixed-ratio voltage converters offer unprecedented levels of efficiency and small form factors, while also presenting unique features like bidirectional operation.

Figure 7: The Vicor BCM6123 fixed-ratio bus converter module offers a 24V output voltage and 62.5A output current while in a 61.0 x 25.14 x 7.26mm ChiP™ package.

Vicor is the only company to offer high-density fixed-ratio converters. The Vicor BCM® products employ a Sine Amplitude Converter™ topology which allows for higher-frequency operation than PWM-based solutions. The BCM family of fixed-ratio converters also comes in a variety of form factors and power ratings to support the needs of a wide variety of high voltage applications. Beyond the BCM family, Vicor offers fixed-ratio converters to meet the needs of many other applications.

The BCM fixed-ratio converter is poised to play a significant role in the growth of battery manufacturing, one of today's fast-growing markets. It supports greater throughput, enhances efficiency and can scale with any application. Regardless of the application or lifecycle phase, fixed-ratio power converters are an exceptional solution for the burgeoning modern battery industry with today is limited by traditional power-conversion approaches.

Vicor and BCM® are registered trademarks of Vicor Corporation; ChiP™ and Sine Amplitude Converter™ are trademarks of Vicor Corporation.

www.vicorpower.com

Sustainable Power Conversion in EVs with Wide-Bandgap Materials and Top-Side Cooling

Infineon develops cutting-edge SiC and GaN technology with innovative, thermally efficient packaging

The world of global mobility is on the cusp of a remarkable shift. In 2024, global EV sales are expected to soar by about 20 percent as governments and consumers try to mitigate the effects of climate change [1]. By 2030, EVs are forecasted to account for at least two-thirds of global car sales [2].

By Daniel Makus, Application Director xEV Power Conversion (OBC, HV DC-DC), and Rafael Garcia, System Architect for OBC and DC-DC Applications, both at Infineon Technologies

With automakers striving to slash EV costs, efficient and sustainable power conversion systems are vital to meet the rising demands and power requirements. To that end, the adoption of wide-bandgap (WBG) semiconductors, such as silicon carbide (SiC) and gallium nitride (GaN), enables efficient, powerful, and long-term cost-effective power solutions. To build on that, innovative technologies like top-side cooling can help designers achieve optimal thermal performance and reduce assembly expenses.

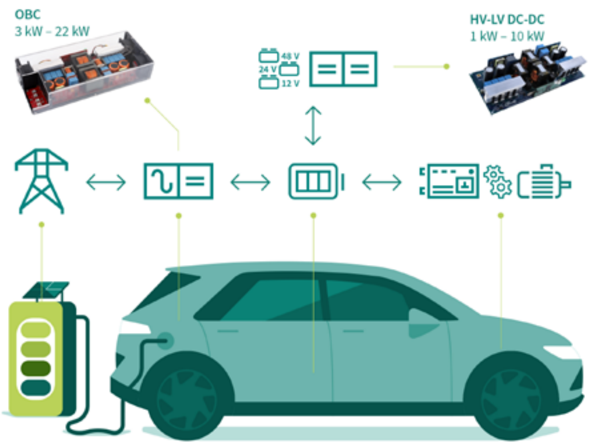

Figure 1: OBC and DC-DC power conversion systems in EVs

Power conversion systems – Importance and emerging challenges

The power conversion systems in EVs, particularly the onboard charger and DC-DC converters, are essential to managing the flow of electricity within the vehicle, optimizing the charging process, and facilitating the integration of various power sources. These power conversion systems are pivotal for the overall performance, efficiency, and user experience of EVs. Their proper functioning is essential to maximize the range, reliability, and functionality of electric cars, making them indispensable in the transition towards sustainable transportation.

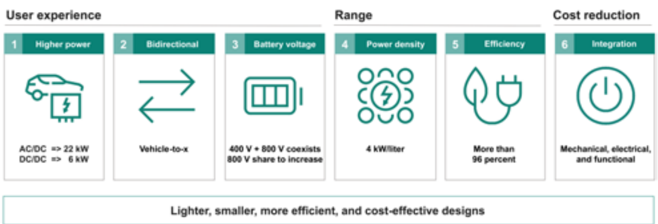

Figure 2: Current EV requirements

Increasing power levels, bidirectional operation support (V2X), and faster adoption of 800 V battery systems have introduced new levels of complexity to OBC and DC-DC power systems – complexity that is heightened due to higher power density, efficiency, and overall cost requirements.

Leveraging WBG semiconductors

SiC and GaN semiconductors have revolutionized power conversion in automotive systems by enabling unprecedented levels of efficiency and performance while coexisting with cost-effective silicon (Si) technologies. SiC-based designs offer high robustness and efficiency in a wide range of temperatures while significantly lowering switching and conduction losses compared to Si-based designs, leading to optimal performance and thermal efficiency. GaN, on the other hand, offers unparalleled efficiency at higher switching frequencies and nearly lossless switching, enabling smaller, more compact devices.

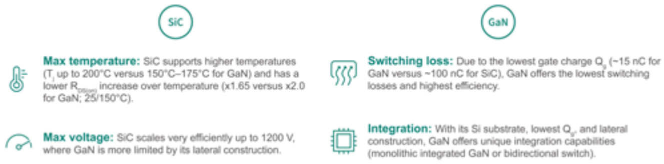

Figure 3: Key benefits of SiC and GaN semiconductors

While both GaN and SiC offer a lot of benefits on their own, they really shine when used together, offering a compelling blend of efficiency, compactness, and affordability in automotive power conversion systems. Designers can leverage this combination to achieve optimal power density and thermal efficiency while enabling new topologies, leading to enhanced vehicle performance and range.

Figure 4 shows some typical implementations of such systems.

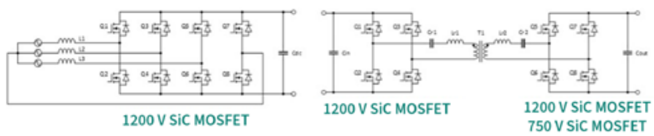

Figure 4: Schematics of 1200 V and 750 V SiC MOSFETs

More and more tier-1 manufacturers are adopting these topologies due to their simplicity compared to the previous generations. For example, in the PFC stage of an 11 kW design, compared to 18 transistors (3x single-phase interleaved) used in Gen 1 topologies, Gen 2 topologies use only eight transistors (three-phase B6 or VSC). Just reducing the number of transistors makes the design way simpler.

Overcoming challenges and complexities in EV power systems

The new topologies use fewer gate drivers as well, and enable a single microcontroller to take over the control loops of both stages of the power supply, i.e., PFC and HV-HV DC-DC. To simplify the design further, some tier-1 manufacturers have decided to eliminate discrete devices and utilize modules with three to four integrated half-bridges.

Despite considerably simplifying the design and reducing the cooling and development costs of the OBC, this approach does not optimize power density and efficiency. This is due to the huge effort required for the EMI filter design and the PFC choke, as they need to filter and switch at voltages higher than those designed for Gen 1 topologies. Certainly, at higher voltages, the switching frequencies cannot be very high (e.g., PFC <50 kHz and HV-HV DC-DC <120 kHz) if a certain efficiency requirement needs to be met (e.g., >95.5 percent). Some publications have demonstrated that adding a ZVS cell to the B6/B8 topology can further increase efficiency and enable higher switching frequencies at the expense of a higher component count.

Additionally, no 900 V-1000 V aluminum capacitors are available for the output of the PFC converter. Hence, designers need to use a series-parallel arrangement of 450 V-500 V aluminum caps to achieve the capacitance necessary to store energy when the B6 topology is configured to work with single-phase grids, e.g., B8, and compensate the 100 Hz/120 Hz ripple.

To further increase power density and efficiency at a lower system cost, topologies with 650 V-750 V transistors can be used. Such topologies will still be compatible with three-phase grids and the 800 V battery architecture. To achieve this, it is necessary to use multi-level converters, as shown in Figure 5.

In Figure 5, the two topologies on the left are hard-switching PFCs, where the top image shows the flying capacitor topology and the bottom image shows an active neutral-point clamp topology. The topologies on the right are resonant HV-HV DC-DC converters, where the top image shows a multi-level CLLC and the bottom image shows a multi-level DAB.

As the automotive industry continues to evolve, a sustainable design is crucial to mitigate the environmental impact of vehicles. By prioritizing eco-friendly materials, energy-efficient powertrains, and recyclable components, automotive solutions can contribute to reducing carbon emissions and conserving natural resources. In power conversion systems, this will play a crucial role in the optimization process, not only

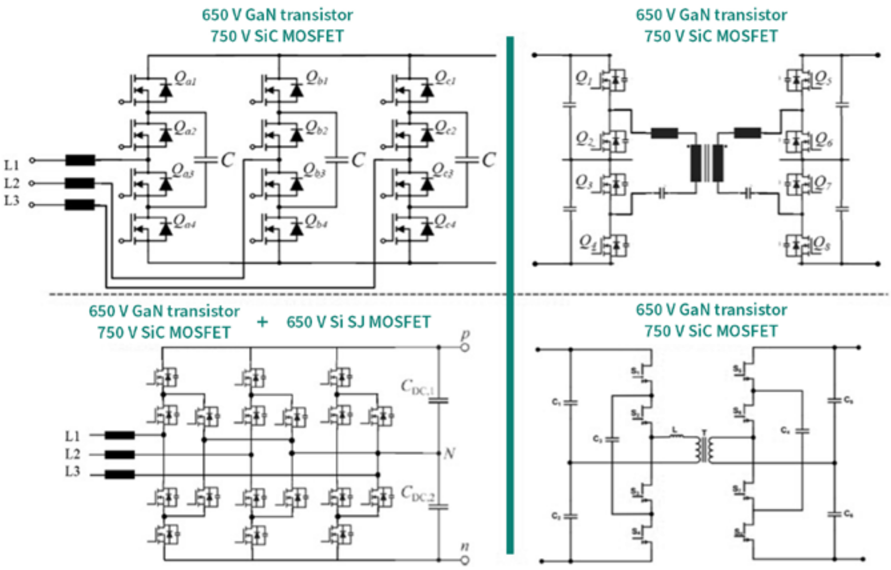

Figure 5: Multi-level converter topologies using WBG devices

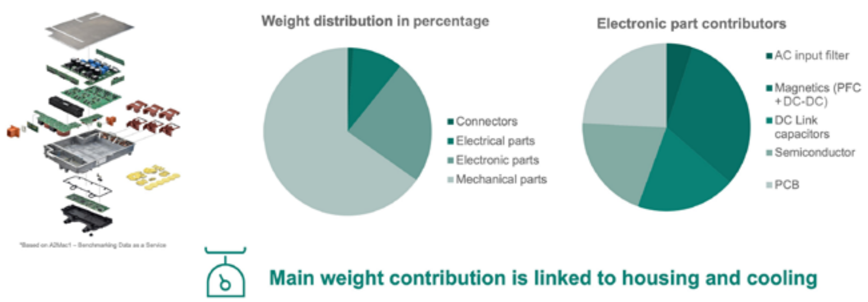

Figure 6: Weight contribution of different components in a power conversion system

for the material selection and their recyclability, but also to reduce the weight and cost of future power systems.

Practical implementation of GaN and SiC in automotive power systems

GaN's superior switching capabilities and high-frequency operation enables novel power electronic topologies to achieve a higher efficiency and power density. GaN also reduces the overall weight of the system by reducing not only the amount of housing, but also the size and number of electrotechnical components, including tons of rare materials, contributing significantly towards higher sustainability.

With the introduction of the lateral structure during the manufacture of GaN power transistors, it is possible to design a bidirectional switch (BDS). Such a BDS will have bidirectional blocking voltage capability without doubling the $R_{DS(on)}$, enabling disruptive topologies that could bring tremendous benefits in terms of power density, reliability, cost, and external component requirements.

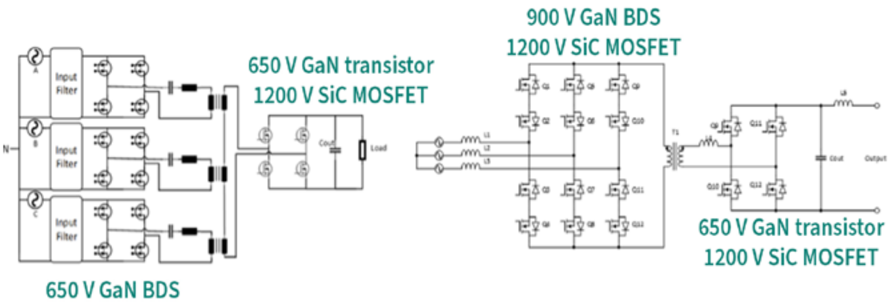

Figure 7: Modular Gen 2 approach using magnetic integration of 650 V GaN and 1200 V SiC transistors (left) and a cycloconverter

Figure 7 (left) shows a very modular approach which includes magnetic integration. Similar to the Gen 1 approach, each module is powering each phase in the three-phase grid, enabling a 650 V device. Depending on the battery voltage, designers can select 650 V GaN or 1200 V SiC transistors.

Figure 7 (right) shows a matrix or cyclo converter – a potential candidate for innovative designs. This topology can easily be implemented with two 1200 V discrete devices connected back-to-back on the primary side and normal devices on the secondary side. The challenge here is to select low-ohmic devices to get the right total $R_{DS(on)}$ (the bidirectional switch has double the $R_{DS(on)}$ of a single device) per position, according to the proper power class and expected power dissipation.

It should be mentioned that the topology is fully resonant, can either be an LLC or DAB, and the switching frequency range will depend on both the output load and input power-fed conditions. As this is a true three-phase topology, considering the maximum input voltage and voltage swells that may happen, the authentic bidirectional GaN switch should have a minimum breakdown voltage of 900 V. Infineon is actively working on designing an automotive BDS GaN switch such that tier-1 manufacturers are ready for mass production of these Gen 3 topologies.

Top-side cooling

In addition to using wide-bandgap technology to improve efficiency, device packaging and cooling become a vital part of the equation and play key roles in enabling more power-dense OBC designs. While through-hole device (THD) packages like TO-247 and TO-220 are still widely used in many applications, they have the disadvantages of high manufacturing costs and of being manually inserted into the PCB before being soldered onto the underside of the board. For these reasons, THD is increasingly being replaced by surface-mount devices (SMD), the placement of which can be automated and results in higher throughput and better reliability.

SMD packages dissipate heat either by bottom-side cooling (BSC) or top-side cooling (TSC). While both BSC and TSC packages can be assembled using automated pick-and-place machinery, TSC provides several advantages over BSC packages like D2PAK and DPAK, which conduct heat generated by the die downwards towards the bottom of the board-mounted device. This direction of heat-conduction is a disadvantage because PCBs are not optimized for very high heat conduction and create a substantial thermal barrier for BSC devices, requiring additional thermal vias to allow the excess heat to dissipate safely.

A negative consequence of this approach is that it makes PCB trace-routing more challenging because large areas of the board are allocated to thermal dissipation elements. An insulated metal substrate (IMS) board can improve the thermal performance of BSC devices but these are more expensive than traditional FR4 PCBs.

The adoption of TSC technology is particularly remarkable and will shape future power-conversion system designs. In TSC devices, the semiconductor die-generated heat is extracted from the top of the package. In TSC devices, the heat generated by the semiconductor die is extracted to the top of the package which has an exposed pad onto which a cold plate (heatsink) is attached as shown in Figure 8.

This approach reduces thermal resistance by up to 35 percent and decouples the thermal pathway from the electrical connections on the PCB. This is significant as it makes PCB design simpler and more flexible, and brings the added benefits of a smaller board area, higher power density, and reduced electromagnetic interference (EMI). Furthermore, the increased thermal performance also removes the need for board stacking. So instead of combining both FR4 and IMS boards, this design makes a single FR4 sufficient for all components and requires fewer connectors.

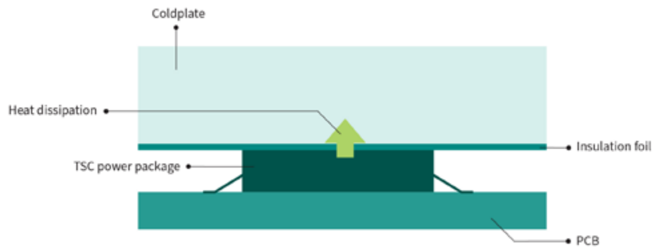

Figure 8: A semiconductor device employing top-side cooling (TSC

These features of TSC reduce the overall bill of materials (BOM), reducing the overall system cost. TSC also helps optimize the power-loop design for increased reliability. This is made possible since the drivers can be placed very close to the power switches. The low stray inductance of the driver switch reduces the loop parasitic, leading to less ringing on the gate, higher performance, and a lower risk of failure. Furthermore, the package concept is JEDEC-compliant and free of royalties, which makes second-source manufacturing easy and available for many suppliers, while other concepts available on the market are proprietary and not easy to reproduce.

Figure 9 summarizes the key benefits of TSC technology in a nutshell.

Infineon has developed double (DDPAK) and quadruple (QDPAK) SMD packaging with TSC for many of its power devices, including its range of CoolSiC™ G6 Schottky diodes, the new SiC MOSFET fam-ily of 750 V and 1200 V devices paired with 650 V Si SJ CoolMOS™, and future GaN-based CoolGaN™ products. Also, the low-voltage power MOSFETs are already available in TSC TOLT packages, which enables the complete system of OBC along with the DC-DC converters to be ready for TSC manufacturing. These devices offer thermal capabilities on par with THD devices and even better electrical performance.

Having a standard height of 2.3 mm for QDPAK and DDPAK SMD TSC packages, with both high- and low-voltage alternatives, helps design complete applications like OBC and DC-DC converters using components having the same height. This reduces cooling expenses compared to existing solutions based on a 3D cooling system.

Figure 9: Infineon's top-side-cooled QDPAK platform for future power-conversion systems

Conclusion

While SiC and GaN technologies occupy the headlines in the battle to achieve greater efficiency and power density from power solutions, and they are vital to minimizing energy losses, extending driving range, and enabling faster charging of EVs, effective thermal management also has a significant role in achieving electrical performance as well as reducing size, weight, and cost of power solutions.

Innovative design of packages, such as Infineon's QDPAK, enables top-side cooling, leading to better thermal performance than the equivalent IMS-based solution. Its simpler construction eliminates multi-board assemblies, reducing component count and cost, especially for connectors. This significantly improves performance and reduces assembly time and expenses.

There is more to explore, with several ideas for more compact, robust, and future-oriented packages in the innovation phase, with the potential to provide numerous advantages for power-conversion designers to improve power density, manufacturability, efficiency, and system cost.

The ability to use both sides of the board significantly improves power density while reducing parasitic elements in the system. While TSC may seem 'new' and in many ways it is, the USP of this solution is that it uses tried-and-tested techniques such as gap fillers, with or without using thermal interface materials, to produce a solution that is elegant and, above all, reliable.

As a leading global semiconductor manufacturer, Infineon has strategically positioned itself in the EV innovation landscape, developing cutting-edge WBG and novel top-side cooling technologies to enable a smooth transition to a sustainable and reliable future of e-mobility.

Watch our on-demand webinar "Solving the challenges in xEV power conversion" – click here.

The presented slides and Q&A document are available for downloading – click here.

References

[1] Bloomberg: Electrified Transport Market Outlook 4Q 2023: Growth Ahead; Online; 2023; https://about.bnef.com/electric-vehicle-outlook/

[2] RMI: EVs to surpass two-thirds of global car sales by 2030, putting at risk nearly half of oil demand, new research finds; Online; 2023; https://rmi.org/press-release/evs-to-surpass-two-thirds-of-global-car-sales-by-2030-putting-at-risk-nearly-half-of-oil-demand-new-research-finds/

About the Authors

Daniel Makus is the Application and Business Development Director for xEV power conversion including OBC and DCDC applications. He is responsible for market research, roadmap development and G2M strategy in xEV applications with a focus on power conversion.

Rafael Garcia is the System Architect for on-board chargers and DC-DC applications for electric vehicles. He focuses on the impact of the major trends in the selection of the different semiconductor technologies. Rafael also works on identifying the key drivers that will lead the next generation of products, thus accelerating the decarbonization of the application.

www.infineon.com

A Versatile High-Performance e-Mobility Platform

High-performance, scalable e-mobility modules like Hitachi Energy's RoadPak™ and other silicon carbide (SiC) semiconductors offer significant efficiency gains in the electric vehicle (EV) powertrain. They drive e-mobility applications like e-vehicles and e-buses, which are more in demand than ever following governmental and global initiatives for renewable and sustainable mobility.

By Tobias Keller, Vice President, Head of Global Product Management & Marketing, Hitachi Energy

To meet these demands, Hitachi Energy developed the RoadPak, a versatile e-mobility platform that is optimised to deliver the highest performance and reliability. It achieves this by using up to 10 SiC chips in parallel, supporting for various chipsets of different generations from various suppliers.

Whether electric or combustion powered, drivers expect a vehicle to function when they want and be able to travel the distance to their destination. This expectation has built up over decades and was achieved in the field of combustion-engine vehicles due to continuous progress and improvement. Today it is rare, provided that all necessary maintenance has been carried out, that a combustion-engine vehicle does not work as expected.

Figure 1: Hitachi Energy's RoadPak™

When we consider the complexity and quantity of components that must all function flawlessly for that engine to run as expected, the result is very impressive and is evidence of outstanding engineering work over many years. This is typically based on a very detailed analysis of possible errors and many of these failure scenarios are tested in detail before market launch, therefore their probability of occurrence is massively reduced.

With the introduction of electrically powered vehicles, the components that form the combustion engine, have been replaced by electronic ones. The requirements for reliability and availability, however, remain the same. It is therefore important to urgently address reliability, availability and safety and present appropriate solutions that maintain performance in these areas.

The switch to electric motors benefits from the fact that electric locomotives have proved to be extremely reliable. An electric locomotive can cover several million kilometres over its lifetime and it's possible that one day, electric vehicles may be able to achieve something similar.

Although the knowledge gained in other applications of electric drive systems, such as electric locomotives, can be useful, the applications are different. For example, locomotives demonstrate relatively constant power with some peak power requirements after stops, but - on balance - maintains a relatively stable load. Electric vehicles have many stops (e.g., at traffic lights or intersections) and must deal with varying speed limits, meaning power requirement changes frequently stops.

The differences in application are reflected in mission profiles, which represent the power required by a vehicle over time in a specific use case. The profiles are slightly adjusted depending on the target audience and can also include very specific requirements

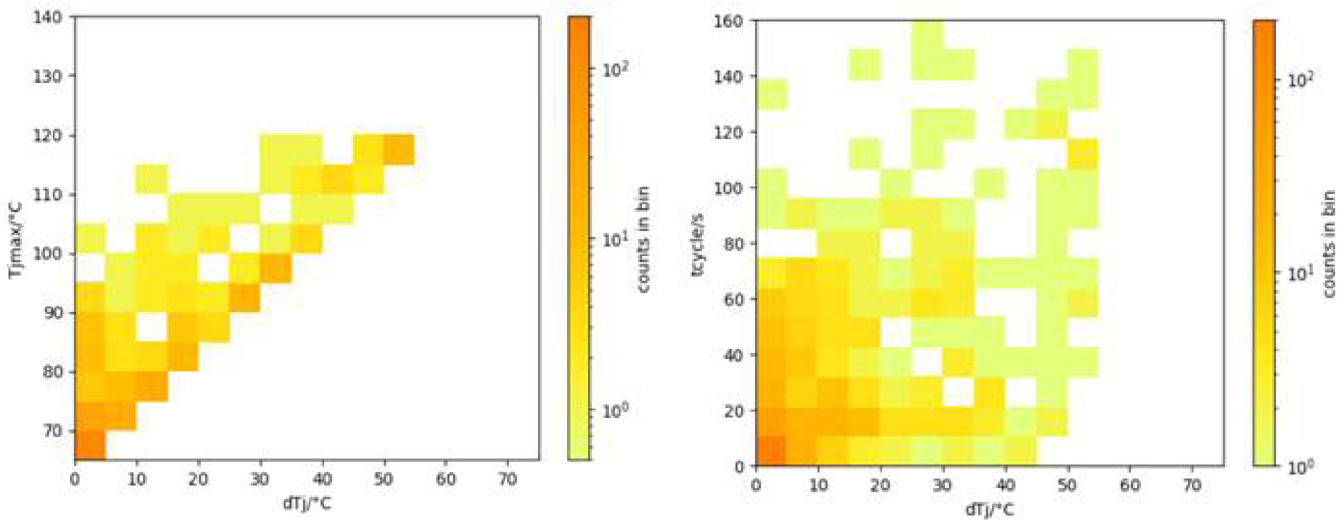

Figure 2: Analysis of 2 typical mission profiles of electric vehicles.

Test type	t_{on} / t_{off} / s	ΔT_j / K	$T_{j,max}$ / °C	Avg. kcyc	End-of-Life (EoL) criteria
PC_{sec}	1.4 / 1.4	90	160	>4,000	N/A
PC_{sec}	1.4 / 1.4	105	175	848	V_{SD} increase
PC_{min}	30 / 30	115	160	145	V_{SD} increase
PC_{min}	30 / 30	130	160	62	V_{SD} increase

Figure 3: Test results of Hitachi Energy's RoadPak™.

such as uphill starts with a trailer or high-speed acceleration for tests on racetracks. Individual use cases are based on frequency or mileage, and several such mission profiles result in a consolidated mission profile that takes multiple use cases into account. A typical time frame to achieve this is, for example, eight years and 400,000 kilometres.

Although an attempt is made to cover all critical operating points, designers must remain realistic as overloading the requirements will lead to an over-dimensioning of individual components. This in turn can result in unacceptable costs.

From the consolidated mission profile, important parameters for power semiconductors, such as maximum junction temperature or the number of thermal cycles, can be deduced. Based on the mission profile, the power semiconductor module can also be designed, and the number of required SiC chips necessary to achieve the required performance can be determined. Ambient temperature (e.g., coolant temperature) is also considered. Furthermore, cycles have a profound influence on the power semiconductor module design and the use of connection and bonding technologies. It quickly becomes apparent whether a conventional solder connection between certain components is sufficient or whether other connection technologies, such as silver sinter connections, a stronger bond that does not melt, are necessary.

The two illustrations provided each indicate the probability of occurrence (counts). The more orange that is visible in the diagrams, the more likely the case is to occur. On the left, the probability of thermal changes in relation to junction temperature is plotted. Thermal changes in the high junction temperature range are much more critical and have an impact on component lifespan. On the right, we see the dependence of thermal load cycles on thermal changes. Here, a high number of cycles with large thermal load cycles is the challenge. In comparison to the same analysis with locomotive mission profiles, the diversity is striking. The distribution of frequently occurring cases is spread across the entire spectrum and not consolidated into a few points.

A more concrete statement regarding mission profiles is made in AQG 324 [1], which introduces load cycle tests, which are divided into two different time ranges: PCsec with switch-on times of less than 5s and PCmin with switch-on times longer than 15s. It is assumed that, especially for power semiconductors, a thermally stable state is already reached after 15s, so longer switch-on cycles do not result in additional heating. The test is defined as a failure test, and various parameters must be continuously monitored.

AQC 324 requires that the thermal resistance (Rth) should show an increase of less than 20%, while the increase in drain-source voltage (VDS) – or the reverse source-drain voltage (VSD) should be below 5%. Particularly in the PCmin test, the dependence of the change in thermal resistance, even to a small extent, on a change in source-drain voltage in MOSFETs presents a challenge. For example, an increase in Rth of <10% can lead to a 5% change in VSD. This is due to the strong relationship between the on-state resistance (RDSon) and temperature.

In these tests it is important for a module with more than one logical switch (e.g., a half-bridge module or a module with six logical switches) that all logical switches are appropriately loaded and included in the assessment.

The junction temperature is an important parameter and is typically measured indirectly through the voltage drop across the body diode. Of course, this measurement is performed on both half-bridges, i.e., all logical switches.

Testing is time-consuming, as many –(in the range of 100,000) cycles are expected. In the case of PCsec with 5s on-time and 5s off-time, this corresponds to 1,000,000s, which is equivalent to 12 days. For 1,000,000 cycles, it would be 116 days. It can also be expected that as the junction temperature increases, i.e., a higher temperature difference between the junction and cooling temperature, the number of cycles decreases.

The behaviour of Hitachi Energy's RoadPak™ can be seen in the following table:

In addition to the on/off time behaviour (ton/toff), the previously mentioned temperature difference between junction and cooling medium (ΔTj) and the maximum junction temperature reached (Tj,max) are shown in the table. To achieve meaningful results, the test must be conducted with multiple samples. In this case, six modules are used in parallel.

Understanding the significance of the results is very important. The larger the difference between the cooling medium temperature and junction temperature, the smaller the values, which shortens to time required for the power semiconductor to successfully complete the specified cycles. This is well-known and understood in the field of silicon semiconductors. The dependence on ton/toff is also clear - the lower these times, the more cycles that can be switched.

For electric vehicles designed for private use, PCsec cycles in the range of 100,000-400,000 are required. For trucks, buses, and taxis, the value should be over 1,000,000 cycles. These values result from the different lifespans of the vehicles. The results from the table confirm that RoadPak from Hitachi Energy meets the expected requirements for both private and public/commercial/industrial use.

www.hitachienergy.com

The Many Interfaces of PCIe® Connectivity

Flexible PCIe Fanout Switch for Industrial Applications

Introducing our groundbreaking single-chip PCIe fanout switch, featuring highly integrated peripherals for seamless connectivity. This compact, yet powerful, chip boasts an embedded USB 3.2 Gen 2 (10G) host controller, 2.5G Ethernet MAC and programmable I/O, making it a versatile solution for diverse applications.

With integrated PCIe physical interfaces offering a 4-lane upstream port and a 1-lane downstream port, the PCI11xxx/PCI12xxx addresses the growing demand for higher bandwidth PCIe sub-systems in embedded applications. Delivering PCIe upstream across a single or multiple lanes accommodates varying system bandwidths.

Designed to fit on various SOM boards, including application-specific carrier boards, the PCI11xxx/PCI12xxx family is the ideal match for automotive telematics. In applications like 4G/5G connections, the down-facing PCIe port connects seamlessly to LTE modem modules, facilitating simple fanout operation and expanding connectivity for port-limited V2X processors.

This family of products is also well-suited for server systems requiring PCIe to USB3 Hub connectivity. In addition, for Edge computing and IoT devices needing PCIe to Superset Combo IO connectivity and automotive infotainment systems demanding USB host functionality, the PCI11xxx/PCI12xxx delivers Gen3 USB host capability without sacrificing a PCIe port.

Versatile and industrial grade, the PCI11xxx/PCI12xxx family provides multiple interfaces, making it an ideal solution for a wide range of applications.

MICROCHIP

microchip.com/PCIePeripherals

GaN ICs simplify Motor Joint Inverter Design for Humanoid Robots

Battery-powered applications such as new-generation robots, drones, and power tools require a reduction in space and a simplification of the design to control electric motors. Optimizing size and components results in innovative solutions that include more functions in a small space without losing efficiency and performance. EPC ePower™ Stage ICs technology helps to simplify and improve the inverter design in advanced motor control applications.

By Francesco Musumeci, Application Engineer, Italy Application Center, Efficient Power Conversion

In inverters for low voltage motor drive applications [1], GaN technology brings crucial improvements such as the switching frequency increase, the reduction of the passive component in the converter input filter (capacitors and inductors), the strong dead-time decrease with the improvement of the output current waveform quality, and the high-power density which contributes to the overall reduction of the converter size. The introduction of monolithic integrated circuits (ICs) in full GaN technology, composed of a switching leg power stage, a half-bridge gate driver with bootstrap supply, and several protection circuits, simplifies the converter's design and allows a noticeable volume reduction. Innovative applications such as motor joints for humanoid robots are significantly improved by motor drive inverters using EPC's monolithic integrated devices because they result in more compact and lighter converter; moreover, the inverter runs cool thanks to their superior efficiency performance and low switching losses of the GaN devices as well as reduction in motor losses by the higher quality of the driving waveforms.

This article introduces the latest generation of GaN integrated circuits (EPC23102/3/4) [3, 4, 5] for inverter applications. Several evaluation boards with new features, discussed in the following sections, have been developed to demonstrate the effectiveness of implementing ICs in inverter performance. In particular, the ICs' temperature versus the motor phase current will be reported and discussed.

GaN advantage

The critical field in a semiconductor material determines the breakdown voltage of a device. For a given breakdown voltage, the higher the electric field, the shorter the width of the drift region. In a GaN transistor, the critical field is an order of magnitude higher than silicon, and the electron mobility due to the two-dimensional electron gas (2DEG) makes the ON resistance low while keeping its dimensions small [2].

GaN technology is based on a planar layout. In reverse conduction, a GaN transistor features an equivalent body diode with no reverse recovery charge (Q_{RR} = 0). Furthermore, GaN devices have parasitic capacitances approximately an order of magnitude lower than their silicon counterparts for a given ON resistance. Smaller parasitic capacitances lead to higher switching capability, higher PWM frequency, and minimum dead time for improved motor efficiency.

EPC2310x: ePower™ Stage IC Features

The ePower™ Stage IC product family integrates input logic interface, high-side level shifting gate driver, and synchronous bootstrap supply, together with eGaN output FETs into one monolithic integrated circuit using EPC's proprietary GaN IC technology; these devices are packaged in a 3.5 x 5 mm FCQFN package. The new generation of Efficient Power Conversion monolithic integrated circuits is composed of three 100 V-rated products. The three ICs (EPC23102/3/4) differ in the ON-resistance ($R_{DS,ON}$) of the power FETs, allowing the devices to be used in different applications. EPC23102 is the lower $R_{DS,ON}$ device with 6.6 mΩ max for high and low side FETs [3], followed by the EPC23103 with 7.7 mΩ max. and the EPC23104 with 11 mΩ max. [4][5]. The devices' structure is described in the block diagram circuit of Figure 1.

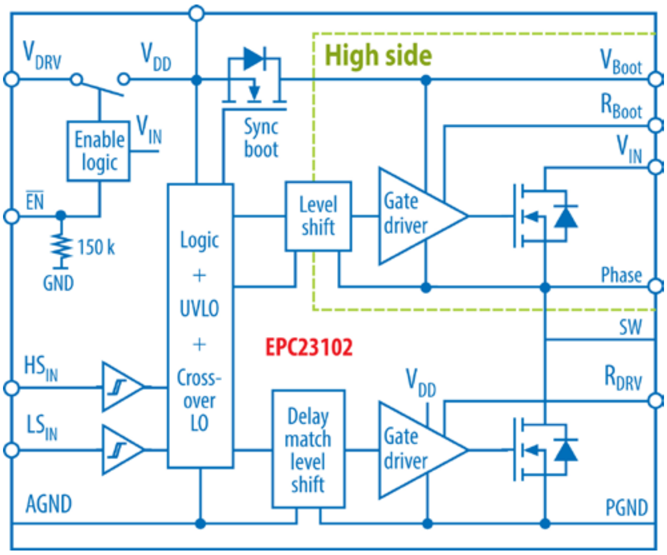

Figure 1: EPC23102/3/4 functional block diagram

Reference designs

EPC has released several reference design boards for motor drive inverters using GaN FETs discrete and GaN integrated circuits. All reference design boards share a similar block diagram and controller connector to help the designer scale the current and voltage during the inverter's platform design phase.

Integrated circuit-based motor drive applications allow for smaller boards and easier design. The new version of the EPC9176 [6] and the new EPC91103 [7] and EPC91104 [8] boards show an example of the simplification and space reduction of a motor drive inverter. The evaluation boards have the same layout but differ in the power stage and the type of phase current sensor. The EPC9176 is equipped with the EPC23102, the EPC91103 mounts the EPC23103, and the EPC91104 mounts EPC23104 devices.

The new reference design boards measure 7.5 x 7.2 cm. The inverter input voltage ranges from 14 V to 85 V. The PCB stackup structure comprises an 8-layer FR4 PCB with 2 oz on the top, bottom, and 4 oz inner layers to reduce the PCB conduction resistance and to have a better heat spreading thanks to the thicker copper. The boards comprise auxiliary power supplies to generate 5 V and 3.3 V from the DC Bus, phase voltage sense, phase current hall-effect sensors, hall/encoder interface for sensored control, and over-current protection circuit as shown in Figure 2.

The most important feature of the reference boards is the simplification of the inverter design, particularly on their top side. As shown in the layout in Figure 2, only the power devices and their respective hall-effect phase current sensors are mounted on the PCB top surface. This facilitates heat spread from the power devices and a better interface with the heat sink mounted on the top. All other components related to analog sensing signals, power supply, and over-current have been placed on the bottom side of the board. The DC-link is composed of ceramic capacitors placed on the top and bottom side of the board, connected to the DC-Bus connector and power devices with alternate tracks of the input voltage VIN and GND also repeated in the internal layers for a better distribution of the DC-Bus current in the layers.

The hall effect current sensors mounted in the new reference boards permit reducing the complexity of the current sensing circuit. The Hall-based phase current sensing solution does not need external conditioning circuits and compared to conventional solutions with shunt resistors, further simplifies the motor drive inverter board design.

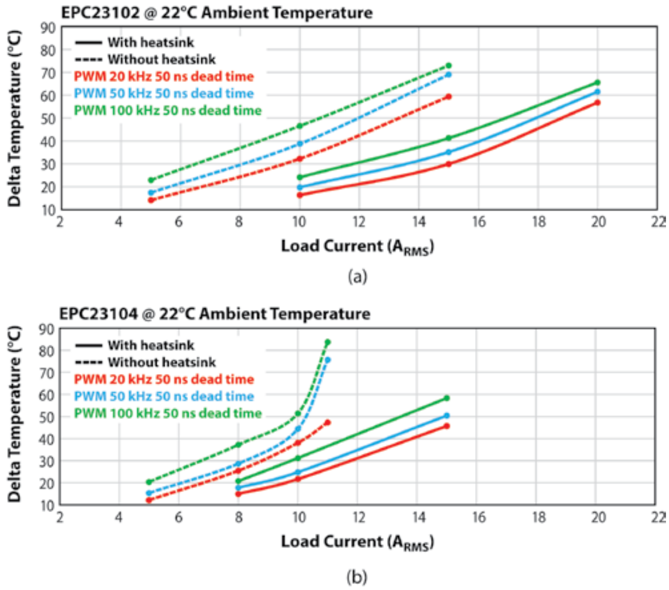

Figure 3: a) EPC3102 and b) EPC23104 temperature rise as function of motor phase current and PWM frequency

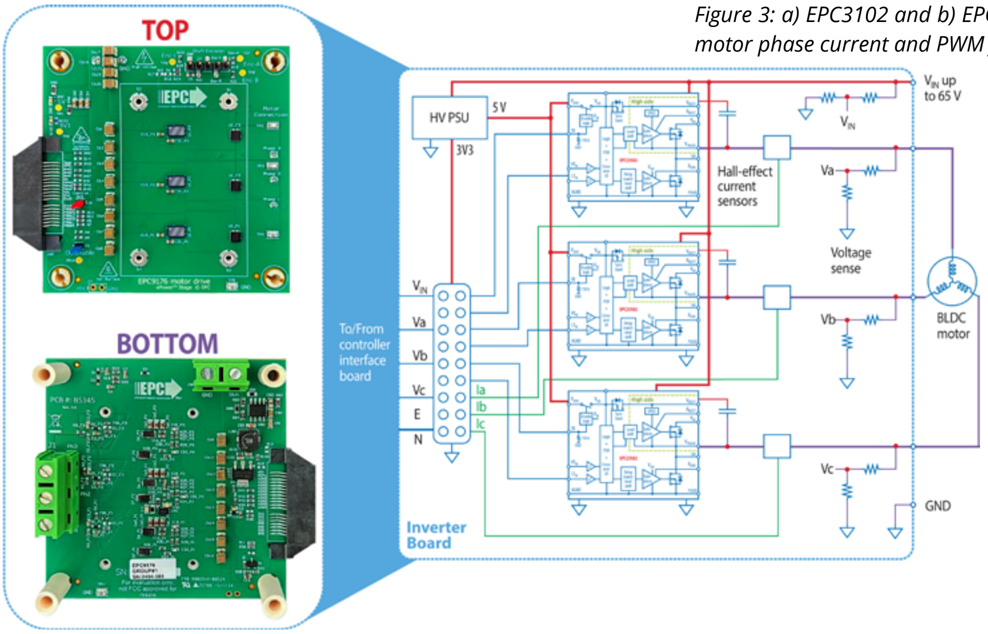

Figure 2: EPC9176 Rev3.0 top and bottom views with system block diagram

Experimental results

Steady-state operation tests with and without heat sink with no forced air cooling are shown in Figure 3 and describe the thermal behavior of the EPC9176 and EPC91104 boards. With a 48 V_{DC} DC Bus, The EPC23102 mounted on EPC9176 can continuously carry 15 A_{RMS} motor phase current without a heatsink, showing a temperature increase of device die with respect to the ambient temperature less than 75 °C for switching frequencies up to 100 kHz and 50 ns dead time. The EPC9176, with a heatsink under passive air cooling (no forced convection), can sustain 20 A_{RMS} with a temperature increase of 65°C for switching frequency up to 100 kHz and 50 ns dead time.

The EPC23104 mounted on EPC91104 presents a different thermal behavior due to the different devices $R_{DS,ON}$. The EPC23104 can reach 10 A_{RMS} without a heatsink and 15 A_{RMS} with a heatsink and passive air cooling, with die temperature increase below 60°C, switching frequency up to 100 kHz, and 50 ns dead time.

Conclusion

Gallium nitride-based Integrated circuits from EPC innovate motor drive inverters. The use of logic-in power-out integrated circuits makes design easier and reduces the dimension of the inverter ensuring greater compactness and weight reduction. Thanks to higher switching frequency, ohmic losses in the motor are reduced, the input filter size is reduced, and the overall system efficiency is increased with a decrease of system-generated heat; shorter dead time allows for silent operation and improves motor performance. Smaller size, less heat generation, and more compactness allow for the realization of inverters integrated into the motors, which are perfect for applications such as humanoid robot joints.

References

[1] A. Lidow, GaN Power Devices and Applications. Chapter 6, First Edition, Power Conversion Publications. ISBN 978-0-9966492-2-3

[2] A. Lidow, M. De Rooij, J. Strydom, D. Reusch, J. Glaser, GaN Transistors for Efficient Power Conversion. Third Edition, Wiley. ISBN 978-1-119-59414-7

[3] https://epc-co.com/epc/products/gan-fets-and-ics/epc23102

[4] https://epc-co.com/epc/products/gan-fets-and-ics/epc23103

[5] https://epc-co.com/epc/products/gan-fets-and-ics/epc23104

[6] https://epc-co.com/epc/products/evaluation-boards/epc9176

[7] https://epc-co.com/epc/products/evaluation-boards/epc91103

[8] https://epc-co.com/epc/products/evaluation-boards/epc91104

www.epc-co.com


plecs
RT Box 3

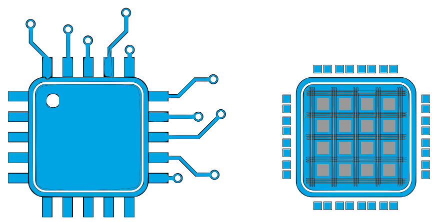

Advantages of Semiconductor-Based Power Modules Over Discrete Components

In the ever-evolving landscape of power electronics, the choice between semiconductor-based power modules and discrete components has a significant impact on the efficiency, reliability, and overall performance of electronic systems. In recent years, semiconductor-based power modules have gained prominence due to their numerous advantages over traditional discrete components. In this article, we explore the key advantages of semiconductor-based power modules before diving into the specific offerings that Vincotech brings to the table.

By Patrick Baginski, Sr. Field Application Engineer EMEA, Vincotech

Advantages of Semiconductor-Based Power Modules

Semiconductor-based power modules integrate multiple components into a single package, resulting in a more compact design compared to discrete components. Modules can easily integrate anything from capacitors to improve switching behavior and stray inductance to shunts for current measurement. Their space efficiency is crucial in size-constrained and space-limited electronic systems such as book-size frequency inverters, renewable energy systems, and uninterruptible power supplies. Semiconductors are placed to ensure small commutation loops that utilizes the efficiency to its maximum and enables some features that are hardly to realize with discrete components.

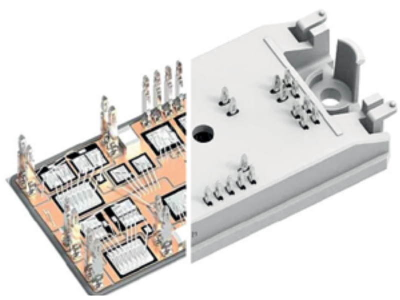

Figure 1: flow 1 IGBT module with integrated capacitors

Another aspect is enhanced reliability. In many applications, reliability is weighted higher than price. Traditional discrete components are prone to reliability issues such as solder joint failures and thermal stress. Semiconductor-based power modules, on the other hand, are designed with advanced packaging technologies that improve thermal performance and reduce the risk of component failures. Their enhanced reliability is essential in mission-critical applications where system downtime is not an option.

Reliability includes thermal performance. Power modules often feature advanced thermal management solutions, such as direct bonding technology, to dissipate heat more efficiently. This lowers their operating temperature, extending the lifespan of the components and ensuring stable performance over time. Different DCB materials come with different thermal properties. While Al_2O_3 is a widely used material, AlN, for example, offers very high thermal conductivity. Because it is more fragile, Si_3N_4 is a good compromise of both materials.

A very important topic is the simplified integration and reduction of assembly costs. Integrating discrete components requires careful consideration of component placement, routing, and thermal management. Semiconductor-based power modules simplify the integration process by consolidating multiple components into a single package. This reduces assembly costs and streamlines manufacturing, resulting in faster time-to-market for electronic systems. Several steps can be spared as modules come with an electrical insulation to the heatsink, can come with a layer of pre-applied thermal interface material, and only need a limited number of screws to be mounted.

Finally, power modules achieve much higher power density compared to discrete components. By tightly packing components in a compact form factor, semiconductor-based modules can deliver more power in a smaller space. This is particularly advantageous in applications with critical power efficiency and size constraints, such as solar inverters and portable electronics like welding machines, and even more critical in embedded drive applications.

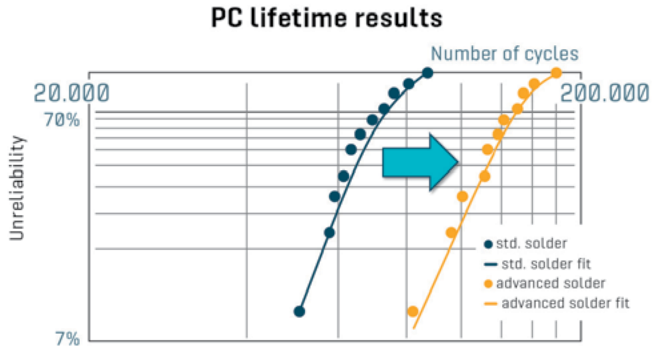

Figure 2: Comparing the power cycling capability of standard versus advanced solder material

Vastly simplified handling and assembly

A deeper comparison between the mechanics of discrete components and power modules reveals vast differences in their handling and assembly. Modules are essentially pre-tested sub-systems. Their manufacturers guarantee that all parts shipped have passed rigorous mechanical and electrical testing. Discrete components, on the other hand, require many additional, largely manual, processes that influence their reliability: Pins need to be bent, thermal interface materials applied, and, in some cases, additional electrical isolation added to the heatsink. Components to be handled include through-hole components such as the TO-220, TO-264, etc. that need to be assembled, fixed, and soldered to the PCB before being mounted to a heatsink. They are connected to form an inverter stage, a PFC circuit, or a brake chopper. Drive applications commonly use bridge rectifiers. The challenge is always to make as-

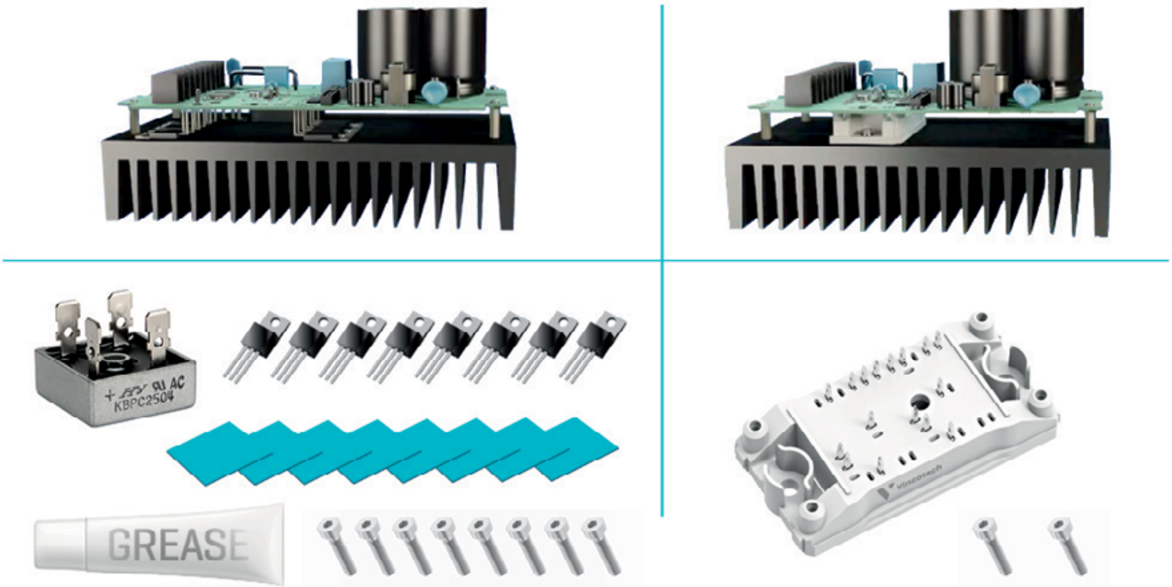

Figure 3: Application with discrete components and with a power module

sembly as stress-free as possible, which can be tough, as discrete components come in different heights.

A comparison of their electrical behavior reveals further drawbacks of discrete components. For one, discrete components cannot be positioned to perform optimally in the case of commutation paths. And, secondly, due to their physical size, discrete components require more space on the PCB and cannot be placed as close to each other as the IGBTs and diodes used in a power module. Consequently, discrete components have a lower power density than power modules.

The figure below highlights differences between using discrete components and a power module in a small power application.

Moreover, parallelizing discrete components requires considering even more components, while power modules can simply be replaced with the next larger housing size. To further facilitate handling, modules can be delivered with solder pins, press-fit pins, and, on request, with pre-applied phase-change material.

Semiconductor-based power modules offer a host of advantages over traditional discrete components, from their compact design and enhanced reliability to improved thermal performance and simplified integration. As a leading player in the industry, Vincotech has contributed significantly to the evolution of power module technology. With its commitment to innovation, customization, and sustainability, Vincotech's offerings empower electronic system designers to meet the demands of today's dynamic and competitive market.

www.vincotech.com

Power Designs Benefit from Material Science Advances – Carbon

In the future of electronics, carbon will play an increasingly important role. This article will explore a few advances in material science in which carbon is expected to revolutionize electronics in the next few years.

By Steve Roberts, Innovation Manager, RECOM Power

Carbon [C] is an essential element. We are carbon-based lifeforms. In combination with oxygen, gaseous CO2 concentration is the barometer we use to measure our contribution to global warming. In solid form, pure carbon can be as soft as graphite or as hard as diamond. Carbon fibers reinforce countless products from airplanes to fishing rods. Radiocarbon 14C dating is an essential tool in archaeology. A more influential element is hard to imagine.

UWBG

Wide Bandgap (WBG) transistors based on Silicon Carbide (SiC) and Gallium Nitride (GaN) have already led to rapid advances in power switching performance. Wider Bandgap materials have a significantly higher intrinsic thermal conductivity and a higher dielectric breakdown voltage than traditional Silicon (Si) based MOSFET power transistors, meaning that the transistor substrates can be made smaller and thinner for the same performance ratings. The smaller size also means that gate and terminal capacitances and resistances are reduced, leading to faster and more efficient switching with lower power dissipation. SiC transistors can handle higher voltages and switch faster and more efficiently than Si-MOSFETs, while High Electron Mobility Transistors (HEMT) based on GaN substrates can switch even faster than SiC-MOSFETS, making them useful for high frequency electronics. The fast switching reduces the required size of the other inductive and capacitive components allowing very compact, efficient and high power density products to be manufactured.

These WBG advantages mean that SiC and GaN transistors are already extensively used in green technologies such as electric vehicles, photovoltaic converters, IoT Networks and eco-design power supplies.

Carbon offers the next generation in this process – Ultra-Wide Bandgap (UWBG) transistors. Instead of SiC or GaN substrates, pure diamond is used, which has an even higher thermal conductivity (4x better than SiC), greater breakdown voltage (6x better than GaN) and a much wider bandgap value than both SiC and GaN (Table 1):

Property	Si	SiC	GaN	Diamond
Bandgap (eV)	1.1	3.0	3.5	5.5
Thermal conductivity (W/cm K)	1.5	4.9	1.3	22
Breakdown voltage (kV/mm)	0.3	2.5	3.3	20
Electron Mobility (cm^2/V s)	1500	400	2000	1060

Table 1: Comparison of basic properties of silicon, WBG and UWBG transistors

The performance of different transistor technologies can be numerated as the Baliga Figure of Merit (BFOM) – the higher the BFOM value, the better. The scale is non-linear because critical performance indicators such as breakdown voltage and conductivity both depend on the critical electric field value, which in turn scales up as a sixth power of the semiconductor bandgap electron voltage. Thus, based on BFOM, WBG transistors are about 730 times better than Si-MOSFETS and a carbon-based UWBG transistor is about 15 625 times better – a massive leap in performance which will be essential for transforming our global energy consumption from polluting fossil fuels to efficient green electrical energy.

Graphene Semiconductors

Graphene is a 2-dimensional form (allotrope) of carbon that is formed from nanolayers that are only one atom thick, with the atoms arranged in a honeycomb-shaped planar lattice. It behaves like a semi-metal, allowing heat and electricity to flow easily along its plane, but not transversely. As a bulk material, it absorbs light strongly across all visible wavelengths, yet it is nearly transparent in single sheets. Microscopically, it is the strongest material on earth as each atom is double-bonded to each of its three neighbors. This rigidity creates an exceptionally high electron mobility, measured at 15 000 cm^2/Vs (compare this value to those in Table 1), so it conducts electricity better than silver.

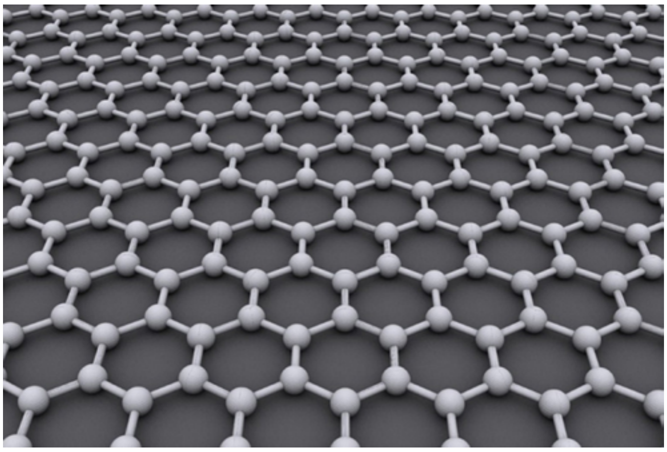

Figure 1: Crystalline structure of graphene (Source: Wikipedia)

Graphene additionally exhibits several unusual electrical properties: it is strongly affected by an external magnetic field, allowing sensitive hall-effect sensors to be built that can operate well at both room temperature and at cryogenic temperatures (down to less than 1°K above absolute zero) and it can be used to make graphene-based FETs (gFETs) that can be used as biosensors. A gFET uses a liquid gate where charged biomolecules affect the channel current, allowing measurements based on ions rather than charge injection. This permits real-time measurements to be made of proteins, biomolecules and nucleic acids, enabling such cutting-edge technologies such as CRISPR gene editing, RNA drug research, detecting the presence of infectious diseases in humans, plants and animals, and cancer research.

Research is continuing into the unique electrical properties of graphene that may open up development of new kinds of electronic devices. One area of development is spintronics, where information can be stored in the angular momentum of electrons (spin-up or spin-down). The regular and rigid array structure of graphene may be an ideal carrier material for a room temperature, atomic level, spintronic non-volatile memory (NVM) which would be faster than conventional RAM and yet retain all the data when switched off.

Carbon Nanotubes

If a graphene sheet were to be rolled into a cylinder, it would become a nanostructure with exceptional tensile strength and thermal conductivity properties. Thermal interface materials made of vertically aligned carbon nanotubes (CNTs) exhibit highly directional thermal conductivity, so heat generated by power electronic devices can be efficiently transferred to a suitable heatsink without excessively warming adjacent components. In tests, thermal conductivities of nearly 15W/°K have been reached – about 3x higher than thermal grease.

In addition, carbon nanotubes can be formulated to act like a semiconductor or a semi-metal, depending on the physical dimensions and/or additional chemical doping. In theory, a carbon nanotube could carry 1000x more current than a similar sized copper conductor and, because of its cylindrical structure, this current could be steered to flow only along the axis of the tube and not laterally, enabling many new kinds of electronic devices.

Other uses of carbon nanotubes are in photovoltaics, sensors, displays, smart textiles and energy harvesters, but the most promising development is new types of Li-Ion batteries that use CNT cathodes (Figure 2). Existing Li-Ion batteries suffer from thermal expansion problems when fast charging or during high discharge rate conditions, which damages the internal structure. The higher mechanical strength of carbon nanotubes can withstand these thermal stresses without degradation. These new CNT cathode batteries can charge from 10% to 90% within 15 minutes and are lightweight, with double the WH/Kg energy density compared with conventional batteries. Furthermore, they will still have 90% of their original capacity after 800 charge/discharge cycles, promising a revolution in electric vehicle driving where a 1000 km range becomes commonplace.

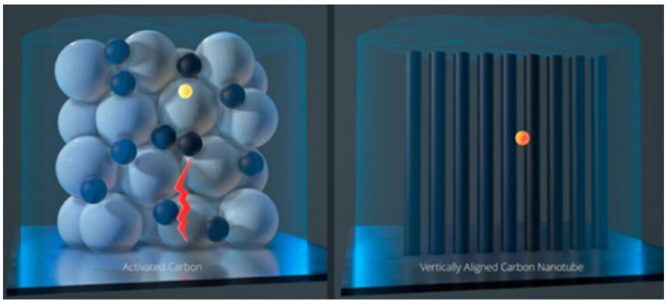

Figure 2: Comparison of a conventional lithium powder cathode (left) with a CNT cathode (right). Source: NAWA Technologies.

www.recom-power.com

Use silicon carbide to rethink soft-switching efficiency

On paper, silicon carbide (SiC) technology has built-in advantages over silicon (Si) in power electronics that make it seem like all that is needed is to use drop-in replacements for existing MOSFETs. That is true to some extent. But it is possible to obtain much more from SiC by paying attention to the ways in which the technology differs from silicon, and how circuit techniques such as soft switching can be optimized beyond what is practical with silicon.

By Mike Zhu, Applications Engineer, Qorvo

SiC's wider bandgap compared to silicon results in higher breakdown voltage and electron mobility, which together reduce on-state resistance. It also enables faster switching speeds compared to silicon, resulting in improved efficiency and the ability to design power electronics systems with smaller form factors. SiC also has a thermal conductivity significantly higher than silicon, allowing for the design of power electronics devices that can operate at higher temperatures without sacrificing performance or reliability.

Whereas circuits based on conventional silicon superjunction MOSFETs need only take account of simple soft-switching techniques, the higher typical frequency of operation means SiC benefits from a careful analysis of when and where losses occur. In turn, that analysis can lead to novel solutions that avoid losses that are inherent to conventional MOSFET-based circuit designs.

For example, a key advantage of a wide-bandgap technology like SiC is the ability to guarantee a higher breakdown voltage for a given on-state resistance. This allows the use of a thinner drift layer that presents less resistance compared to the thicker layers needed for bulk-silicon devices. At the same time, the composition of the crystal lattice delivers higher carrier mobility. The net result is considerably higher conductivity.

The junction field-effect transistor (JFET) is the best option to minimize drain-source resistance. In a MOSFET, the carriers must pass across the surface of the p-base (p-well) region through a resistive inversion channel at the MOS-interface before entering the n-type drift region. However, in a JFET, there is no such inversion channel. By using a high bulk majority carrier mobility, the JFET approaches the theoretical limit of on-state resistance compared to breakdown voltage. Qorvo's SiC JFET-based devices allow a transistor design with a greater safety margin on breakdown voltage compared to MOSFET designs, and an on-state resistance nearly half that of competing parts.

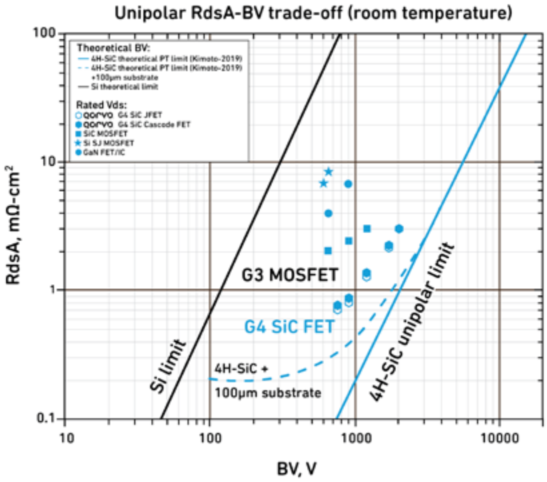

Figure 1: Qorvo's Gen4 SiC FETs exhibit roughly half the RdsA of traditional SiC MOSFETs

Conventionally, using a depletion mode JFET on its own introduces circuit design challenges. As a normally-on device, it needs a negative voltage to turn off completely. However, SiC MOSFETs have low threshold voltages, so negative gate voltages are not uncommon in real-world circuits. Applying negative voltages prevents the accidental turn-on of the transistors at temperature extremes where the threshold voltage may drop below nominal levels.

Qorvo's solution combines an SiC JFET with a low-voltage silicon MOSFET in a cascode structure where the SiC JFET gate-to-source voltage is the inverse of the Si MOSFET drain-to-source voltage. This cascode structure is illustrated in Figure 2. In the cascode configuration, the external gate drive controls a low-voltage Si MOSFET drain-to-source voltage, which indirectly drives the high voltage SiC JFET. This cascode configuration provides control that is familiar to engineers used to working with silicon superjunction MOSFETs. The lower operating voltage of the MOSFET contributes less than 10% to the overall on-state resistance of the pair of devices. To aid integration, Qorvo supplies this configuration in a single package.

The cascode structures provide control over switching through the Si low-voltage MOSFET, decoupling the control logic from the high-voltage JFET. Such a decoupling provides the opportunity to optimize the gate control voltage range and gate charge for the low-voltage Si MOSFET without sacrificing the full performance advantages of the SiC JFET. Unlike conventional SiC MOSFETs that typically require gate voltage as high as 18V to fully activate the device and achieve the full benefit of low on-state resistance, the cascode architecture allows use of lower maximum gate-control voltages and eliminates the need for negative voltages in the off-state. This narrowing of the voltage range reduces gate charge by 50% (from 18V / -4V to 10V / 0V), potentially reducing losses during switching, particularly for soft-switching applications at light loads.

Switching to SiC with a JFET structure significantly shrinks die size. Qorvo's device has an almost ten-fold reduction in die area with the same power-handling ability of silicon superjunction devices. SiC's thermal conductivity and superior efficiency offsets the increase in thermal resistance that accompanies a significantly smaller die. Any further increases in thermal resistance are offset through the use of silver sintering for die attach, which provides a six-fold improvement in thermal conductivity compared to conventional solders.

The application of a cascode structure to an SiC JFET further improves efficiency by reducing stray capacitances that affect silicon superjunction devices and SiC MOSFETs. The lower stray capacitances also improve density by driving the switching frequency higher than is practical with silicon devices and even SiC MOSFETs.

The benefits are most apparent in soft-switching circuit architectures. While soft-switching techniques used with silicon devices tackle some of the most obvious sources of loss due to the turn-on and turn-off phases of the switching cycle, the fast-switching capability of the latest generation of SiC transistors addresses more subtle issues that are generally missed.

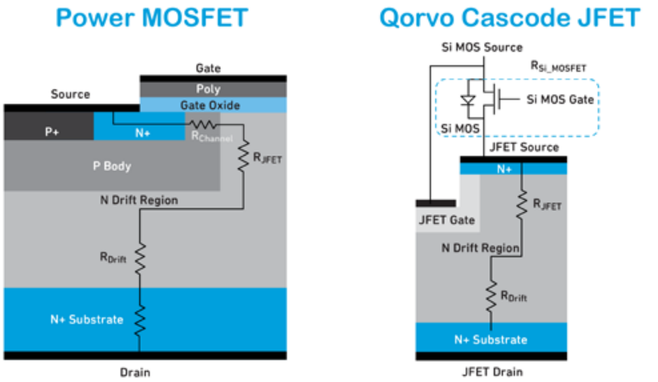

Figure 2: Cross-section view of planar SiC MOSFET (left) and Qorvo cascode SiC FET (right). The dominant channel resistance (Rchannel) of SiC MOSFET is replaced by a much lower $R_{DS(on)}$ low-voltage Si MOSFET in cascode structure.

Many circuits based on silicon devices employ zero-voltage switching (ZVS). Its primary purpose is to reduce the voltage between the drain and source during the transistor turn-on transition before current begins to flow freely through the transistor channel. Ideally, the device drain-to-source current (I_{DS}) and drain-to-source voltage (V_{DS}) have almost zero overlap, thus eliminating turn-on switching loss. The output capacitance (i.e. sum of the drain-source capacitance and the capacitance between the gate and drain) is normally fully charged to the DC link bus voltage during device turn-off in the previous cycle and is recycled into the load to avoid losses during the next ZVS turn-on event.

ZVS turn-on with a conventional Si device can lead to a period of dead time in the switching cycle that can last as long as 300ns due to the high output capacitance of silicon devices. At a switching frequency of 500kHz (2µs period), a 300ns dead-time during both turn-on and turn-off transitions represents 30% of the duty cycle. The SiC JFET delivers a key advantage over Si MOSFETs because it has 10x lower output capacitance that takes less time to clear, especially at low drain-to-source voltage bias where output capacitance increases significantly for Si MOSFETs. Silicon superjunction devices have strong nonlinearity in the CV curve at low drain-to-source voltage bias, which leads to high voltage transition time near the bus voltage and 0V during the switching transition in a half-bridge topology. This reduces the length of the dead time needed for ZVS which can be traded for higher-frequency operation or more power delivered to the load.

Due to the long voltage transition time and relatively high turn-off switching loss, designs for ZVS circuits using Si devices are limited to switching frequencies below 150kHz. With the fast-switching capability of the Qorvo SiC FET, the switching frequency boundary is pushed beyond 500kHz. Similar to turn-on switching loss, efficiency improves if the overlap between the fall in current and rise in drain-source voltage during turn-off is minimized.

However, EMI becomes more challenging with increased switching speed. Designers must diligently minimize PCB parasitics from critical current commutation loops early in the design phase to fully exploit SiC's fast-switching capability. But there is a limit on how much optimization can be achieved when safety requirements (e.g. clearance, creepage, etc.) are considered. Once the circuit design is finalized, there are two popular ways to further fine tune turn-off drain-to-source voltage spikes and ringing. One is using high gate resistance (R_g) to slow device switching speed. A more effective and efficient way is to use a snubber circuit, as shown in Figure 4, with low gate resistance. In other words, use small gate resistance to allow fast switching of SiC devices, and use snubber RC to control V_{DS} spikes and ringing. The device snubber C_s provides V_{DS} peak overshoot control while C_d minimizes power loop stray inductances by being placed very close to the fast-switching half-bridge. R_s and R_d provide damping for V_{DS} ringing.

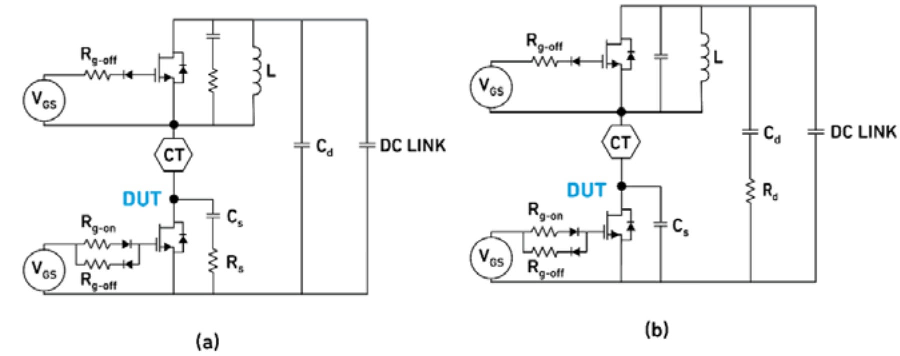

Figure 4: DPT schematic with an RC snubber on both switches for (a) hard-switching and (b) ZVS soft-switching

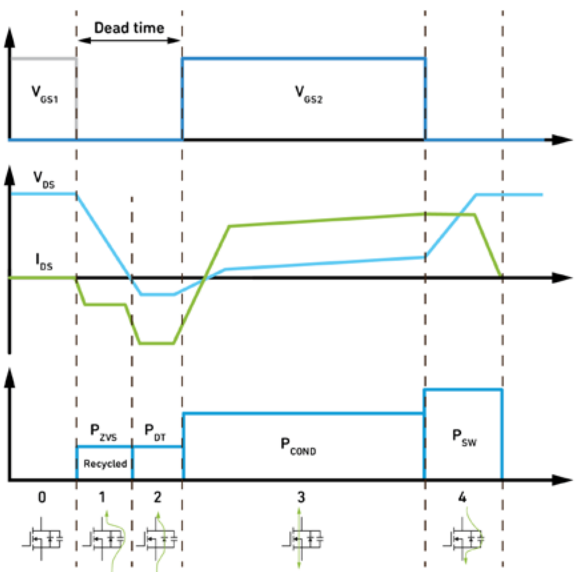

Figure 3: Illustration of key waveforms and loss distribution in ZVS soft switching applications

A common misconception is that using a snubber is inefficient. For a half-bridge topology - typically used in ZVS applications such as LLC or PSFB - using a snubber is much more efficient than using high gate resistance because the added drain-to-source capacitor does not generate any turn-on loss. During the turn-off dv/dt phase, the displacement current of the freewheeling device will further decrease the turn-off current of the device that has been actively turned off, thus reducing voltage and current overlap to greatly reduce turn-off loss (E_{off}). The displacement current level is determined by the equation I = C*dv/dt. C is the equivalent output capacitance and includes both device output capacitance (C_{oss}) and the extra snubber C_s paralleled across the device drain-to-source. With extra snubber capacitance between the drain and source and high dv/dt (i.e. low gate resistance), the displacement current will be higher. This leaves less current to overlap with V_{DS} for the active-turn-off device, thus reducing turn-off switching loss. This approach allows us to contain the V_{DS} ringing and spikes without sacrificing as much device switching speed, had we instead used a high R_g solution. Figure 5 shows double pulse test turn-off waveforms - both with and without a snubber - to intuitively demonstrate that using a snubber with low gate resistance greatly reduces voltage and current overlap, which in turn reduces turn-off switching loss.

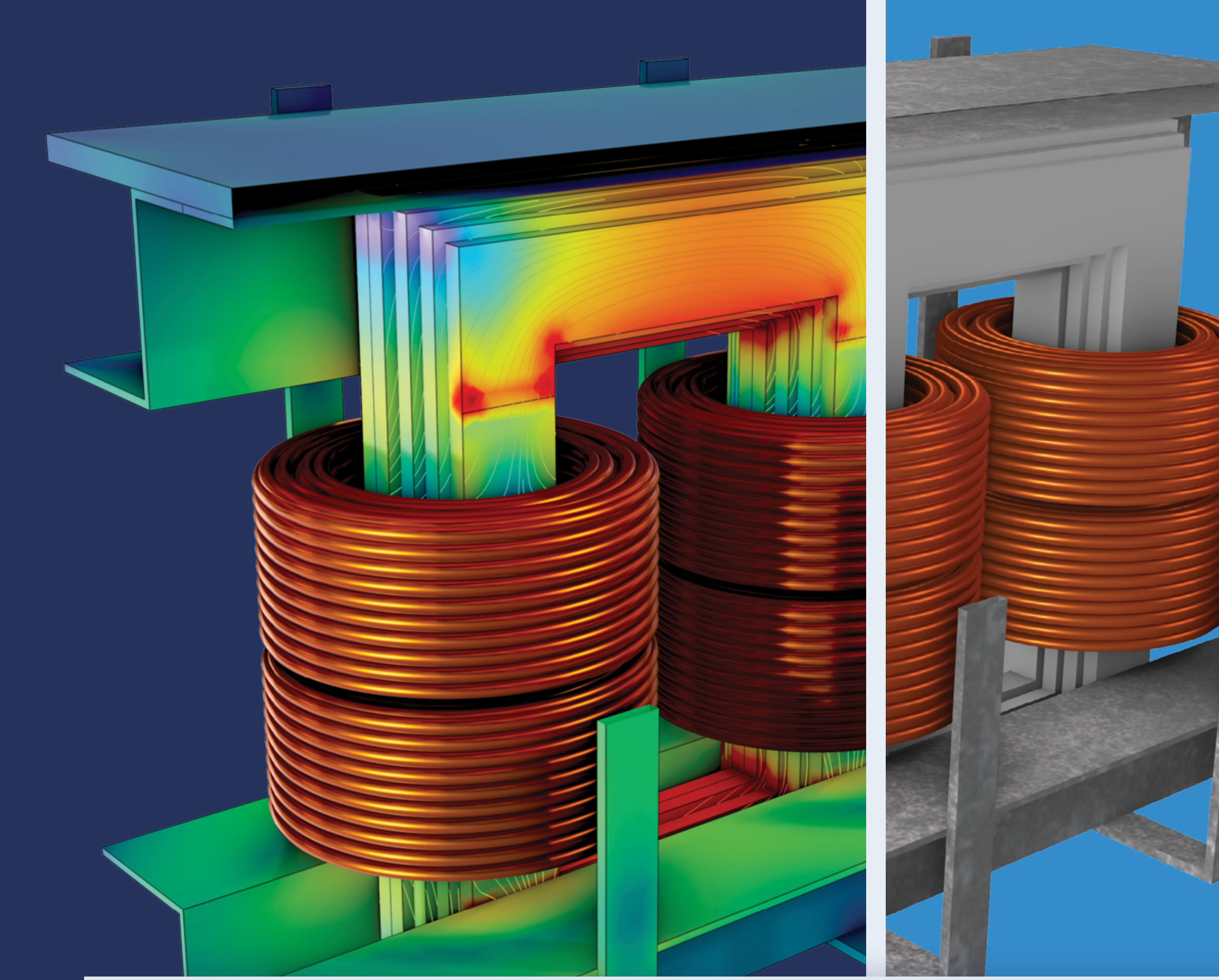

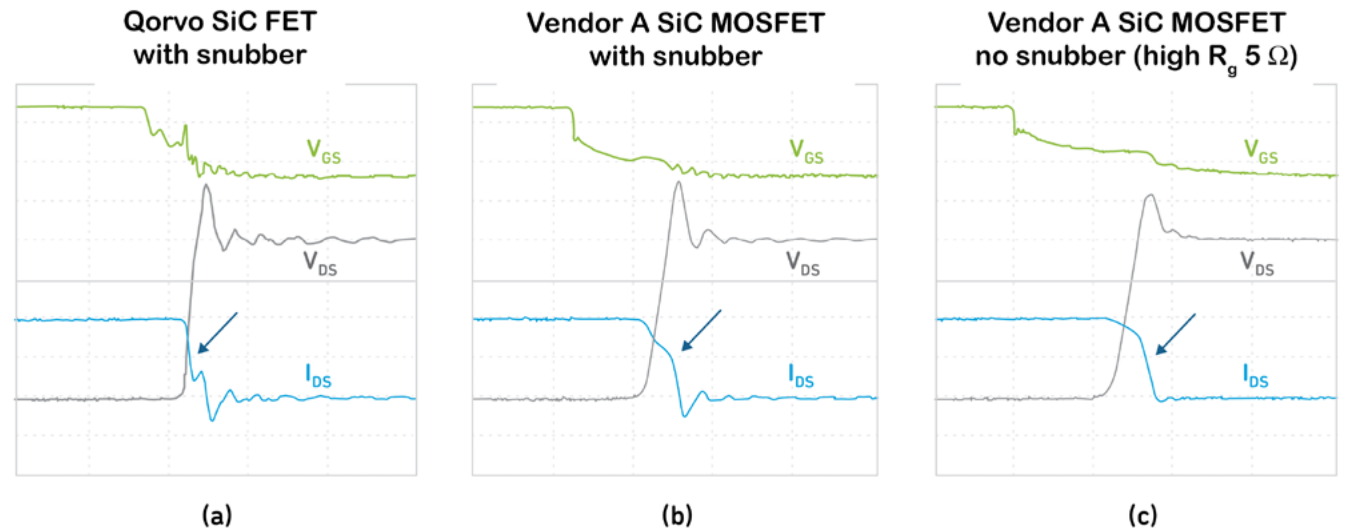

Figure 5: 800V V_{DS}, 100A I_{DS} turn-off waveforms for Qorvo's SiC modules in E1B packaging: (a) UHB100SC12E1BC3-N (1200V, 100A E1B module) with snubber (660pF, 4.7Ω, R_{goff} 2.2Ω), (b) Vendor A 1200V, 100A SiC module with snubber (660pF, 4.7Ω, R_{goff} 2.2Ω), (c) Vendor A 1200V, 100A SiC module without snubber (R_{goff} 5Ω)

The savings possible through the use of snubbers emphasizes the importance of leveraging soft-switching circuit architectures when using SiC to maximize efficiency. Snubber circuits present less of a benefit in hard-switching designs, where the energy stored in C_S from the turn-off cycle is often wasted as heat in the device channel during the next turn-on cycle. However, even with this turn-on loss penalty of using a snubber, the overall switching loss (i.e. the sum of turn-on and turn-off switching losses) is still much lower than simply using high gate resistance at full load (i.e. the device's rated current level).

Referencing the waveforms from Figure 5 for a double pulse test conducted with an 800V bus voltage and 100A load current, the analysis summarized in Figure 6 reveals that adding a snubber results in a 50% reduction in losses for the SiC MOSFET module from vendor A. The combination of using Qorvo's JFET-based devices with a snubber delivers an additional 74% reduction in turn-off switching loss. This makes it possible to increase the switching rate threefold and drive a reduction in the size of external passive components. Citing the simulation of a 50kW PSFB (phase-shifted full bridge), the 74% reduction in turn-off switching loss also helps drive a 10% reduction in junction temperature (Figure 7). Ultimately, better thermal performance leads to smaller heatsinks and cooling structures; combined, the two translate into a reduction in converter volume.

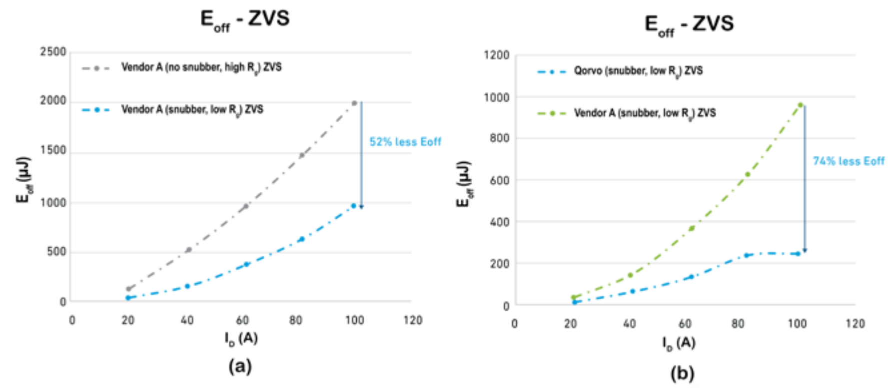

Figure 6: DPT test results at 800V V_{DS}, 100A I_{DS} for turn-off switching loss for Qorvo SiC modules in E1B packaging: (a) Vendor A 1200V, 100A SiC module with snubber (660pF, 4.7Ω, R_{goff} 2.2Ω) and without snubber (R_{goff} 5Ω), (b) Qorvo UHB100SC12E1BC3-N (1200V, 100A SiC module in E1B packaging) with snubber (660pF, 4.7Ω, R_{goff} 2.2Ω) and Vendor A with snubber (660pF, 4.7Ω, R_{goff} 2.2Ω).

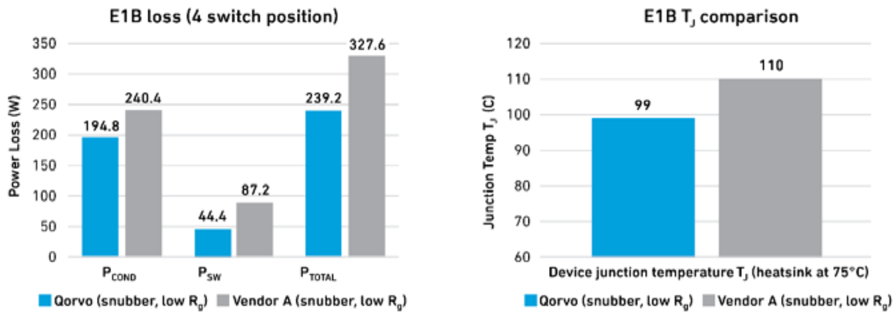

Figure 7: FET loss from simulation of a 50kW phase-shifted full bridge. Application conditions: 50kW, 800V V_{IN}, 400V V_{OUT}, 150kHz, deadtime 150ns, heatsink temp 75°C

Though SiC has inherent advantages over silicon in power-electronics design, reassess both device selection and circuit topology to gain the best performance possible. Fast switching coupled with the combination of a snubber circuit and the inherent low drain-to-source resistance of the Qorvo SiC cascode JFET configuration enables dramatic leaps in efficiency and power density for ZVS soft switching applications.

www.qorvo.com


"Meet the TOP EXPERTS
for SiC and GaN!"
Bodo's
Wide Bandgap
EVENT 2024
December 3-4
Hilton Munich Airport
Mark your Calendar!
Day 1
Opening Roundtable
& Come Together
Day 2
Conference
& Tabletop Exhibition
bodoswbg.com
Bodo´s Power Systems®

pcim
EUROPE

Nuremberg, 11 – 13 June 2024

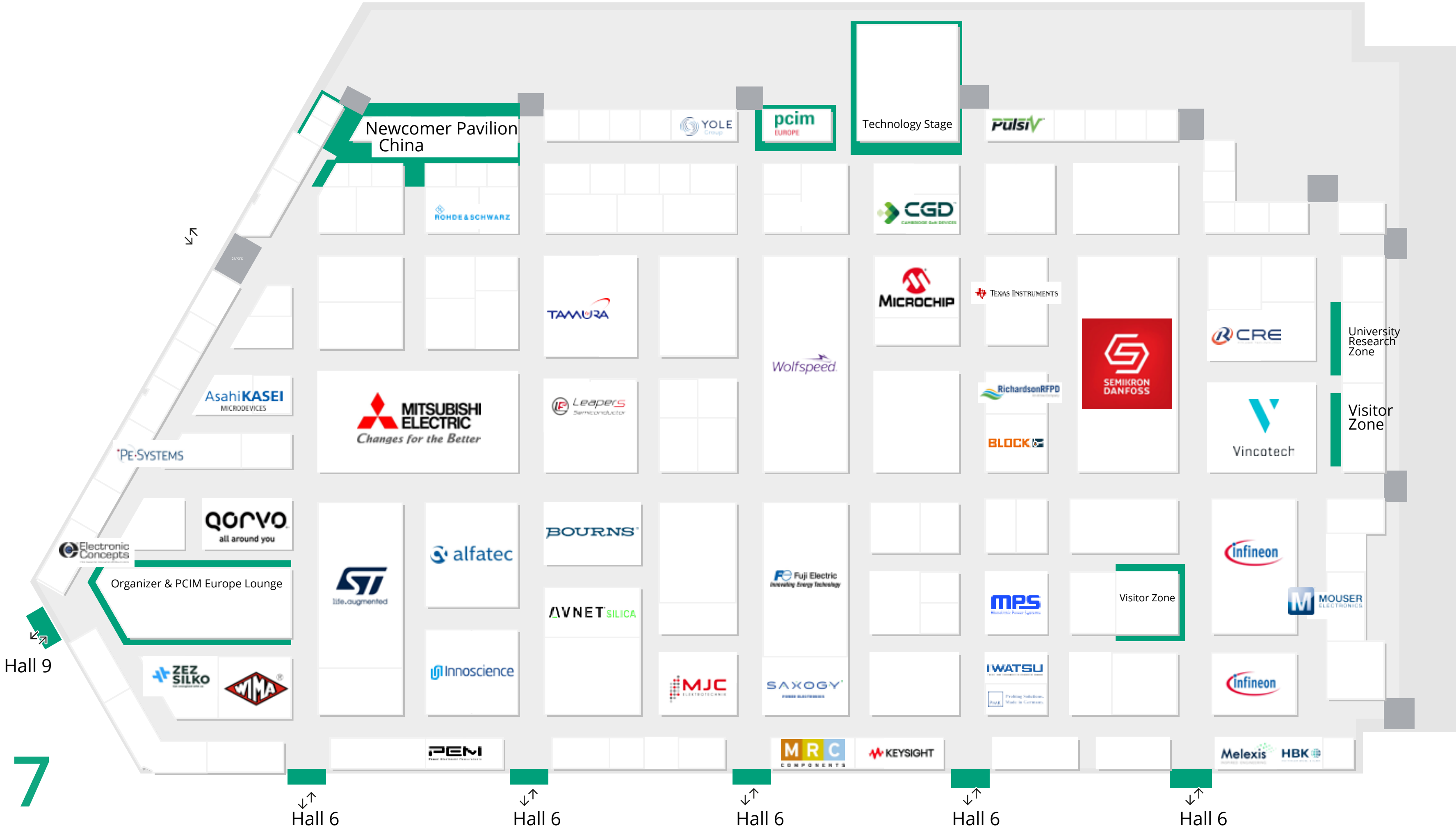

Hall 7

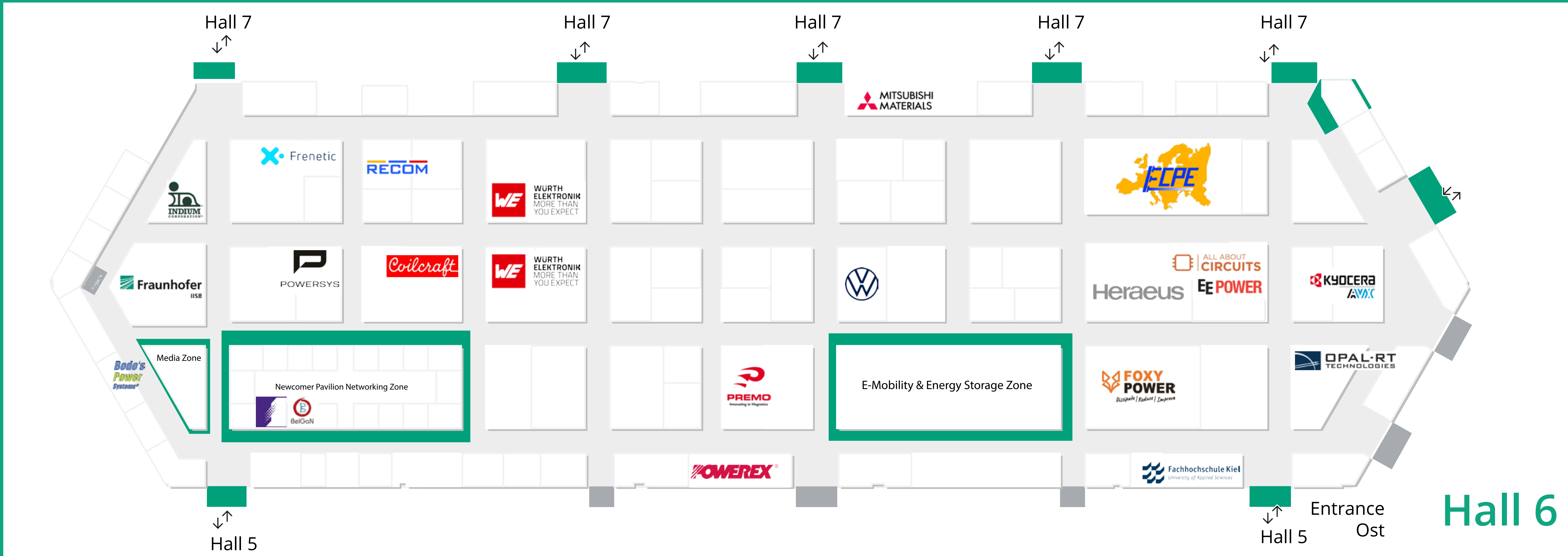
Hall 7
Hall 7
Hall 7
Hall 7
Hall 7
MITSUBISHI MATERIALS
Frenetic
RECOM
WÜRTH ELEKTRONIK MORE THAN YOU EXPECT
ECPE
INDIUM CORPORATION
Fraunhofer IISB
POWERSYS
Coilcraft
WÜRTH ELEKTRONIK MORE THAN YOU EXPECT
ALL ABOUT CIRCUITS
Heraeus
EE POWER
KYOCERA AVX
Media Zone
Bodo's Power Systems
Newcomer Pavilion Networking Zone
BelGaN
PREMO
E-Mobility & Energy Storage Zone
FOXY POWER
OPAL-RT TECHNOLOGIES
POWEREX
Fachhochschule Kiel
Hall 5
Hall 5
Entrance Ost
Hall 6

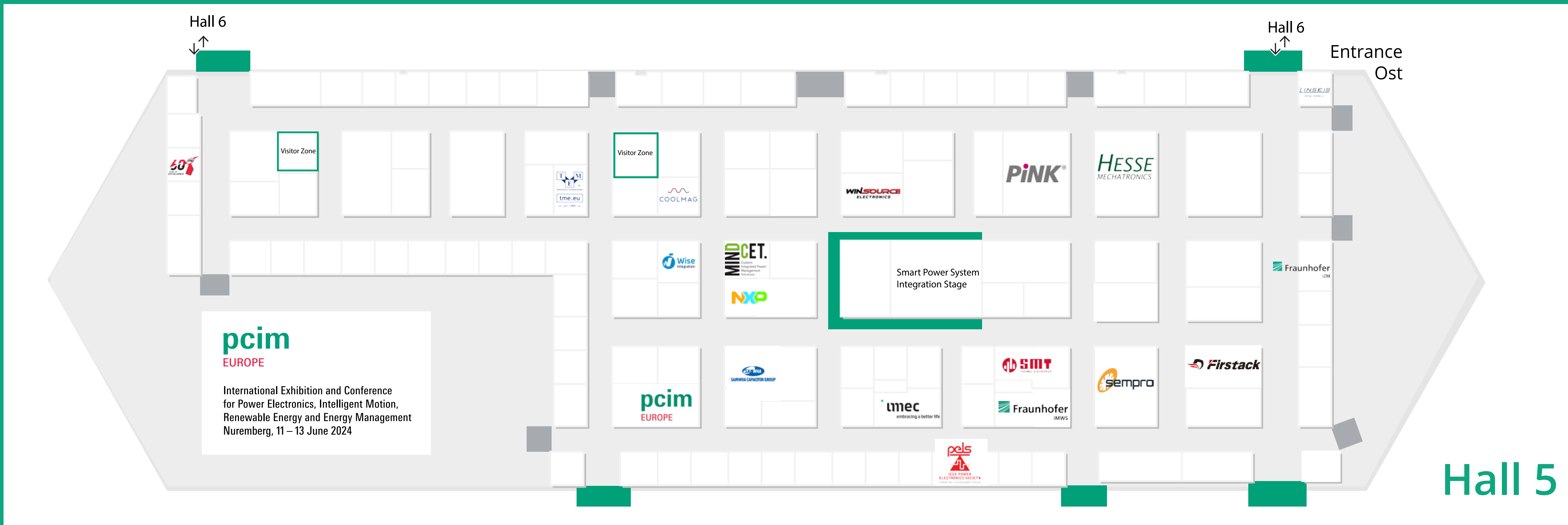
Hall 6
Hall 6
Entrance Ost
LINSEIS
Visitor Zone
tme.eu
Visitor Zone
COOLMAG
WINSOURCE ELECTRONICS
PINK
HESSE MECHATRONICS
Wise integration
MIND CET.
NXP
Smart Power System Integration Stage
Fraunhofer IZM
pcim EUROPE
International Exhibition and Conference for Power Electronics, Intelligent Motion, Renewable Energy and Energy Management
Nuremberg, 11 – 13 June 2024
pcim EUROPE
SAMWHA CAPACITOR GROUP
imec
SMT
Fraunhofer IMWS
sempro
Firstack
pels
IEEE POWER ELECTRONICS SOCIETY
Hall 5

Hall 9

11:20 - 12:15
(GMT+1)
12. Jun '24

Panel Discussion: SiC Wide Bandgap, The Future of Power - Part 1

Presenter Bodo Arlt Bodo's Power Systems	Speaker Carlos Silva WeEn Semiconductors T...	Speaker Evangelos Theodossiu Vincotech
Speaker Stefan Häuser Semikron Danfoss	Speaker Mrinal K. Das onsemi	Speaker Pierre Delatte CISSOID
Speaker Eugen Stumpf Mitsubishi Electric Europe		

13:15 - 14:15
(GMT+1)
12. Jun '24

Panel Discussion: SiC Wide Bandgap, The Future of Power - Part 2

Presenter Bodo Arlt Bodo's Power Systems	Speaker Guy Moxey Wolfspeed	Speaker Kevin Speer Microchip
Speaker Peter Friedrichs Infineon Technologies AG	Speaker Aly Mashaly Rohm Semiconductor	Speaker David Sheridan Alpha and Omega Semic...
Speaker Virgiliu Botan Hitachi Energy		

14:20 - 15:20
(GMT+1)
12. Jun '24

Panel Discussion: GaN Wide Bandgap, The Future of Power

Presenter Bodo Arlt Bodo's Power Systems	Speaker Giorgia Longobardi Cambridge GaN Devices	Speaker Llew Vaughan-Edmunds Navitas Semiconductor
Speaker Dilder Chowdhury Nexperia	Speaker Philip Zuk Transphorm	Speaker Alex Lidow Efficient Power Conversi...
Speaker Thomas Neyer Infineon Technologies	Speaker Harald Parzhuber Texas Instruments	Speaker Balu Balakrishnan Power Integrations

Using FRD MOSFETs to Achieve High Efficiency, High Power Density, and Maximize Reliability in Power Supplies

The "Super Junction" technology has dominated the power MOSFET market where the breakdown voltage exceeds 600V due to its superior figure-of-merit. This article outlines issues engineers need to consider when designing Super Junction-based power devices. It provides an optimized solution that enhances efficiency, power density, and reliability in power supply applications.

By Ziwei Yu, Application Manager; Jorge Ramos, Sr. Application Engineer; Wendi Wang, Staff Engineer; and Richard Zhang, Sr. Director of MOSFET, all Alpha & Omega Semiconductor

As shown in Figure 1, one of the first considerations is that the p columns extend from the base region to create a "charge balance" in the drift area for higher doping concentration, namely lower resistance in the corresponding region. The extended junction area leads to a drawback of excessive reverse recovery charge.

Furthermore, Figure 2 shows a typical half-bridge configuration in which the current freewheels through the body diode of the high-side MOSFET during the dead time before the low-side MOSFET turns on. The body diode reverse recovery happens when the low-side MOSFET starts to turn on. The low-side MOSFET sees a negative current spike due to the reverse recovery charge of the high-side MOSFET. This causes an excessive turn-on loss in the low-side MOSFET. At the same time, the high-side MOSFET sees a high slew rate voltage rise and a spike voltage during the Tb period, which can cause an overstress on the device.

Ultimately, as shown in an example in Figure 3, a 600V SJ device failure is caused by the body diode recovery when the forward current and the current slew rate are beyond the device's safe operation limit.

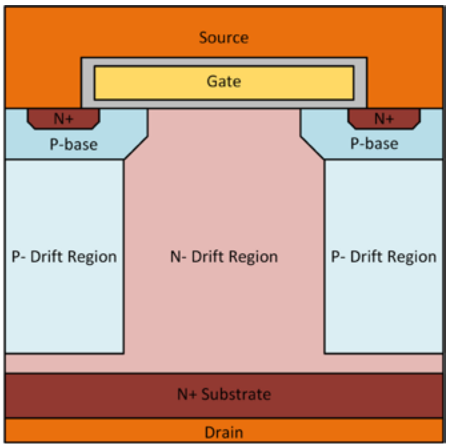

Figure 1: P-N junctions in Super Junction MOSFETs

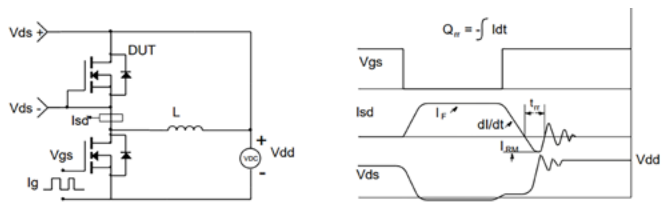

Figure 2: Body diode reverse recovery in half-bridge circuit

An issue to be aware of is that body diode reverse recovery in Super Junction-based power devices has deeply impacted the selection of HV power devices for power supply designs. Figure 4 shows a typical circuit in AC/DC power supply. In the PFC stage, SiC Schottky diode instead of a synchronous rectifier FET is used as the high-side device because the switching loss caused by the reverse recovery of a synchronous rectifier is too high with the target switching frequency (usually above 50kHz).

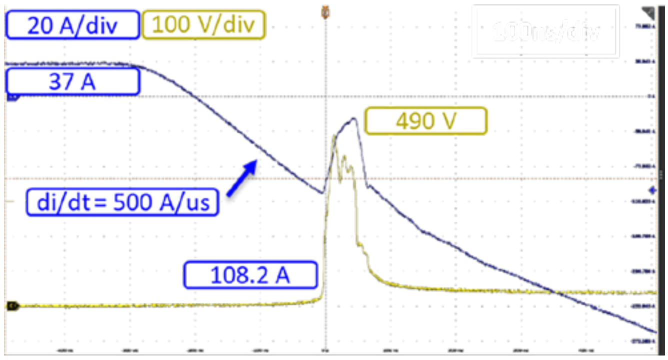

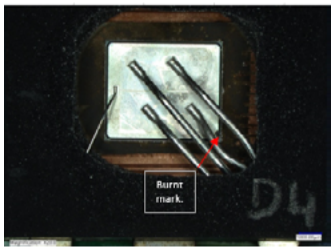

Figure 3: Illustrates a device failure caused by the body diode reverse recovery

In the DC-DC stage, the soft-switching LLC circuit is used where hard commutation of the HV devices does not happen in normal operation mode. The device's hard commutation causes the body diode to reverse recovery; thus, it will not be seen in this case. However, hard commutation can happen in the LLC circuit during abnormal operation conditions such as start-up and short-circuit transients. Protections against such transients are normally required in the controller design of the LLC circuit. Failure to prevent the hard commutation in the LLC circuit could lead to a failure in the HV devices due to the very snappy body diode reverse recovery transient.

There are circumstances where the HV device body diode reverse recovery can't be avoided. For example, cycle-by-cycle hard commutation protection is not available in high-power LLC converters with digital controllers. In high-voltage motor drive applications, active devices (MOSFET/IGBT) are needed for both high - and low-


SAXOGY®
POWER ELECTRONICS
pcim EUROPE
Hall 7
Booth 135
POWER MANAGEMENT
SAFETY EQUIPMENT
THERMAL MANAGEMENT
YOUR DUT
TEST BENCHES
INDUCTIV & RESISTIV LOADS
SPECIAL FUNCTIONS
With us, everything revolves around your DUT.
Select one piece or use complete solutions.
We speak power electronics
precise I safe I adaptiv
Find out more about this topic.
www.saxogy.de

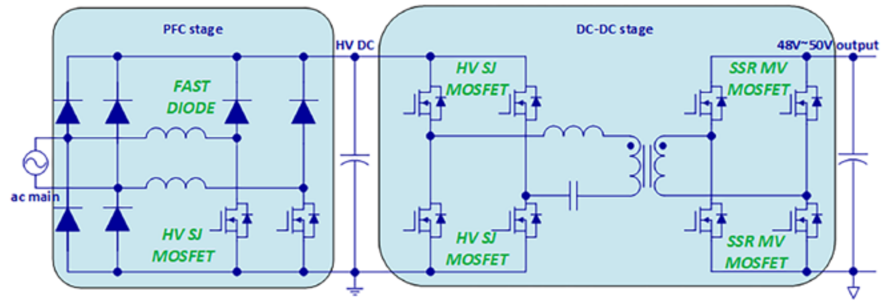

Figure 4: Typical AC/DC power supply circuit structure

side switches. Improved body diode performance regarding the reverse recovery charge and reliability is a key requirement for the HV power device in these applications.

An Optimized solution: αMOS5™ FRD technology

The αMOS5 FRD MOSFET platform developed by Alpha and Omega Semiconductor (AOS) is specifically optimized for low reverse recovery charge and switching robustness. Electron irradiation is applied in this technology to control the lifetime of the bipolar carriers during the reverse recovery phase. It creates defects to serve as recombination centers and accelerates the process of electron/hole pair recombination of the FRD during the forward biasing and the reverse recovery stage, significantly reducing the total number of excessive charges stored in the FRD drift region.

Comparing the Qrr waveforms of the same Super Junction structures, but with different carrier lifetime control, the ER-processed part shows a significant reduction in Qrr value. Suppressed Qrr means that a smaller power spike level will surge through the FRD, thus suppressing the risk of thermal failure.

It is important to note that the MOSFET active/termination transition region is the most vulnerable to reverse recovery failure as it passes high current density with its limited area size. A key benefit of the αMOS5 platform is that it employs a conservative termination design to evenly spread the electric field across the transition region. This optimization prevents localized hot spot burnout due to excessive power density during the reverse recovery tb phase.

Test Results and Conclusion

The safe operation condition regarding the body diode reverse recovery is validated with AOS αMOS5 FRD MOSFET tests. The test result is provided in the device datasheet. Figure 6 shows the test waveform of AOS' AOK042A60FD 600V 42mΩ αMOS5 SJ

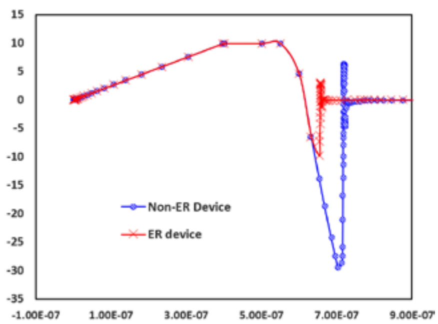

Figure 5: ER Controlled reverse recovery waveform

MOSFET, and two competitors with similar B_{Vdss} and R_{dson} specifications. The test was conducted with 50A forward current and 1000 A/us slew rate at three different temperatures. As given in Table 1, the AOK042A60FD passed the test at 200°C, while the competitors failed the test even at lower temperatures.

It is worth noticing that AOK042A60FD shows the lowest drain voltage slew rate in the T_b period waveform. This helps the

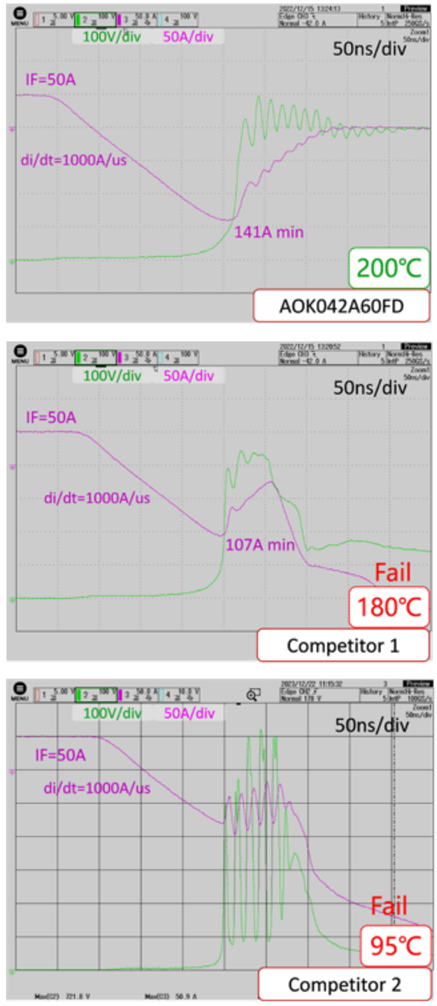

Figure 6: Body diode reverse recovery test performed on two competitive products and the AOK042A60FD αMOS5 FRD MOSFET (VDD = 400V, IF = 50A, di/dt = 1000A/us)

DUT	IF (A)	di/dt (A/us)	dv/dt (ns)		
			25°C	150°C	200°C
AOK042A60FD	50	1000	104 (pass)	46 (pass)	38 (pass)
Competitor 1			160 (pass)	92 (pass)	74 (fail)
Competitor 2			134 (pass)	122 (fail)	

Table 1: Body diode reverse recovery robustness test result for AOK042A60FD

device survive the harsh reverse recovery transient, as well as improve the device's EMI performance. The test result shows that the AOS αMOS5 FRD SJ device provides highly effective body diode robustness in the reverse recovery transient, which is crucial in bridge-type applications such as LLC converters to ensure the highest system reliability in abnormal and transient conditions.

www.aosmd.com

The 1/3-2/3 Weighting Mystery

The most prominent factor for determining the service life of a power-electronic system is the temperature development at the semiconductor itself. For this reason, it is very important to determine the chip temperature as accurately as possible.

By Dr.-Ing. Martin Schulz, Global Principal, Application Engineering, Littelfuse

The determination of a power semiconductor's temperature often is not a trivial task. This is partially, because strictly speaking there is no such thing as "the chip temperature".

All specifications in data sheets and in calculations on service life refer to a mathematical construct of a virtual chip temperature or virtual junction temperature T_{vj}.

The so-called in-situ measurement is the method of choice to measure the chip temperature in the laboratory. Here, the chip to be measured is first heated to precisely defined temperatures using a calibrated heating plate. A small measuring current is then injected, and the resulting forward voltage is measured. There is a linear relationship between the forward voltage and the temperature of the chip, provided that a constant and precisely known current is flowing.

The current must be chosen small enough, so that it does not itself contribute to the heating of the semiconductor. At the same time, it but must be sufficiently large to generate a measurable voltage.

Values around 1% of the nominal current of the semiconductor to be tested have proven to be reasonable.

In turn, the chip-temperature can be determined from the correlation, which is unique and reversible, if the previously used current is used and the voltage on the component is known.

The result of this laboratory measurement is based on a constant chip temperature and, due to the external heating, there is a homogeneous temperature distribution in the chip. This special case, which does not reflect the conditions in the real application, provides "the chip temperature" or the "junction temperature" T_j.

In the real application, however, there is a temperature gradient across the chip's surface; the chip is hotter in the center than it is at the edges, especially at the corners. The reason for this is that more heat can be transferred to the surrounding assembly and connection technology at the edges and corners than in the center of the chip.

The effect can be clearly seen in measurements such as those displayed in Figure 1, which are taken using an infrared imaging camera (IR).

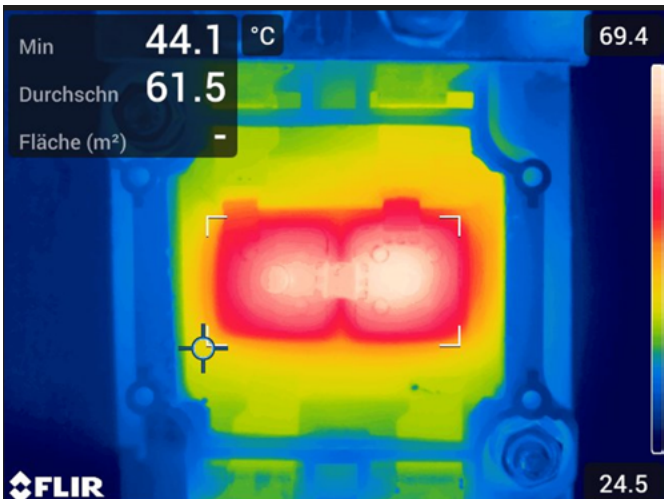

Figure 1: IR image of two diodes connected in parallel under DC load

Alternatively, a sensor placed on the chip is often used, for example a type K thermocouple. Although the sensor then provides a temperature value, this does not necessarily represent the value required for characterization and service life determination. One advantage of this measurement is that it is possible to measure during operation at high voltage and high current, provided the measurement equipment meets the requirements for the protection of equipment and personnel. This is important as the sensor is in galvanic contact with the chip and therefore carries a potentially lethal voltage.

The temperature sensor is often placed in the center of the chip, so that it at least reliably delivers the maximum value. If the thermal relationships are known precisely enough, conclusions can also be drawn from the maximum value to the average value.

The virtual chip temperature T_{vj}, which represents an average value of the temperature over the entire chip surface, is always of interest when considering the service life and thermal design. If it can be implemented, the in-situ measurement also precisely provides this value in the real setup, as only one voltage at one current needs to be measured. Averaging is an inherent part of this measurement setup. The measured voltage represents the chip temperature as if it were homogeneously distributed.

Reliability tests at semiconductor manufacturers are also monitored using the in-situ method. Here the approach is close to the application as the chip is actively heated. The information on load cycling resistance based on this method already includes the fact that the maximum temperature value on the chip is higher than the temperature specified. This approach can therefore be considered conservative and is ideally suited to characterization measurements and quality assurance processes.

Another way to calculate the mean value is by evaluating IR images. This method also allows the observation of semiconductors in real operation and provides precise and application-related information. For evaluation, the software belonging to the IR camera usually allows an area of interest to be defined and the correlating mean value within it to be determined. This procedure is used in Figure 1; the area under consideration comprises two diodes connected in parallel.

The disadvantage of this method is that the observed semiconductors must not be potted. Potting compounds, even if they are optically transparent, block the emitted infrared radiation, making this way of measurement impossible. Consequently, such setups cannot be operated with high voltages because the lack of insulation can lead to arcing and malfunction or even destruction.

A frequently used alternative evaluation consists of determining the temperature T_M in the center and the temperature T_E in one corner of the chip and performing a 2-to-1 weighting.

The virtual chip temperature then results in $T_{vj}=1/3\cdot(2\cdot T_M+T_E)$. This is possible both from the IR image and using two correctly positioned temperature sensors.

It is no coincidence that even this seemingly simple method delivers accurate values. The precision can be explained by the thermal conditions along the chip diagonals.

From one corner to the diagonally opposite corner, the temperature across the chip develops along a dome-shaped curve. A good approximation of this shape is either a parabola or a sinusoidal curve. Due to the simple relationships, the sinusoidal curve is the preferred one here.

The mean temperature results from the effective value of the sine curve and the offset. Figure 2 depicts the curve that can be assumed in this case.

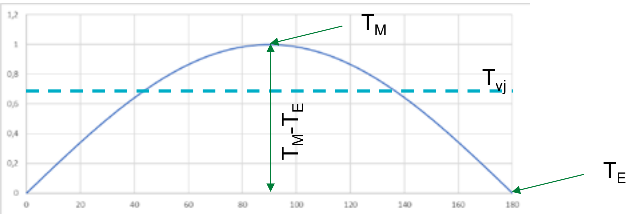

Figure 2: Temperature distribution along the diagonal of a chip

The required mean value corresponds to the RMS value, which is calculated from the amplitude (T_M-T_E) and the offset T_E as

$$T_{eff} = T_{vj} = \underbrace{\frac{1}{\sqrt{2}}(T_M - T_E)}_{\text{RMS-Value}} + \underbrace{T_E}_{\text{Offset}}$$

In another notation, the equation can be rewritten as

$$T_{vj} = \frac{1}{3} \cdot \left[\frac{3}{\sqrt{2}} \cdot (T_M - T_E) + 3 \cdot T_E\right]$$

With the approximation $\frac{3}{\sqrt{2}} \sim 2$ the result is:

$$T_{vj} = \frac{1}{3} \cdot [2 \cdot T_M + T_E]$$

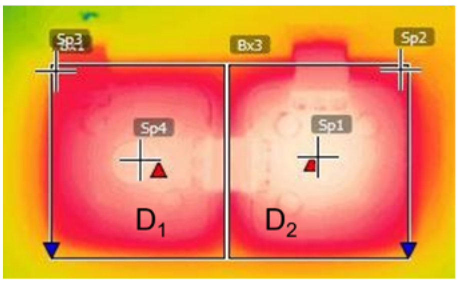

Bx3	Max	108,6 ° C
	Min	67,7 ° C
	Average	96,0 ° C
Sp1		107,7 ° C
Sp2		77,9 ° C
Bx1	Max	103,9 ° C
	Min	65,4 ° C
	Average	92,1 ° C
Sp3		75,6 ° C
Sp4		102,5 ° C

Figure 3: IR-evaluation of a thermal measurement

A comparison of the three methods for averaging - in-situ, area average and 2/3 approximation - results in slightly different numerical values. If the tolerances of the respective measuring techniques are considered, it turns out that the values usually only deviate slightly from each other in the range of ±1 K.

Figure 3 gives an insight into the data obtained using an IR camera from a measurement on two diodes connected in parallel within a semiconductor module.

The measuring points Sp_1 and Sp_4 in the middle of the diodes and Sp_2 and Sp_3 at their corners, which are clearly visible in Figure 3, are used for the 1/2 weighting. These measuring points were placed by hand, so there are also tolerances here. Based on the local values determined, the virtual chip temperatures for the diodes are:

$$T_{vj,D1} = \frac{1}{3}(2 \cdot T_{SP4} + T_{SP3}) = \frac{1}{3}(2 \cdot 102{,}5 + 75{,}6)°\text{C}=93{,}5°\text{C}$$
$$T_{vj,D2} = \frac{1}{3}(2 \cdot T_{SP1} + T_{SP2}) = \frac{1}{3}(2 \cdot 107{,}7 + 77{,}9)\ °\text{C}=97{,}8°\text{C}$$

The evaluation of the mean value over the entered areas Bx1 and Bx3 and the automatically displayed maxima and minima provide:

$$T_{vj,Bx1} = \frac{1}{3}(2 \cdot 103{,}9 + 65{,}4)°\text{C}=91°\text{C}, \quad \overline{T_{avg,cam}} = 92{,}1°\text{C}$$
$$T_{vj,Bx3} = \frac{1}{3}(2 \cdot 108{,}6 + 67{,}7)°\text{C}=95°\text{C}, \quad \overline{T_{avg,cam}} = 96°\text{C}$$

As a result, this means a temperature of 92.25±1.25°C for diode D1 and a temperature of 96.4±1.4°C for diode D2. Although in both cases neither the true maximum nor the true minimum was met, the deviation of the values finally determined is negligible.

What is the practical use and gain for developers? Determining the chip-temperature is crucial to support simulation results that are often starting points when predicting the lifetime of a system under development. Chip-temperature measurement during operation tends to be challenging. Thus, the recurring request is, to get a customized power device with a thermal sensor attached to the chip. Instead – and if chip-sizes allow to do so - placing two sensors will get a very accurate result of the chip-temperature, even under operating conditions. The very similar results all methods lead to also substantiate how robust the 1/2 averaging is when there is a setup with two thermocouples.

www.littelfuse.com

A High Voltage eFuse for automotive Applications

This article introduces the proof of concept for a new eFuse system, which achieves a short-circuit detection response time of below 160ns under the test conditions at 650A of short-circuit current in an 800V system.

By Thomas Langbauer, Team Leader Architectures & Topologies, Silicon Austria Labs; Thomas Feibel, Senior Research Engineer, Silicon Austria Labs; Zhen Huang, Junior Scientist, Silicon Austria Labs; Ichiro Okada, Lead Expert Magnetic Sensor Products, Asahi Kasei Microdevices Corporation; Takahisa Shikama, Manager Field Application Engineer, Asahi Kasei Microdevices Europe

In electric and hybrid vehicles, many fuses, such as conventional thermal fuses, are used for protection of systems such as onboard chargers, auxiliary systems, BMS, and junction boxes.

Fuses are well known and a common solution for system protection of electric machines, which are relatively robust against overcurrent. However, to protect SiC and GaN based power semiconductor devices used in onboard chargers against surge currents such as short-circuits that occur in the order of microseconds, both accuracy and response time of conventional fuses may not be sufficient. The new eFuse system, which detects these surge currents precisely within the order of nanoseconds and cut off the current, will be the key to protecting system in next-generation EVs.

The challenges with thermal fuse:

- There are several challenges to be considered to protect the system from overcurrent with fuses.
- Fuses can interrupt the current within the order of tens of milliseconds, and its fusing current is relatively inaccurate.
- A surge-like current, such as a short-circuit, may damage the device before the fuse blows.
- Once the fuse blows, the system cannot resume normal operation until the fuse is replaced.

EV systems are composed of various types of components relatively robust against overcurrent and power semiconductor devices that are susceptible to damage from surge current such as short-circuits.

Thermal fuses, which are still widely used today, interrupt the overcurrent by melting an internal conductor when the overcurrent occurs. However, due to their operating principle, melting fuses require from a few milliseconds to several tens of milliseconds from the occurrence of a surge current to cut off the current. Therefore, it is difficult to protect semiconductor power devices from damage caused by surge currents that occur in the order of microseconds, such as short-circuits. Also, to protect components other than power devices, it is necessary to consider and design for a margin as well, since the fusing current is subject to variations and temperature dependency.

Furthermore, once a fuse blows, the system cannot return to normal operation, so even temporary and rare surge currents, such as lightning or short-through current due to noise, etc., will not allow the system to resume until the fuse is replaced. A new protection system with semiconductor switches that solves the challenges of conventional fuses is preferable for the protection of next-generation EVs.

The solutions with eFuse system:

In this proof of concept, we developed a new eFuse system that solves the above issues of fuses.

- Fast and precise surge current detection.
- Accurate setting of current cut-off thresholds and response time to cut-off.
- Current interruption and recovery operation using semiconductor switches

The eFuse system is designed to handle different modes of operation, i.e., short-circuit and overcurrent, and generates current cutoff triggers in three circuits: short-circuit detection, dI/dt detection, and overcurrent protection (Figure 1). This circuit configurations allow better current turn-off controls for different operating modes, resulting in a more flexible protection system than fuses.

Fast and accurate current detection is necessary to protect SiC, GaN, and other semiconductor power devices against damage due to short-circuit currents and other causes. Here we adopted the CZ39xx series current sensor from Asahi Kasei Microdevices (Figure 1), which are ideal for this application. With its 4MHz bandwidth, less than 100ns of response time, and fast settling from switching noise make it suitable for this application. In addition, thanks to

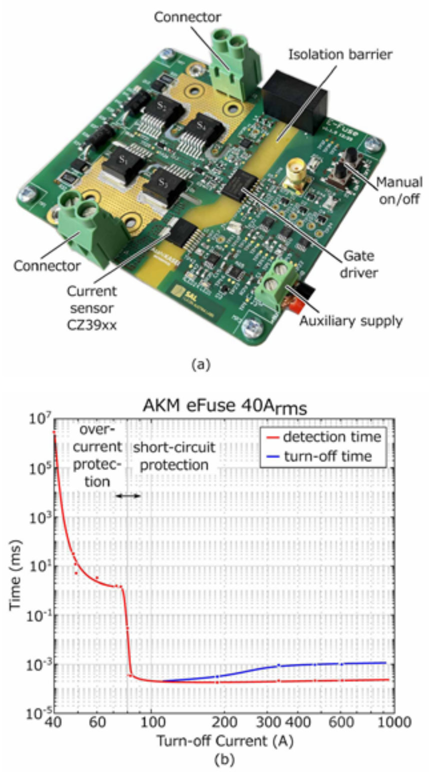

Figure 2: (a) Proof of concept board of eFuse system and (b) characteristic curve of eFuse system

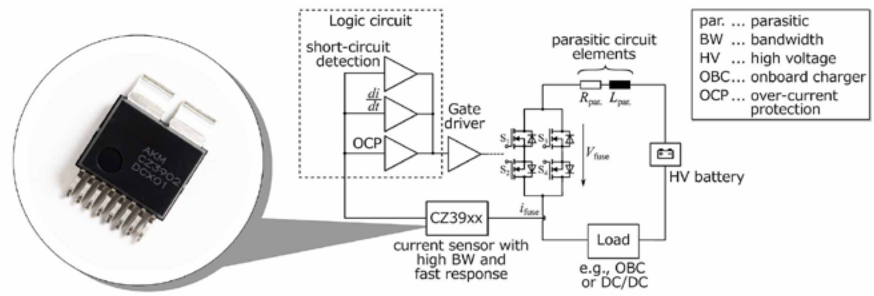

Figure 1: eFuse system diagram including the CZ39xx series current sensor

the III-V compound semiconductor Hall element technology, it is robust against strong magnetic field of over several hundred milli-Tesla.

These circuits employing the CZ39xx series current sensor, peripheral circuits including control logics, and semiconductor switches composed of SiC power devices are mounted on a single compact PCB.

This has resulted in eFuse, a protection device that can be resettable without replacing any components and has cut-off characteristics that match the cause of abnormal currents, such as short circuits or overcurrents.

Result of proof of concept:
Figure 2a shows an actual proof of concept board of the eFuse system. SiC FET is adopted for switching devices and the circuit is designed for 800V reinforced isolation and a short-circuit current up to 1kA. Figure 2b shows a characteristic curve of the eFuse system. The measurement results of response time from when the current exceeds the threshold to when the detection trigger occurs is plotted in red, and the response time to when the current is shutdown to 0A is plotted in blue. The eFuse system achieves a response time of less than 250ns for surge current of over 80A for short-circuit mode. On the other hand, response time for an overcurrent of less than 80A is designed slower than the response time for surge current detection to avoid unnecessary shutdown.

Figure 3 shows the measurement result of a short-circuit current detection. Focusing on the output voltage waveform of the current sensor, the response time from trigger point of overcurrent detection to the generation of current cutoff trigger is less than 160ns. As a result, the eFuse system achieves faster current detection and current interruption than was possible with conventional thermal fuses.

Conclusion
This newly developed proof of concept realizes a new eFuse system, which solves the challenges of conventional thermal fuse-only protection system. With a fast and accurate current detection solution, the eFuse system can provide the overcurrent protection which is needed for next-generation EV systems. Additionally, the current sensor employed in the eFuse not only supports its function but can also be effectively utilized for controlling the current in connected subsystems such as DC/DC or OBC converters.

www.akm.com

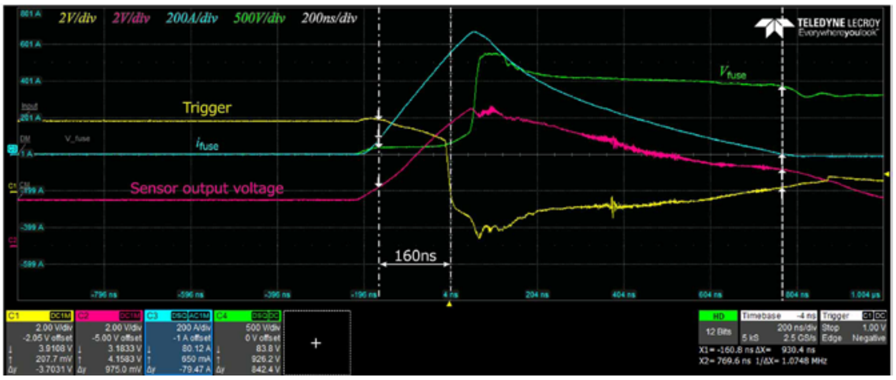

Figure 3: short-circuit protection measurement

Enabling Electrification of Aerospace with highly configurable and customizable integrated Actuation Solution

*Traditionally aircraft have been using hydraulic actuators to maneuver primary and secondary flight controls, landing gear, braking system, and deicing systems.
Electrification of aerospace sector is driving transition from hydraulic actuators to power electronics drive to reduce weight, complexity and maintenance requirements while improving reliability.*

By Amit Gole, Product Marketing Manager for integrated Power Solutions, Microchip Technology

Microchip has a strong legacy of providing standard as well as highly customized power electronics solutions in either silicon (Si) IGBT or silicon carbide (SiC) technology to reduce design cost, time, resources and complexity for aviation and defense customers.

Our new cost-effective, plug-and-play Integrated Actuation Power Solution combines a Hybrid Power Drive (HPD) and a compatible driver board that provides intelligence, scalability, design flexibility, reliability, faster time to market and high-power density for aircraft power system applications in More Electric Aircraft (MEA), cargo planes, small planes, defense avionics, electric Vertical Takeoff and Landing (eVTOL) aircraft, drones and multicopper.

Airplanes have several flight controls that help it to maneuver on land and in the air. An airplane rotates in bank, pitch, and yaw while also moving horizontally, vertically and laterally. The four fundamentals (straight-and-level flight, turns, climbs and descents) are the principal maneuvers that control the airplane through the six motions of flight. On land, the rudder is used to taxi the airplane left, right or straight. In the air, both primary flight controls and secondary flight controls are used. Primary flight controls consist of rudder to control the yaw, along the vertical axis, elevator to control the pitch up and down along the lateral axis, and aileron to control the bank or to turn the airplane along the longitudinal axis, which coordinate rudder and elevator as necessary.

Secondary slight controls consist of trim, flaps and spoiler. Trim control surfaces are required to offset any constant flight control pressure inputs provided by the pilot. Pitching moments may also be generated by extension and retraction of flaps, landing gear and other drag producing devices, such as spoilers. Primary flight controls are a must and hence the name while secondary flight controls help to enhance the motion of the airplane in the air with finer control.

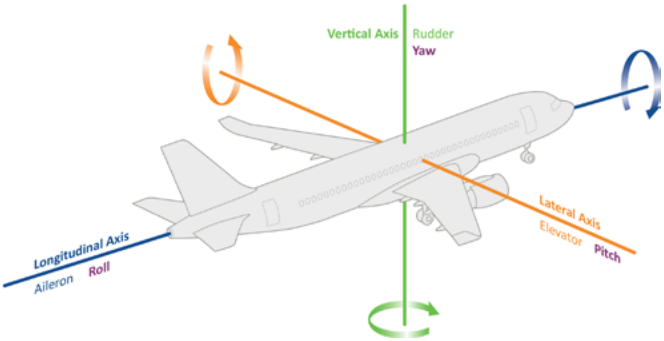

Figure 1: Primary Flight controls from FAA Airplane Flying Handbook

In addition, there are many other tasks that are performed by the actuator namely deicing, landing gear operation, power door opening and deicing.

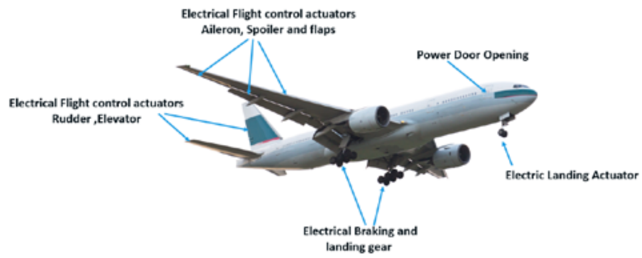

Figure 2: Airplane Actuation Applications

The flight controls get active as the plane gains speed in the air and encounters a large amount of force. To move these surfaces, pneumatic actuators were used in the early 20th century. Around the 1930s, aircraft started using hydraulic actuators. These hydraulic actuators consist of centralized hydraulic reservoir, filters, pumps and incompressible liquid to move the actuators with aircraft engine directly driving the hydraulic pumps. These actuators eventually moved to electro-hydraulic actuators that maintained the centralized hydraulic fluid reservoir, while electric motor being used to drive the centralized hydraulic pumps. Most of the old generation aircraft in service use this technology. The key issue with this central hydraulic system is maintenance, plumbing, frequence changes in filters, higher weight, bulkier systems and higher energy consumption.

With the invention of actuation technology there is a transition from traditional hydraulic systems (EH) to Electrohydraostatic actuators (EHA), Electrical back up hydraulic actuators (EBHA) and Electromechanical Actuators (EMA) with the end goal to replace the central hydraulic system with Fly by Wire (FBW) to reduce system weight, power consumption, complexity and maintenance all while improving reliability.

Electro hydrostatic actuation (EHA): Electro hydrostatic actuation (EHA) system eliminates the need for central hydraulic systems These systems use electric power for aircraft flight control-surface actuation that results in reduced aircraft weight, efficient power consumption, and improved maintainability.

EHA systems are power-by-wire actuation systems that utilize aircraft electric power for flight control surface actuation. These systems are highly energy efficient and provide an overall weight benefit to the aircraft. EHA technology is power-on-demand actuation that results in reduced overall aircraft power consumption. EHAs result in improved maintainability since there are no hydraulic connections between actuation equipment and the vehicle system. EHAs consist of a fixed displacement, high speed, reversible pump driven by a brushless DC electric motor. Actuator position is controlled by the pump rotation direction and actuator piston velocity is controlled by pump rotational speed. The actuator output force is a function of the electric motor output torque.

Electrical backup hydraulic actuation (EBHAs): EBHA system is like that of EHA Systems. However, it is generally used to provide back up for the central hydraulic systems and has similar advantages as those of EHA.

Electromechanical actuation (EMAs): EMA systems are power by wire system that eliminates the need for central hydraulic systems, as well as any sort of hydraulic elements because of its use of mechanical actuators. Electric motor is dedicated and located at each mechanical actuator on the aircraft. These type of actuators remove the use of pumps and instead use mechanical gearbox or similar arrangement powered by an electric motor. This mechanical gearbox drives rotary to liner conversion to move the flight controls.

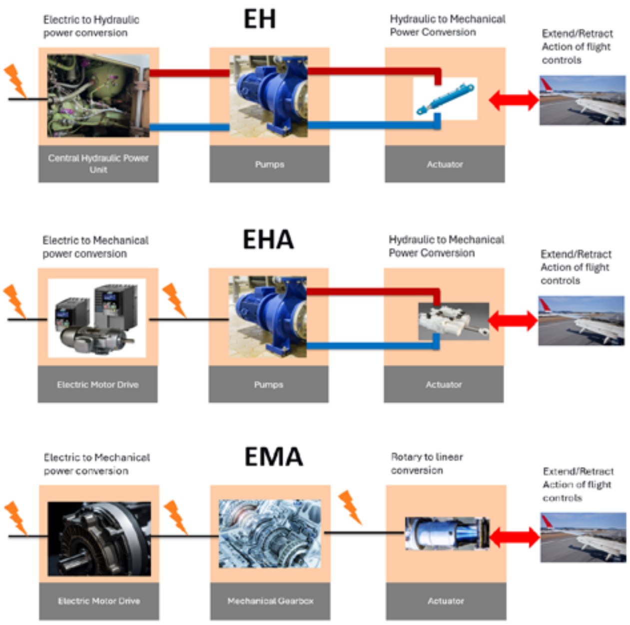

Figure 3: Types of Actuators, Transition to EHA and EMA is the first step in decarbonization

The key benefit of this transition from centralized hydraulics systems to EHA/EBHA and EMA includes but is not limited to significant weight savings, increased performance, enhanced safety due to improved reliability in demanding conditions, reduced maintenance cost and lower operating life cycle costs. All these factors together reduce the carbon footprints of the airplane. The bigger the airplane the more significant the benefits. This transition needs rugged, reliable, cost efficient, compact power electronics drive to run the motors that in turn drive the actuators.

As aircraft evolve to More Electric Aircraft (MEA) and eventually to fully electric aircraft, actuation systems will be one of the first systems that is likely to get electrified. This gives us the opportunity to provide solutions for applications including but not limited to commercial, cargo and smaller training aircraft, in addition to the defense sector, eVTOL, drones and multi-copters.

Figure 4 shows an example of More Electric Aircraft (MEA) that will need power electronics solutions for 24 flight controls, 5 landing gear, 10 fuels pumps and 8 doors. This demonstrates the need for power solutions that enable the change towards decarbonization.

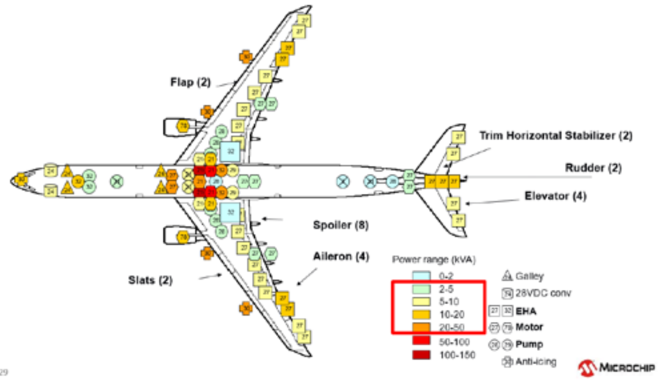

Figure 4: Opportunities in MEA

There are multiple growth drivers that enable the demand for actuation electrification:

- Electrification of commercial and cargo airplanes
- Growth in passenger traffic
- Fleet modernization
- Electrification of military and defense airplanes
- Fully electric/H2/hybrid smaller aircraft
- Electric VTOL (EVTOL) use for public and cargo transfer
- Drones and multi-copter usage for service and agriculture

Figure 5: Market segments and growth drivers

Some of the key forecasts and analyses from the commercial aviation market reinforce the potential for an expanding electric actuation market.

Fleet modernization: Airlines will require the latest, most efficient and lowest-emission aircraft. As of the year 2022, only 25% of the commercial fleet has been electrified.

Passenger Traffic: Passenger traffic is expected to grow at 3.6% from 2019 to 2041 and will increase the number of aircraft to satisfy this demand.

New generation planes: By 2041, the new generation of airplanes will represent more than 95% of the fleet. Since these planes will use electrical actuation instead of hydraulic, the demand is likely to be higher. When compared to 2021, only 20% of the fleet represented new planes.

In summary, there is a demand of more than 40,000 new airplanes considering both growth (>23,000) and replacement (> 17,000) by 2042.

To enable this transition, the capability to integrate different power electronic components for functions like motion of power control but also to provide configurability, standardization, modularity, and reliability to meet the aerospace standards.

Power Module

The actuator generates a translational motion in the forward and reverse direction, which gets converted into rotational motion for flight controls. To replace the traditional hydraulic system with power electronics, we need to have several capabilities. Depending on the nature of flight control, the configurations could be mandatory or optional.

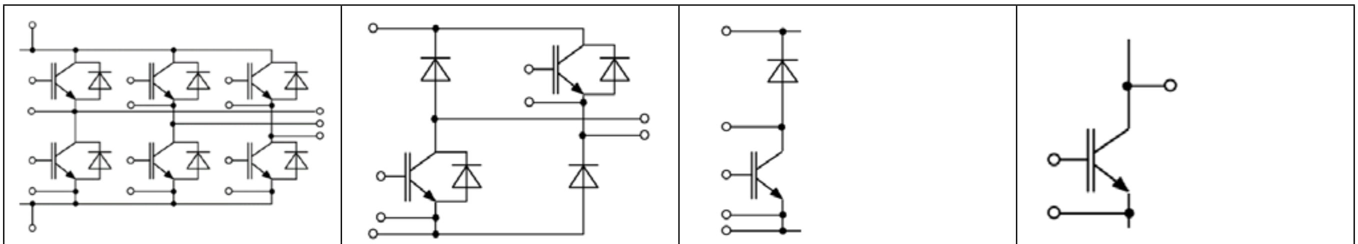

1. Motor drive to control the rotational motion of flight control.

2. Solenoid drive to hold the flight control at desired position. This featured is important for flight controls that are needed to be hold such as Flaps.

3. Brake chopper to limit DC bus voltage due to regeneration from motor, allowing energy to freewheel via external braking resistor.

4. Soft starter to control the inrush current at the start of the motor; this is achieved by soft start switch

Figure 6: Integration of multiple topologies in one compact power module

The power range of the typical actuator ranges up to 25 kW for operating pressure of 5000 Psig with stroke length of 10 inches. These ratings vary depending on the applications but provide a very generic rating that is commonplace in the aviation industry. The DC link voltages are primarily 270V and 540V. The electric motor switching frequency varies between ~2 to 10KHZ. Due to the higher voltage involved it is important to have fully isolated module with enhanced thermal capabilities to provide low power loss and high efficiency to enable smaller weight and footprints. It is essential to have 650V to 700V power modules for 270V DC link and 1200V for 540V with the ability to provide derivatives up to 1700V, if required.

Both Hybrid SiC (IGBT + SiC D) and SiC are recommended to provide optionality to the customer. For relatively high frequency, full SiC, including SiC MOSFETs and Schottky diodes, helps to reduce switching losses while hybrid SiC balances the benefits versus cost when the Fsw is relatively lower. The low junction to case thermal resistance and Silicon Nitride (Si3N4) substrate improves the thermal performance of the module. Use of Aluminum-Silicon Carbide (AlSiC) baseplate further reduces the weight while extending the reliability of the solution. This results in high-power density, which helps to shrink the size and weight of the solution, thereby allowing greater power density in the given area. This is a critical differentiator in aerospace applications. Lower thermal losses reduce the cooling requirements and improve the overall efficiency of the converter, impacting the power consumption positively.

The Integrated Actuation Power Modules need to have very low package inductance. The rate of change of current (di/dt) could be substantially higher due to high switching frequency (Fsw). This high di/dt with higher stray inductance results in higher overall inductance and higher voltage overshoot during the switch turn-off. [V overshoot = V & L di/dt]. Having lower overshoot improves the ruggedness of the power module.

It is also important to have temperature monitoring that can be easily implemented to control temperature conditions and improve protection. Monitoring of DC bus, Inverter, and solenoid current with feedback to control circuity enhances durability of the power module.

Test	Conditions
High Temperature Cycle	DO-160G, Section 4, Cat. D2 (100 °C)
Low Temperature Cycle	DO-160G, Section 4, Cat. D2 (-55 °C)
Cold Temperature Start-Up	10 starts, -55 °C
Temperature Variation	DO-160G, Section 5, Cat. A (>10 °C/minute)
Altitude	DO-160G, Section 4, Cat. D2 (Underpressurized area) (50,000 feet)
Humidity	DO-160G, Section 6, Cat. C (55 °C, 95% RH)
Operational Vibration	DO-160G, Section 8, Cat. R, Curve E1 (11g)
Operational Shock and Crash Safety	DO-160G, Section 7, Cat. D (20g, 11ms, saw-tooth)

Figure 7: Qualification test plan

To comply with the high standards of aviation, qualification as per DO-160G for flight conditions like Low/High temperature cycling, cold start up, altitude of 50,000 feet, cold temperature -55 Deg C, humidity, shock s and vibrations), highly accelerated life testing (HALT), RoHS, partial discharge test and AS9100 adherence are key.

Fully integrated actuation solution

While most of the customers can design their own driving circuitry compatible with power module, having fully integrated solution for actuations provides an all- in-one solution minimizing the design efforts, cost associated with projects, accelerates time-to- market, complexity and lack of flexibility associated with system designing for MEA actuation.

The gate driver board should provide the PWM signal to the power module based on the inputs from higher level system. This may include all the switches of the inverter, solenoid drive, soft starter and brake switch. Apart from providing the gate signals, the driver should be able to provide isolation and continuous monitoring of following parameters and provides output to LVDS:

- DC link bus voltage
- DC link bus current
- Phase current output of inverter
- Solenoid current
- Temperature of power module

The driver board should have the voltage across the shunts in power module and provide current measurement signals as isolated differential output for phase current, bus current and solenoid current. The driver board should also measure the DC link bus voltage and provide an isolated differential voltage output.

In normal operation, the driver board would receive PWM switching signal inputs from a higher–level system and provides the gate–drive signals to the power module to control the functioning of three-phase inverter bridge switch, solenoid switch, soft–start switch and brake switch.

Microchip's Integrated Actuation Solution

Microchip's cost-effective, plug-and-play Integrated Actuation Power Solution combines a Hybrid Power Drive (HPD) and a compatible driver board that provides intelligence, scalability, design flexibility, reliability, faster time-to-market and high-power density for aircraft power system applications in MEA, cargo planes, small planes, defense avionics, electric Vertical Takeoff and Landing (eVTOL) aircraft, drones and multicopper. The HPD modules range from 5 kVA to 20 kVA and have the same footprint. These modules include a three-phase inverter with temperature and output current measurements and options for a brake chopper, solenoid drive and soft starter. They can be configured with

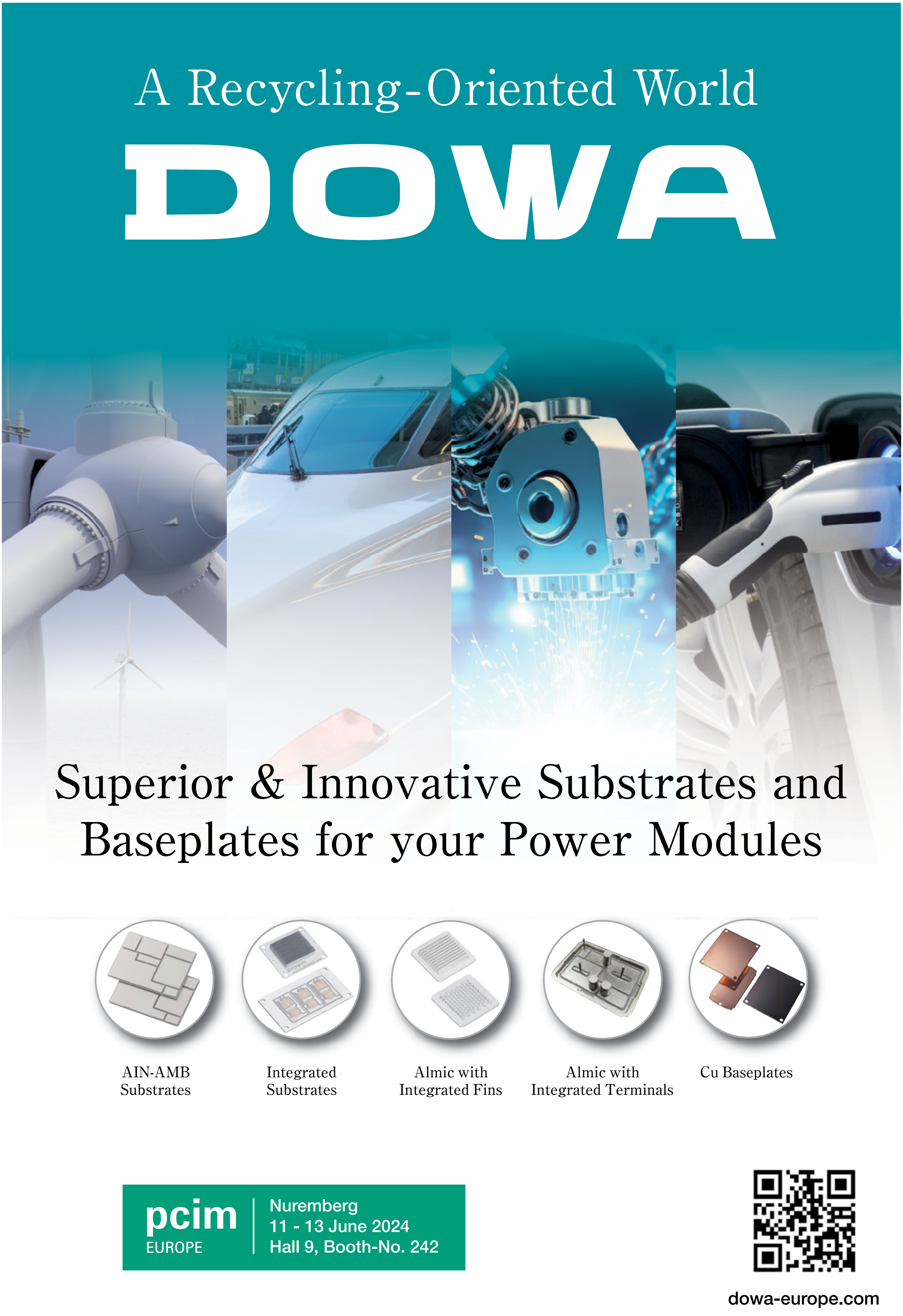
A Recycling-Oriented World
DOWA
Superior & Innovative Substrates and Baseplates for your Power Modules
AlN-AMB Substrates
Integrated Substrates
Almic with Integrated Fins
Almic with Integrated Terminals
Cu Baseplates
pcim EUROPE
Nuremberg
11 - 13 June 2024
Hall 9, Booth-No. 242
dowa-europe.com

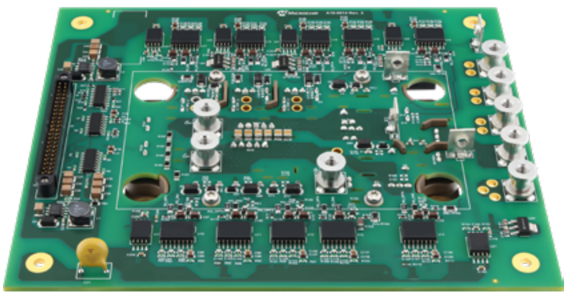

Companion Driver Board
Compatible to with Microchip SP6HPD power module
- SP6HPD soldered directly on the driver board
- Direct temperature sensor output (from SP6HPD)
- Environmental Ruggedness
- Maximum 110 °C. Altitudes up to 50,000 feet
- RoHS compliant. Conformal coating
- Galvanically Isolated
- Partial discharge across isolation barrier
- Single power supply (VCC): +15V (typ.)
- UVLO on input VCC and internal bias supply
- LVDS control inputs from higher level system
- Differential outputs for current and voltage telemetry
- Protections: DESAT, Soft turn-off, Active Miller Clamping and Shoot through

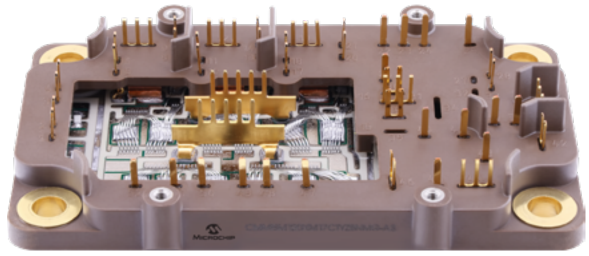

Power SP6HPD Module
- Efficient Power semiconductors (Si IGBT / mSiC™)
- Low weight / Low profile / Low-Inductance
- High thermal performance (Si3N4)
- Wider Temperature range (-55°C)
- Easy mounting
- RoHS Compliant
- Designed to meet DO-160
- AS9100 and Custom Versions Features

Integrated Actuation Solution

Figure 8: Integrated Actuation Power Solution

Silicon (Si) or Silicon Carbide (SiC) switches. The isolated gate driver board can manage the intricacies of driving MOSFETs and Insulated-Gate Bipolar Transistors (IGBTs) at a higher switching frequency. The press-fit connector enables the board to be attached easily to the top of the HPD module in accordance with DO-160 and AS9100 standards for the aerospace industry. You can also order an HPD module and a driver PCB assembly separately for design freedom and adaptability.

Key Benefits of Microchip's Integrated Actuation Power Solution
- High level of integration and flexibility -Includes inverter, brake chopper, solenoid drive, soft starter, thermal sensors, telemetry outputs and gate driver board
- Modular and adaptable SiC/IGBT solution with nominal DC link up to 540 VDC and power rating up to 20 kVA
- Isolated gate drive board with shoot-through detection, multiple protections and high-speed Low-Voltage Differential Signaling (LVDS)

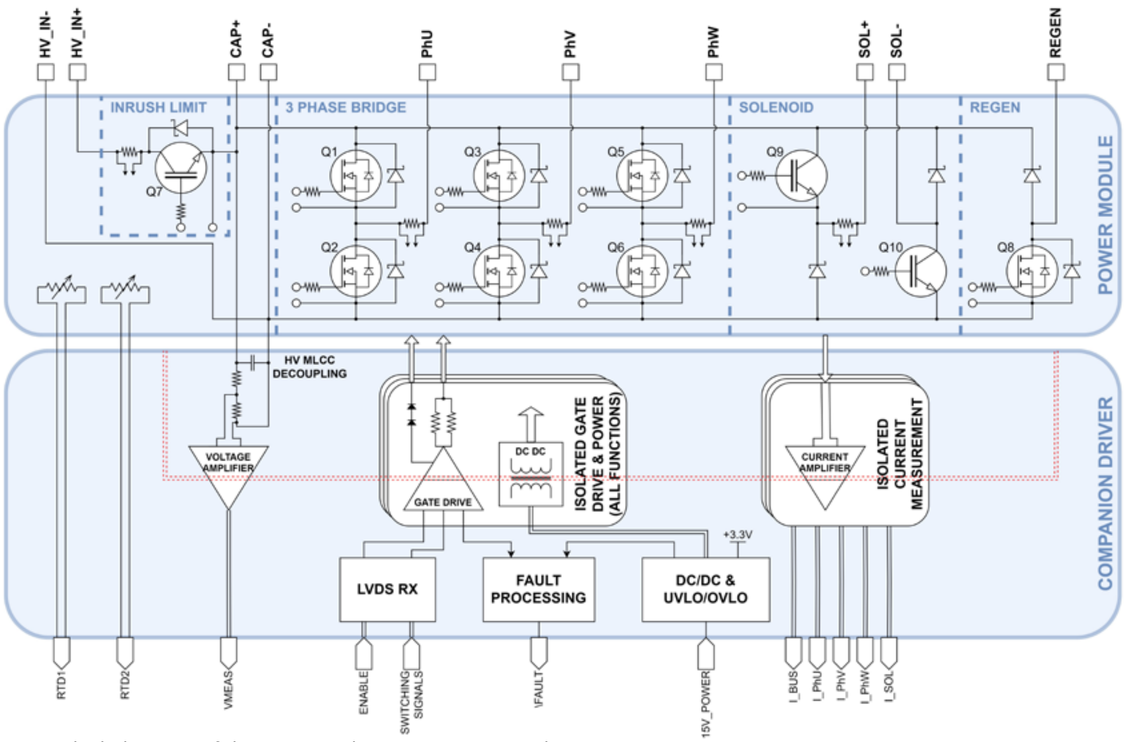

Figure 9: Block diagram of the Integrated Actuation Power Solution

- Cost-effective, high-reliability and rugged solution
- High power density with reduced weight, smaller footprint, optimized design, and efficient semiconductors
- Faster time to market -Easy-to-use modular design with integrated functionality reduces the number of components and testing requirements
- Flight-proven standard and custom solutions available up to 1700 V

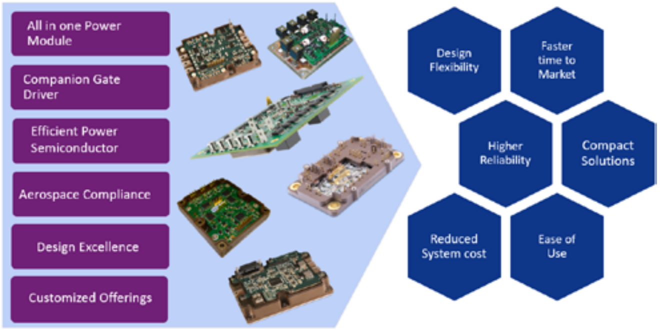

Figure 10: Value proposition of Integrated Actuation solutions

References:
- Airplane Flying Handbook, FAA
- Electro Hydrostatic Actuation: An attractive Energy-Efficient option for Machine Builders. Achim Helbig, Ph.D, Moog, Innovation Projects Manager 2014
- Primary Fixed-Wing Actuation Systems Collins aerospace collinsaerospace.com
- Electro hydrostatic Actuation Parker.com
- Airbus Global Market Forecast, https://www.airbus.com/sites/g/files/jlcbta136/files/2023-06/GMF%202023-2042%20Presentation_0.pdf

www.microchip.com

Accurate and reliable Junction Temperature Measurements with Fiber Optic Sensors

Obviously, junction temperature (Tj) is a critical parameter for determining the power cycling capability of power semiconductor devices. It is actually essential for thermal characteristics extraction of IGBT, elaboration of lifetime laws and study of stability of power dies.

The new generation of fiber optical temperature sensors enables more reliable direct measurement of this critical parameters to improve ageing and failure modes analysis of power modules. They can also predict module end of life with embedded instrumentation and enable preventive maintenance over corrective actions through condition monitoring.

By Charles Leduc, Sales and Marketing VP, Opsens Solutions

Power cycling and Mission profiling

Accurate Junction Temperature is critical and essential for thermal characteristics extraction of IGBT, elaboration of lifetime laws and study of stability of power dies. Ageing and failure modes of power modules have been elaborated through these processes. These measurements are usually done in controlled conditions over relatively short period of time. Sensors are rarely fixed permanently to the die or the wire, allowing reuse.

Advantages of fiber optic sensors

- Outstanding repeatability and consistency of measurements
- Sensor could be packaged for module with and without gel
- Small rigid head could be placed precisely
- No risk to technicians (no energy to be transferred)
- Response time in ms range

Figure 1: Sensor deployed on die through silicon gel (Courtesy of Aalborg University)

Reference

[1] Z. Wang, B. Tian, W. Qiao and L. Qu, "Real-Time Aging Monitoring for IGBT Modules Using Case Temperature," in IEEE Transactions on Industrial Electronics, vol. 63, no. 2, pp. 1168-1178, Feb. 2016, doi: 10.1109/TIE.2015.2497665.

Condition Monitoring

Active monitoring has the objective to predict potential problems on power modules hard to reach or integrated in critical systems such as offshore power generator, subsea environment, high power density multichip modules, critical infrastructures (high speed train) …

Real-Time Aging Monitoring for IGBT Modules Using Case Temperature:

Wind turbines usually operate in remote, harsh environments and are subject to various subsystem failures. It was reported that the IGBT module is a top ranked subsystem contributing to the overall failure rate and downtime of wind turbines. Owing to a rising concern over the long-term reliability of wind turbines, there have been significant interests in developing online health monitoring technologies for major wind turbine subsystems. Therefore, to ensure the safe operation and reduce the maintenance cost via condition-based maintenance for wind turbines, it is critical to monitor online the aging of the IGBTs used in wind turbine power converters [1]

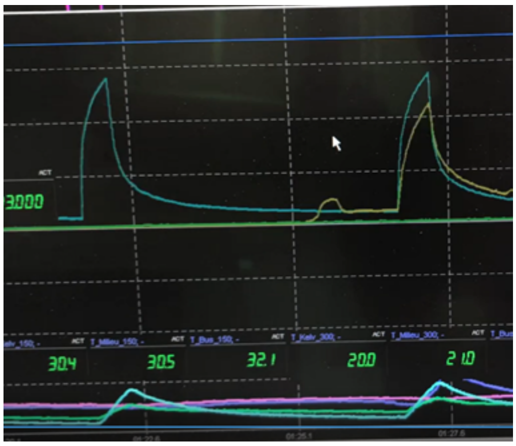

Figure 2: Sharp temperature variations during power cycling (Courtesy of Gustav Eiffel University)

Optical sensors are the perfect tool to predict aging based on temperature:

- They do not require any maintenance/calibration after installation
- Installation of sensor do not require any modification of the industrial converter design and package
- Power module can operate at full power and full voltage (representing real operating conditions) after instrumentation.

https://opsens-solutions.com

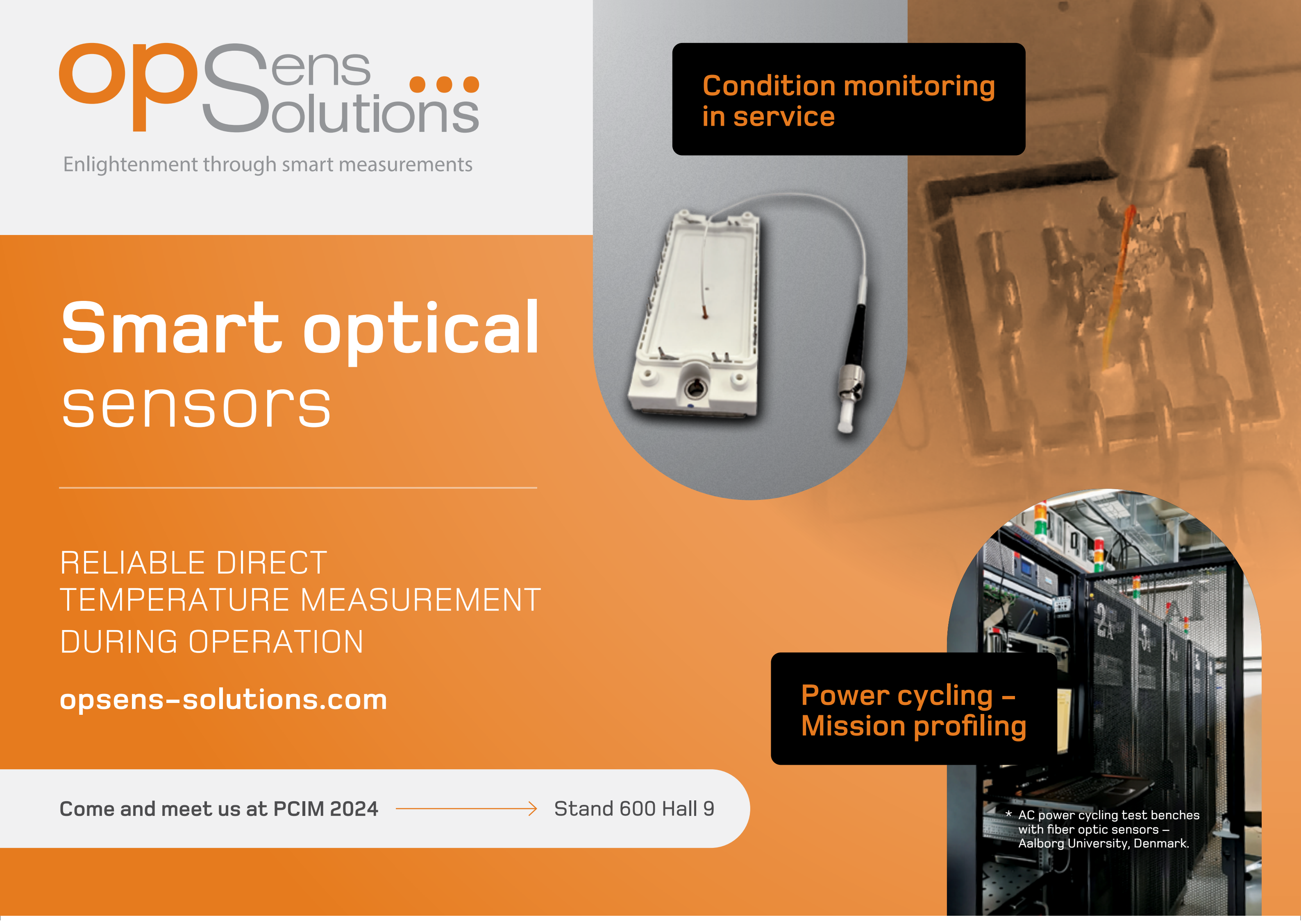
opSens Solutions
Enlightenment through smart measurements
Condition monitoring in service
Smart optical sensors
RELIABLE DIRECT TEMPERATURE MEASUREMENT DURING OPERATION
opsens-solutions.com
Power cycling – Mission profiling
Come and meet us at PCIM 2024
Stand 600 Hall 9
* AC power cycling test benches with fiber optic sensors – Aalborg University, Denmark.

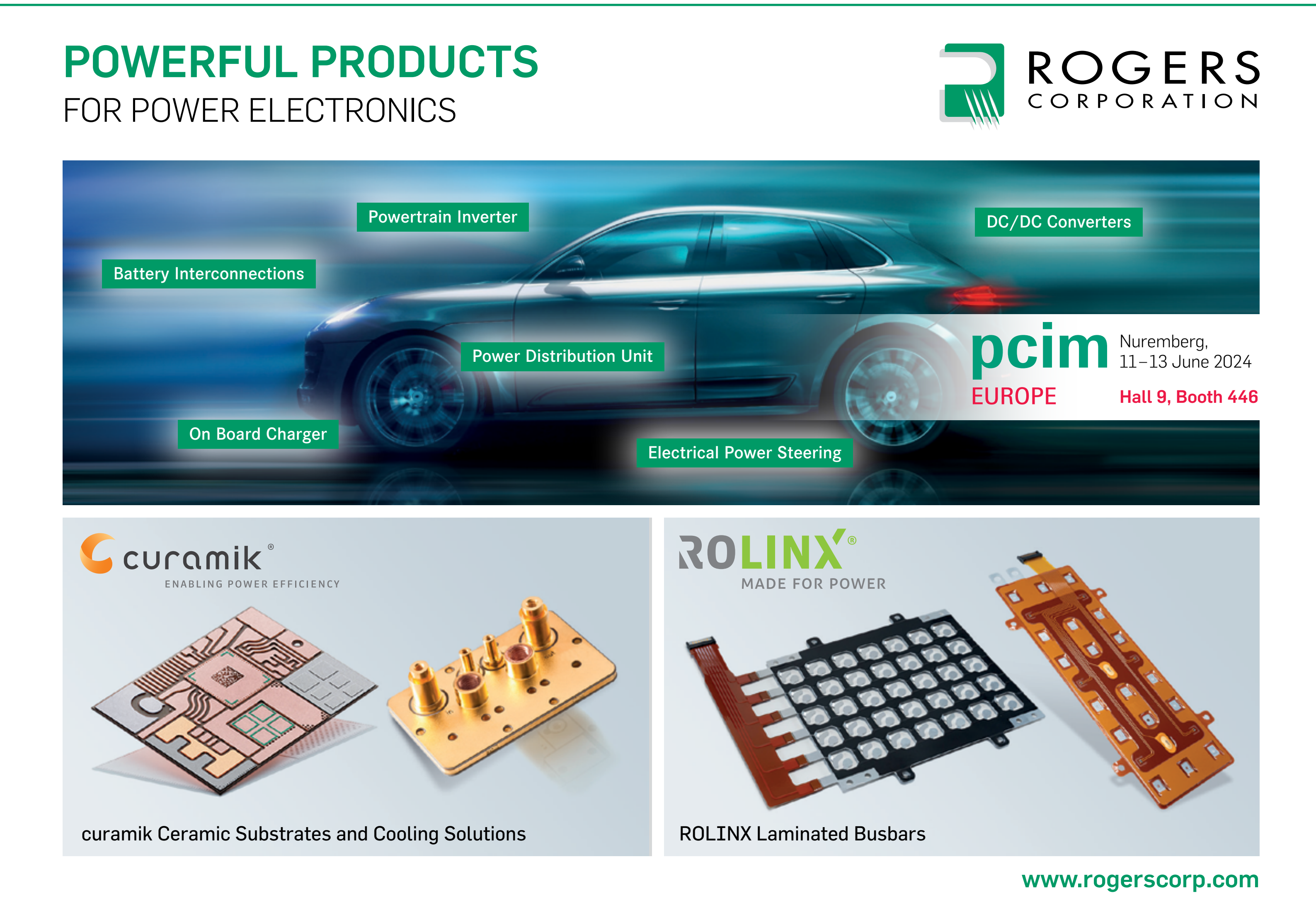
POWERFUL PRODUCTS
FOR POWER ELECTRONICS
ROGERS CORPORATION
Powertrain Inverter
DC/DC Converters
Battery Interconnections
Power Distribution Unit
On Board Charger
Electrical Power Steering
pcim EUROPE
Nuremberg, 11–13 June 2024
Hall 9, Booth 446
curamik
ENABLING POWER EFFICIENCY
curamik Ceramic Substrates and Cooling Solutions
ROLINX
MADE FOR POWER
ROLINX Laminated Busbars
www.rogerscorp.com

Engineered Substrates with ultra-low resistivity Polycrystalline SiC Base

Game Changers in SiC Power Device Performance and Reliability

Since the introduction of the first commercial single-crystal SiC wafers in the early 1990's, no change has been made to their composition, only changing their diameter and reducing their defectivity over time. SmartSiC™ is an engineered substrate based on a new paradigm, combining on a single substrate a high-quality top layer made of single-crystal SiC bonded over a highly-electrically conductive polycrystalline SiC handle wafer. This allows for unprecedented gains in terms of device performance and reliability.

By G. Picun, WBG Business Development Manager, SOITEC; Dr. L. Zumbo, R&D Staff Engineer, STMicroelectronics; Dr. E. Guiot, WBG Product Design Manager, SOITEC; G. Bellocchi, R&D Staff Engineer, STMicroelectronics; A. Guarnera, SiC Power Devices Design Group Manager, STMicroelectronics; S. Rascunà, Advanced Research Senior Manager, STMicroelectronics; A. Imbruglia, Funded Projects Advanced Design Program Manager & Expert, STMicroelectronics; G. Arena, Sr. Director of R&D Technology Development, STMicroelectronics; M. Saggio, R&D Design Director, STMicroelectronics

Introduction

Silicon Carbide (SiC) technology in power electronics is playing a crucial role in driving the transition towards electric mobility and enhancing the efficiency of renewable energy systems. With the increasing demand in the market, power semiconductor companies are under pressure to rapidly scale up their production capacity. Despite significant enhancements in the quality and availability of 4H-SiC material, the challenge of producing low defect density and high performance SiC wafers for optimal yields still persists.

In response to this pressing need, a groundbreaking SiC engineered substrate (called SmartSiC™) has been introduced to address the industry's requirements. The unveiling of a dedicated manufacturing line in September 2023 marks a significant milestone, signaling the start of high-volume manufacturing for this innovative SiC substrate. This strategic initiative is poised to revolutionize the landscape of SiC technology, offering a breakthrough solution to the current manufacturing constraints and paving the way for enhanced efficiency and performance in power electronics applications.

The fabrication of the SmartSiC™ substrates relies on the Smart Cut™ technology and offers significant advantages in the fabrication of SiC devices. Here's a breakdown of its key features and benefits:

- High-Quality SiC Top Layer: The Smart Cut™ technology facilitates the transfer of a high-quality SiC layer on top of a handle wafer, serving as seed for the drift epitaxy to be grown. This process is crucial for optimizing device yield and reliability, ensuring that the resulting devices meet stringent quality standards.
- Low Resistivity Handle Wafer: The technology incorporates a low resistivity handle wafer with a typical resistivity of 2mOhm.cm (standard SiC material resistivity is around 20mOhm.cm) [1]. This feature is essential to enhance device conduction, while also enabling the minimization of switching losses, ultimately improving the overall performance of applications based on SiC devices.
- Compatibility with Different Wafer Diameters: The Smart Cut™ technology is compatible with any substrate diameter and currently being used for both 150mm and 200mm wafers.

Based on the characteristics described here above, the obtained SmartSiC™ Engineered Substrate consists of a sub-micron thickness (between 400 and 800nm) high-quality, single crystal 4H-SiC top layer bonded on top of a polycrystalline SiC handle wafer. The final engineered substrate has a thickness of 350µm for 150mm wafers, and 500µm for 200mm wafers. This composition ensures the structural integrity and performance of the substrate, contributing to the reliability and efficiency of SiC devices.

Additionally, by enabling the reusability of initial single crystal donor wafers due to the low thickness of the top single crystal layer, the SmartSiC™ technology offers the most efficient usage of hard to obtain SiC boules. Compared to conventional wafering processing of SiC material, which typically allows the extraction of a maximum of 50 wafers per boule, the Smart Cut™ technology allows for the preparation of up to 500 engineered substrates from the same boule. This substantial increase in productivity represents a significant cost-saving and resource-efficient solution for SiC device fabrication.

The Smart Cut™ process applied to the manufacturing of SmartSiC™ engineered substrates is shown in Figure 1.

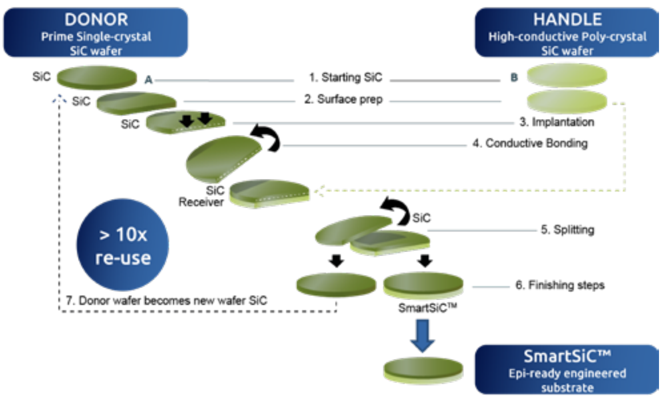

Figure 1: Smart Cut™ technology adapted to silicon carbide

Description of devices used as test vehicles

To investigate the advantages of SmartSiC™ engineered substrates versus standard single-crystal 4H-SiC wafers, n-type, 13mOhm / 650V Gen2 planar SiC MOSFETs were manufactured on both types of substrates and processed simultaneously as a single batch.

The single-crystal, 4H-SiC wafer, considered as the reference, is Nitrogen-doped with a typical resistivity of 20mOhm.cm, whereas the poly-SiC handle wafer of the SmartSiC™ substrate has a higher Nitrogen-doping and a typical resistivity of 2mOhm.cm. The drift epitaxy is Nitrogen doped, with a doping concentration $N_D \approx 2x10^{16}cm^{-3}$. Phosphorus and aluminum implantations were used to form respectively source and body regions. The gate oxide was a 55nm thick SiO_2 layer, while highly doped n-type poly-Si was used as gate electrode. The structures of the test vehicle MOSFET on the standard single-crystal SiC wafer and on the SmartSiC™ substrate are shown in Figure 2.

Results and Discussion

The results obtained on the 13mOhm 650V Gen2 planar SiC MOSFETs are presented and discussed in this section.

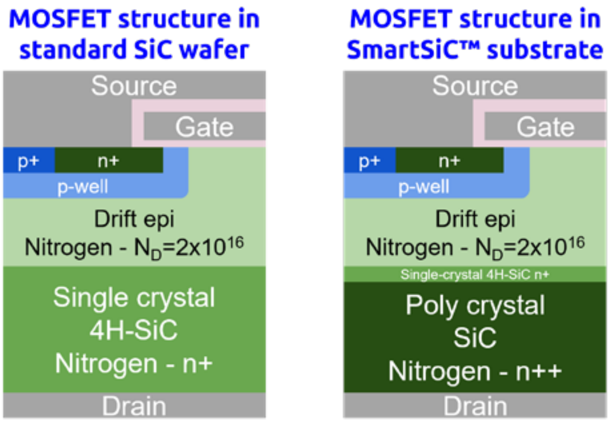

Figure 2: Structure of the Gen 2 planar SiC MOSFET used as test vehicle as implemented on single-crystal 4H-SiC wafer (left) and on SmartSiC™ substrate (right).

The comparison of device's R_{DSon} is presented in Figure 3. Results show an average reduction of the on-resistance of around 24% favorable to the SmartSiC™ substrates. This improvement is due to the much lower resistivity of the poly-SiC handle wafer of SmartSiC™ substrates, as well as its capacity to make much lower resistivity metal contacts (back-side drain contact in this case).

Such a strong reduction of R_{DSon} (~24%) is close to what it can be expected during the transition from a given device generation to the next one.

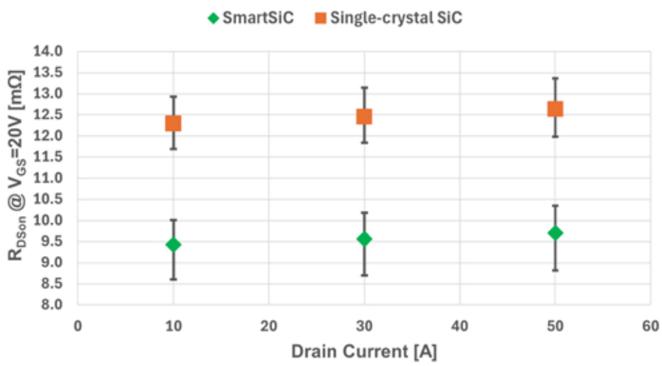

Figure 3: R_{on} comparison for a 13mOhm / 650V Gen2 SiC MOSFET manufactured in single-crystal SiC and SmartSiC™ substrates.

Threshold voltage and drain leakage current for the same device manufactured in single-crystal SiC wafer and SmartSiC™ substrate are respectively presented in Figure 4 and Figure 5. The results show an equivalent behavior on these parameters for both types of substrates.

Figure 4: V_{th} comparison for a 13mOhm / 650V Gen2 SiC MOSFET manufactured in single-crystal SiC and SmartSiC™ substrates.

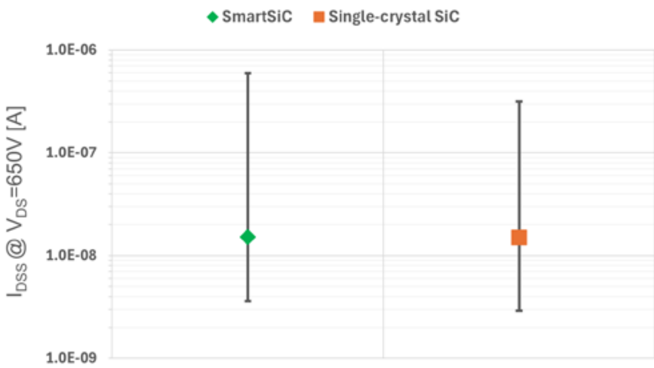

Figure 5: I_{DSS} comparison for a 13mOhm / 650V Gen2 SiC MOSFET manufactured in single-crystal SiC and SmartSiC™ substrates

Perspectives of SmartSiC™ potential for other devices

As shown in the previous sections, in contrast to standard single-crystal SiC substrates with an electrical resistivity of around 20mOhm.cm, polycrystalline SiC material can achieve resistivity levels as low as 1mOhm.cm, with a typical value around 2mOhm.cm [1]. Additionally, the high doping level of polycrystalline SiC contributes to lowering the contact resistance well below 10µOhm.cm² [2]. These characteristics enable SmartSiC™ substrates to increase the device's current density, thus allowing the reduction of the device die size, for both MOSFETs and diodes.

In particular for FETs, although the total gain is dependent on the initial device specific resistance (Ron.A) and die thickness, Figure 6 shows that the more advanced the FET technology, the higher the gain obtained. By initial Ron.A we mean that of the device when manufactured on a single-crystal SiC wafer. As an example, for a FET with an initial Ron.A of 2.8mOhm.cm² and a die thickness of 180µm, figure 5 shows that when manufactured on SmartSiC™ substrates, the new Ron.A is 15% lower (a gain of 15%). Notice that this gain is independent of the device's voltage rating.

The value of 2.8mOhm.cm² taken in the previous paragraph corresponds to the current state-of-the-art case of a 1200V SiC MOSFETs [3]. However, when looking at the device generations to come in the next years, Ron.A gains (reductions) in excess 20% can be expected, always presenting the advantage of "at least" one additional generation when using SmartSiC™ engineered substrates.

An extreme gain case takes place today with state-of-the-art JFETs, the preferred choice for 400V and 800V solid-state circuit breakers (SSCB) for electrical vehicles (EV). Taking as an example a 750V SiC JFET with an initial Ron.A of around 0.7mOhm.cm² [4], gains of around 30% can be expected.

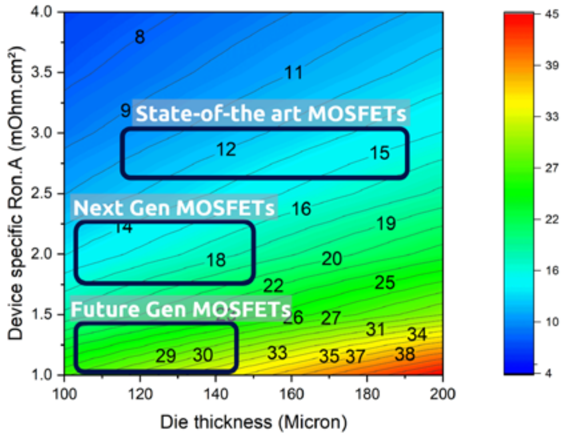

Figure 6: Ron.A reduction enabled by SmartSiC™ use for 1200V SiC MOSFETs as a function of the initial Ron.A and die thickness.

Last but not least, SmartSiC™ engineered substrates show at first analysis, to be further confirmed with specific electrical evaluation, a valuable ruggedness against bipolar degradation. This degradation phenomenon appears on SiC substrates due to the gliding (extension) of basal plane dislocations (BPD) within the SiC crystal when exposed to high levels of bipolar current (due to electrons and holes simultaneously). This takes place generally during the reverse conduction of SiC MOSFETs, when current goes through the PiN-type body diode of the transistor.

To validate such ruggedness, epitaxied standard single-crystal SiC wafers as well as SmartSiC™ substrates were exposed to stress conditions aimed at revealing bipolar degradation. this was carried out by using the E-V-C technique developed by ITES, Co. (Japan) [5]. After stress, it appears that both the number of Shockley staking faults (SSF), the indicator that bipolar degradation takes place, and their typical size are lower in the case of SmartSiC™, compared to the results obtained in standard SiC wafers. The results suggest that the SmartSiC™ design possesses an inherent ruggedness advantage against bipolar degradation over single-crystal wafers. This characteristic was previously evaluated through a forward-current stress test conducted on a 4H-SiC epitaxial layer subjected to proton irradiation [6].

Conclusions

Under the current context of accelerating the deployment of SiC devices for the decarbonization of the mobility and power conversion industry, SmartSiC™ offers unmatched characteristics allowing for higher power density and more reliable applications.

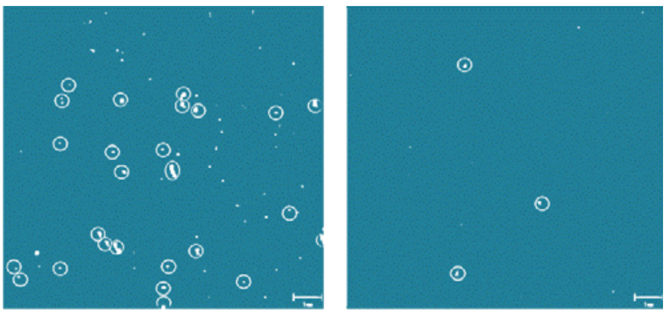

Figure 7: Typical 10x10mm observation fields post UV illumination (here 150 W) 420nm BPF PL of bipolar degradation severity between bulk+epi (left) vs. SmartSiC™+epi (right).

Results obtained from MOSFETs made on single-crystal SiC wafers and SmartSiC™ substrates shows that this latter offers gains equivalent to those obtained when moving from a device generation to the next one.

The gains validated on currently available device generations show that the advantages of SmartSiC™ would still be more noticeable in future device generations, but also in other devices with much lower Ron.A such as JFETs.

The works necessary to obtain the results presented here have been carried out within TRANSFORM project [7] (funding from the Key Digital Technologies Joint Undertaking under Grant Agreement No. 101007237).

References

1. Séverin Rouchier et al., 150 mm SiC Engineered Substrates for High-Voltage Power Devices, Materials Science Forum, Vol. 1062, pp 131-135.
2. Annealing-free ohmic realized by bonded SiC substrate , Advanced Power Semiconductors 2020
3. Mario Saggio, Silicon Carbide: a game changer in power electronics, CS International, April 16-17 2024, Brussels, Belgium
4. Michael Paluszek et al., Wide Band-Gap Semiconductor Amplifiers for Plasma Heating and Control, ARPA-E Fusion Summit, April 26-27 2022 San Francisco, California, USA
5. Kazumi Takano et al., Effective Method (Selective E-V-C Technique) to Screen out the BPDs that Cause Reliability Degradation, Materials Science Forum, Vol. 1062, pp 273-277
6. Harada et al., Suppression of stacking fault expansion in a 4H-SiC epitaxial layer by proton irradiation, Nature, Scientific Reports volume 12, Article number 13542 (2022)
7. https://www.sic-transform.eu/en

www.soitec.com
www.st.com

Electrical Energy Reliability and Efficiency

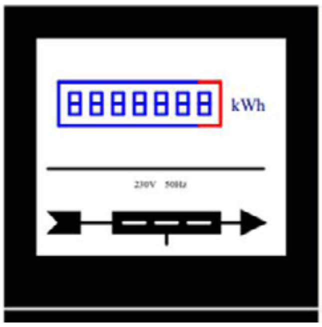

Voltage converters are the backbone of many technical systems. Depending on the application, the required power supply unit is realized by transformer, rectifier AC/DC converter. When high-performance switching power supplies were not yet available, 50 Hz transformer solutions were used almost exclusively.

By Willi Spiesz, Managing Director, Grau Elektronik

Electrical energy is provided almost exclusively as three-phase current with a system voltage of 10 ...30 kV~ in the power supply plunts and transported over long distances at voltages of 380kV~. The electronic DC voltages like 5V, 12V, 24V were transformed down from the high transmission voltage via transformers down to 220V~/230V~ voltage by means of a transformation ratio, rectified, smoothed and stabilised. Features for selecting a power supply are of course the price, reliability, availability, decision whether using standard components or special solutions, the required power, needness of wide-range input yes/no 110V~ ... 230V~ with/without power factor, operating temperature, EMC, efficiency, MTBF, form factors such as size, weight, plug and the type of installation. In the 1970s, as already mentioned, the solutions very often still consisted of the components 50Hz transformer, bridge rectifier and smoothing, possibly with downstream U-stabilisation. The question is, to what extent should the acquisition costs be the sole deciding factor in the purchase decision? Operating, maintenance and replacement costs may be a factor that should not be neglected. It is worthwhile using a more energy-efficient solution after just 24 - 36 months of operation time. For industrial goods, depreciation periods of 10 years are often applied. However, the machines often run twice as long. It is now necessary to consider whether and to what extent the use of an energy-saving solution can reduce the operating system costs for the energy supply company!

Many electronic devices require a stable DC voltage. Energy is transmitted by means of AC voltage plants supply and networks. This means that a DC voltage must first be generated from an AC voltage at the point of use. The method of voltage generation affects both operational safety and operating costs.
Before the introduction of high-frequency power supply solutions, which have now assumed a dominant position with the advent of fast-switching, low-impedance semiconductors, solutions with 50 Hz transformers, bridge rectifiers and smoothing capacitors were predominantly used to convert the 220V~ / 230V~ mains voltage to 24V and other frequently required DC voltages. The transformer solutions enable galvanic isolation between primary (230V~) and secondary circuits (e.g. 12V, 24V, ...).

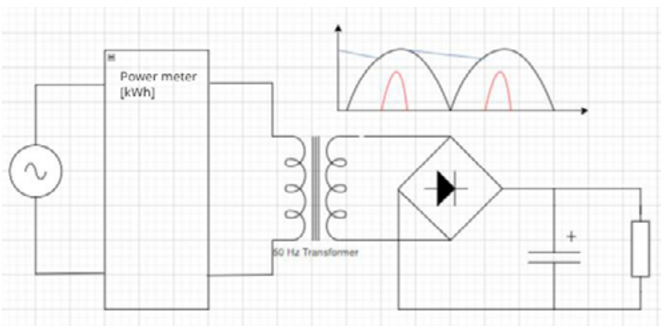

Figure 1: Classical 50 Hz transformer – rectifier solution causing high energy costs

Due to the special way of loading the transformer with the bridge rectifier and smoothing electrolytic capacitor, a pulsed current flow results in the 230V~ primary circuit.

The electricity meter is calibrated in effective values. The pulsed current flow results in a different RMS value for the current, which is calculated, despite the same charge carrier flow.

$i = C * dU / dt$ (1)

$i = dq / dt$ (2)

From equation (1) follows by conversion:

$i * dt = C * dU$ (1a)

On the DC side, a certain power or energy is required to perform the work.

$dW = u * i * dt$ (3)

Substituting the expression from equation (1a) into equation (3) results in

$dW = u * C * dU$ (3a)

If both sides are integrated, the result is

W (work, labour, energy) = $\int dw$
$= C * \int U*dU = ½ * C*U^2$ $W = ½ * C*U^2$ (4)

From the square of the voltage in the formula, you can see straight away that the energy or work does not change linearly with the voltage. The higher the crest factor $\xi r = î / Ieff$, the higher the electricity costs.

Energy, Work

$W = P * t$ (5)

A capacitor, an accumulator can now be filled in various ways, i.e. 'filled' with electrical charge carriers (q). Of particular interest in this context is the energy required for this on the AC side.

Example: On the DC side, an electrical power of P = 50W with a voltage U = 24V is required. The energy in the storage unit (battery) should be sufficient for an operating time of t = 24h.

E = 50W * 24h = 1'200Wh (6)

The current I is calculated as follows:

I = P/U = 50VA / 24V = 2.08A (7)

The battery has a storage capacity of C = 2.1A * 24h / 24V (8)

The charge in the battery: Q = I * t = 2.08A * 24h = 50 Ah (9)

This charge must be supplied by the AC voltage source. In addition, the AC voltage source must of course also provide the losses in the circuit components involved. These losses will be omitted for the sake of clarity.

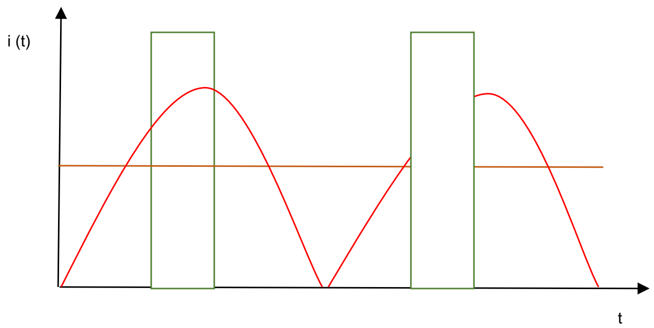

Figure 2: Red line shows rectifier input voltage, green line impuls current with high harmonics and poor power factor

The amount of charge supplied must be the same when charging with direct current or alternating sine current (rectified value) and with pulsed current (red), otherwise the battery, the accumulator and the capacitor would be charged at different rates. The surface areas for the charge must therefore be the same size.

Q = I * t direct current

Q = 2 * î / π Sine after bridge rectifier

Q = iRE * tp tp = T/12 with a typ. Current flow angle of Φ = 30° for bridge rectifiers with smoothing electrolytic capacitor.

The effective value of the input current, which is also billed, is calculated as follows:

I_{Eeff}^2 = 1/T ∫(6*I)²dt = 1/T * 36 * T/6

This results in $I_{eff,puls}$ = √6 = 2.45 times greater.

The crest factor is therefore: ξ_r = î / I_{eff} = 6 * I / √& * I = √6 = 2.45

In many mains applications in the 10W to 75W power range, high energy costs often occur unnoticed when consumer devices that use non-linear components in their inputs, such as bridge rectifier circuits, are connected to the 230V~ mains. The so-called power factor λ for such appliances is often only between 0.3 and 0.6. As the energy meters of the energy supply companies are calibrated in effective values, it is important to ensure efficient energy consumption of the consumer appliances. Otherwise it will be expensive. As long as electrical energy cost 5 - 6 cents, this consideration did not play such an important role. But with today's costs of 20 cents /kWh upwards, this is wasted money.

As the integration takes place inside bottom and top boundaries (the current flow in the example takes place between 60° and 90° corresponding to T/12 in relation to 2 sine half-waves), this means twice within one complete cycle T.

Therefore $i_{RE,puls}$ will 6 x higher than the I for the eual charge transfer towards the secondary path.

Assumption energy costs: 20 Cent/kWh

P Load	50 Hz Tranformer + smooth cap.	Annually costs	PFC solution	Difference annually
	kWh	€	kWh	€
25W	55.55W * 365 *24h = 486.6	97,32	28W * 365 * 24 = 245.4	49.08
50W	111.1W * 365 *24h = 973.2	194,67	56W * 365 * 24h = 490.8	98.16
100W	222.2W * 365 *24h = 1'946.6	389,33	112W * 365 * 24h = 981.6	196.42

However, in order to transfer the same amount of charge to the DC voltage side 24V, a different amount of work (energy) must be applied to the AC voltage side.

In order to compare only the influence of the waveforms, the time (t) of charging must be set to the same value!

Energy for 1 complete charge

a) Direct current E = 24V * 2.08A * 24h = 1,200Wh

b) Alternating current sine waveform

P = U_{Eeff} * I_{Eeff} = 50W (without losses, in the transformer, rectifier)

The following applies to the secondary side:
Q = 50Wh ➔ î = 50Ah/24h = 2.083A * π / 2 = 3.25A

This results in I_{Aeff} = î / √2 = 2.31 A

$U_{E,eff}$ = 230V~ ➔ I_{Eeff} = 50VA / 230V_{eff} = 0.217A

c) If the energy is transferred in pulses to the secondary DC voltage side, the following ratios result:

required electrical charge Q = 50Ah

$i_{RE,pul}$S =? ➔ I = 1/T ∫ $i_{RE,puls}$ * dt

$i_{RE,puls}$ = 6 * I as the charge carrier transport takes place per sine half-wave in T/12, i.e. 2 x per complete sine input oscillation. Consequently, the current must be greater by a factor of 6 so that the same amount of charge is transferred to the secondary side in T/6 of the period duration T.

Calculated under following assumptions:

ξ_r = 2,22 o. Power Factor PF = 0.45 and 365 * 24h operation time

η = 0.92

ξ_r o. PF = Power Factor ; λ = real power / apparent power

η = efficiency

Switch-mode power supplies with a sinusoidal current consumption can help here. However, there are differences in the way they work. Classic solutions are a step-up converter consisting of a storage choke, MOSFET trs. rectifier diode, smoothing capacitor and IC circuit with various additional components, which initially generates an intermediate circuit voltage of approx. 380V ... 400V DC from the rectified mains voltage. A downstream DC/DC converter, also in high-frequency operation f ≥ 50kHz, then generates the required secondary voltage of 5V, 12V 24V, galvanically isolated from the mains side, short-circuit and open-circuit proof.

However, Grau Elektronik power supply units use a PFC transformer solution that is following a sinusoidal input current curve and therefore having a low crest factor and high power factor λ with a maximum reduction in circuit components. By using transient-resistant components, a mains transient of 1.6 ... 2.3 * $U_{E,nenn}$ for t <= 0.1msec can also be handled.

www.grau-elektronik.de

Understand the Thermal Behavior of SiC for Efficient Power Design

Silicon carbide (SiC) has numerous advantages over traditional silicon process technologies in power electronics. It combines higher electron mobility with a wider bandgap and better thermal conductivity.

By Chip Brakeville, VP of Sales and Marketing, SemiQ

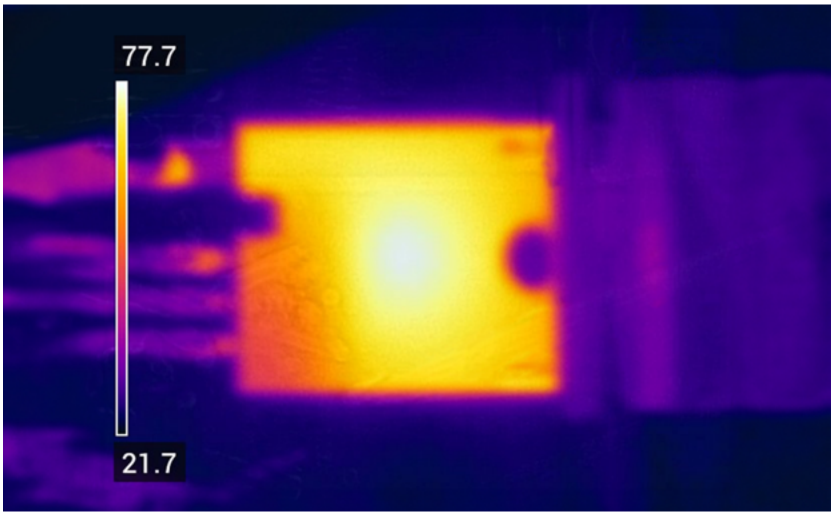

Thanks to these properties, SiC devices tend to exhibit lower on-state resistance ($R_{ds(on)}$) compared to silicon devices of similar ratings. As well as the higher carrier mobility, this lower resistance is assisted by the much higher breakdown field strength SiC offers over silicon. That property enables the use of a thinner drift layer in the device structure.

Perhaps SiC's most important advantage for many industrial designs that other technologies cannot readily address lies in its ability to perform well at elevated temperatures without excessive carrier leakage. A major contributor to this is SiC's lower intrinsic carrier concentration. However, to maximize the potential of SiC in designs that need high-temperature compatibility, it is important to understand how devices respond under conditions that will impact performance and efficiency.

In their work on SiC device design and manufacture, SemiQ engineers have carried out extensive tests that demonstrate the behavior of MOSFETs across the entire temperature range. These tests provide important data points that indicate how to take best advantage of SiC's thermal and electrical properties.

The tests carry through to manufacturing for the QSIC 1.2kV SiC MOSFET modules, with all parts undergoing testing to 1.4kV to ensure reliability. To guarantee stable gate threshold voltage and gate-oxide quality for each module, SemiQ conducts gate burn-in testing at the wafer level. In addition to the burn-in test, various stress tests, including gate stress, high-temperature reverse-bias (HTRB) drain stress, as well as the combined high humidity, high voltage, and high-temperature stress test (H3TRB), are used to ensure parts are compliant with automotive and industrial quality standards.

In the company's work on characterizing SiC devices, SemiQ has showed how the presence of both negative and positive temperature coefficients of on-state resistance over the full operating temperature ranges can influence design decisions where maximum reliability is needed. The company performed experiments on its 1.2kV SiC MOSFET in a calibrated oven using the Keysight B1505A Power Device Analyzer. To ensure the effects of ambient temperature were shown clearly, the experiments were conducted only after sufficient time had elapsed after the oven was set to its target temperature for devices to heat or cool to the correct level. During experiments, self-heating was mitigated by the use of short pulse widths and low duty cycles.

Experiments demonstrated that around room temperature, the $R_{DS(on)}$ of a SiC MOSFET reaches its minimum. Below this temperature, resistance can increase dramatically depending on the applied gate-source voltage. Lower voltages increase the temperature sensitivity, which also increases the temperature at which the temperature coefficient shifts towards positive.

The negative temperature coefficient below room temperature has implications for situations where devices are operated in parallel. If the system commences operation in low ambient temperatures, the effect can lead to one of the devices passing much more current and overloading due to thermal runaway. However, increasing gate-source voltage to around 18V-20V reduces the coefficient and with it the risk of an imbalance developing.

Though threshold voltage tends to reduce with increasing temperature, thanks to the reduction in bandgap voltage, maintaining a high gate-source voltage is important to overall device performance. This is the case even at higher temperatures. Experiments show that drain current tends to decrease with temperature. There

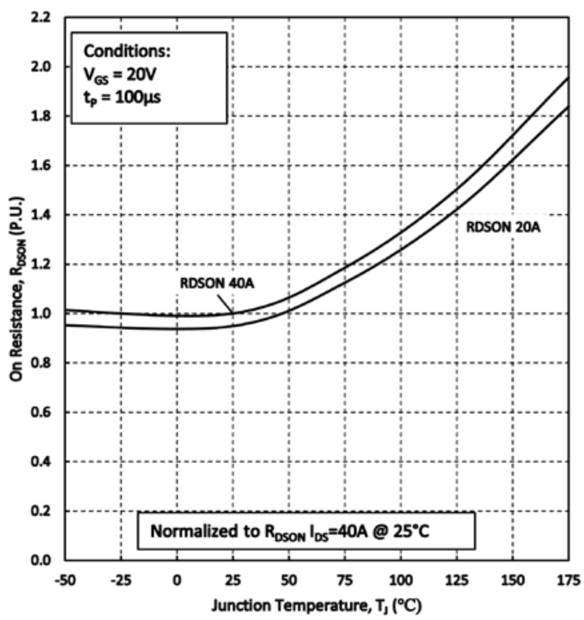

Figure 1: Normalized on-resistance vs. temperature.

are several factors that contribute to this response. Carrier mobility changes with temperature and the bandgap reduces, which has an impact on intrinsic carrier concentration. This also leads to a temperature-dependent lowering in threshold voltage.

However, SiC MOSFETs will continue to show a significant improvement in $R_{DS(on)}$ when the gate-source voltage is increased. Although 10V is above the typical threshold voltage of a SiC MOSFET, conduction losses at this level would most likely lead to a thermal runaway

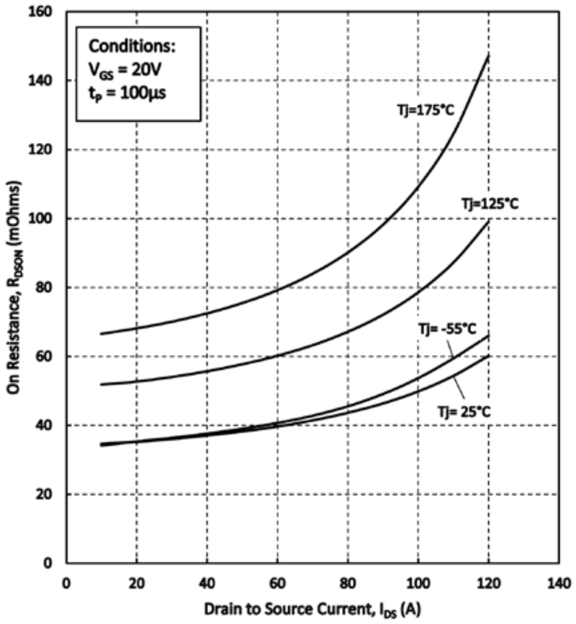

Figure 2: On-resistance vs. drain current for various temperatures.

of the device. Operating at 20V or above delivers better overall performance. When the device is turned off, because of the temperature dependence of the threshold voltage, SemiQ's recommendation is to maintain a gate bias of –5V. This low voltage prevents any unintended parasitic turn-on effects and ensures correct behavior at temperatures as high as 175°C where the threshold voltage can fall to as little as 1.8V from its typical level around 3V.

At elevated temperatures, the positive coefficient of SiC MOSFETs will increase conduction losses. However, it may be important to also consider the impact of drain current, which can also have a substantial impact on losses. Typically, on-resistance increases with drain current. It increases by around 50% from 20A to 120A. Combined with the increase in resistance with temperature, this can lead to a resistance of less than 40mΩ for SemiQ's 1.2kV SiC MOSFET to around 140mΩ at 175°C when passing a current of 120A. Circuit designers may choose to operate devices in parallel to pass less current through each device where on-state resistance needs to be kept as low as possible.

Figure 2 illustrates the relationship between on-resistance and drain current across a range of temperatures (-55°C, 25°C, 125°C, and 175°C). At -55°C and 25°C, the device exhibits lower on-resistances and decreased variability compared to those observed at 125°C and 175°C. Typically, SiC MOSFETs show a negative temperature coefficient (NTC) at lower temperatures until reaching a specific threshold, after which they transition to a positive temperature coefficient (PTC).

The body diode's effect on switching behavior is another area where circuit designers can focus to take full advantage of SiC's properties and use higher switching frequencies. One effect of the body diode is reverse recovery current, caused by minority charge carriers being cleared from the MOSFET's body diode when the device is switched back on. This reverse recovery current is translated into energy losses, which directly affects the efficiency of the power converter. The forward voltage of the body diode in SiC device is also higher than with silicon. For this reason, to minimize losses, it is important to avoid making use of the body diode outside of the dead time in the switching cycle.

However, compared to conventional silicon devices, those built on SiC processes tend to exhibit short recovery times when devices are turned off. This reduction provides the opportunity to increase switching frequency. That in turn lets designers use smaller external passive components in the support circuitry, which helps cut power-converter volume and costs.

A double-pulse test (DPT) provides valuable insight into detailed turn-on and turn-off performance. DPT is used to turn transistor on and off at different current levels as shown. By adjusting the switching times, the waveforms can be observed over the full range of operating conditions. The use of two pulses is important as it allows evaluation of reverse recovery current. Other effects include ringing caused by high changes in current with time (di/dt) that interact with parasitic inductances and capacitances in the device that may form resonant LC circuits.

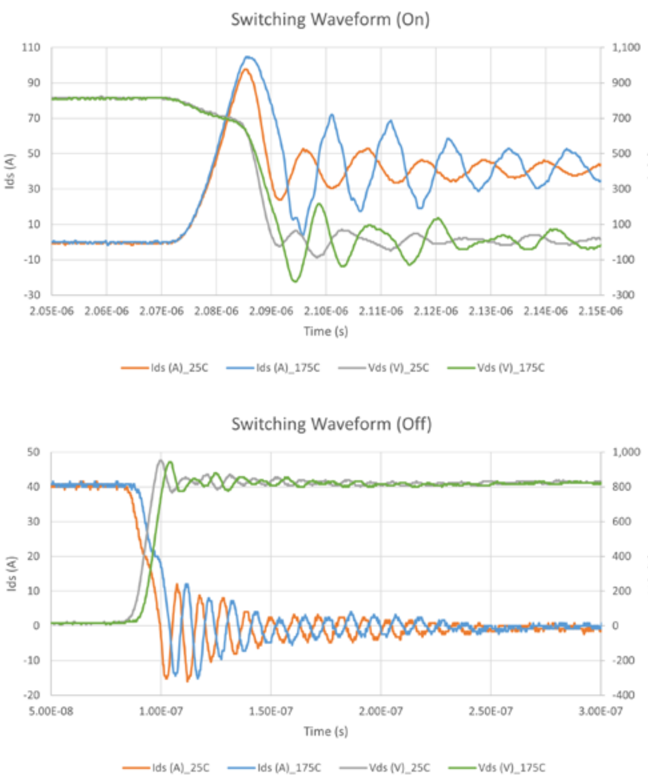

Figure 3: (a) Turn-on V_{ds} and I_{ds} switching waveforms at 25°C and 175°C (b) (a) Turn-off V_{ds} and I_{ds} switching waveforms at 25°C and 175°C for GP2T040A120J with a DC bus voltage of 800V, a load current of 40A, and using an external gate resistance of 4.3Ω mΩ.

To study the effects of temperature on this behavior, SemiQ carried out tests on devices in TO-263-7L packages. In this testing configuration, only the device-under-test was subjected to heating, and surface-mount pads used to connect it to the PCB. A calibrated external clip-on heater was used to maintain a controlled temperature.

Tests demonstrate that the reverse recovery time tends to increase with temperature. This leads to turn-on losses exhibiting an upward trend at elevated temperatures. However, turn-off losses remain relatively constant. Tests also showed that turn-on waveforms have higher ringing than turn-off waveforms. Though turn-off involves a rapid change in voltage, the parasitic elements may not form as strong of a resonant LC circuit during this phase, leading to relatively lower ringing. The result is that circuit designs that focus on reducing the effects of the body diode and ringing, which can be ameliorated by snubbers, are most important during the turn-on phase, especially if the device is expected to operate at the high end of the temperature range.

Though there is often a margin of safety set by device manufacturers to ensure MOSFETs can withstand their rated breakdown voltage, tests have shown that this voltage increases with temperature. Taking as an example a 1.2kV SiC MOSFET, this device demonstrates a breakdown voltage of at least 1520V at −50°C, rising to 1570V at 150°C. Though the drain leakage current also tends to increase with temperature, largely caused by the thermal generation of carriers, the positive temperature coefficient of the breakdown voltage masks this effect in practice.

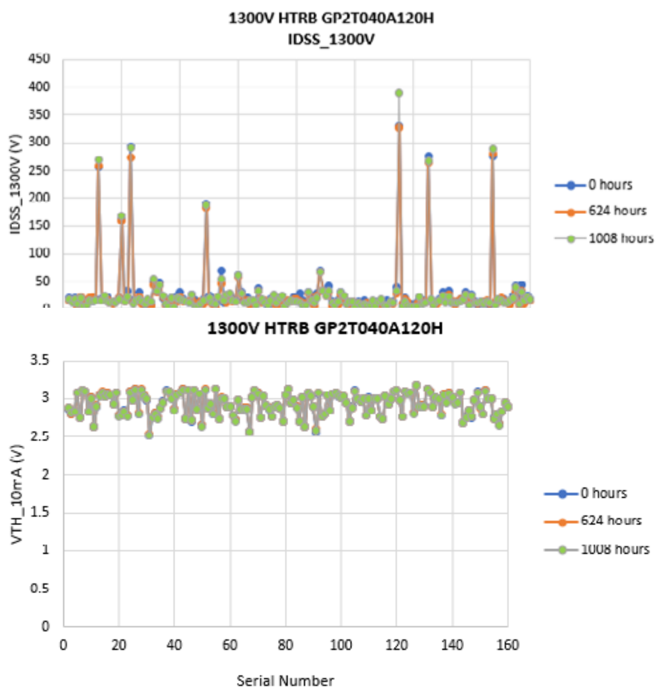

Figure 4: HTRB Test Results at 175°C and 1300V Reverse Bias.

SemiQ's careful study of the behavior of its 1.2kV SiC MOSFET provides valuable information on the static and dynamic characteristics of this type of device. For designers aiming to take advantage of SiC's ability to handle higher power-converter switching frequency, it is important to consider temperature-dependent losses. Turn-on losses exhibit an upward trend at elevated temperatures, but turn-off losses remain relatively constant. By paying attention to these differences, designers can compensate for these effects and gain the full efficiency improvements made possible by SiC technology, as demonstrated by the company's QSIC 1.2kV MOSFET modules.

Backed by more than 54 million hours of HTRB and H3TRB stress testing, the modules enable power-conversion efficiency as high as 98%, which helps improve thermal stability and enhance reliability. These benefits make the SiC modules ideal for a wide range of applications, including power supplies for DC power equipment, inverters, motor drives, electric-vehicle charging stations and more.

www.semiq.com

Accurate Current Sensing for Automotive Design

Isolated current sensor technology is becoming increasingly important for vehicle design

Current sensing is already a vital part of automotive design ranging from simple resistance-based measurement to more advanced sensors developed to analyze the behavior of fuel-injector systems. As electrification gains momentum, current sensor technology is poised to play an even more significant role, adapting to the specific requirements of these new vehicles.

By Ben Xie, Technical Marketing Manager, NOVOSENSE Microelectronics

A major design change that accompanies the evolution of the electric vehicle (EV) is the need to detect currents accurately in high-voltage subsystems and protect the advanced controllers that need to interpret and act on these signals. There are now numerous locations at which current sensors in high-voltage domains are needed, ranging from the fast battery charge circuits to heating units.

HV current sensing applications

One of the most important targets for accurate current sensing lies in the battery management system (BMS). Batteries are sensitive to overcharging and the trend towards fast high-voltage charging at 800V makes this measurement even more critical. By monitoring current information, the BMS can accurately sense battery estimation, detect and diagnose faults and ensure that charging is completed in a safe manner.

In EV motor control units, feedback provided by changes in current levels can accurately determine real-time power and torque, providing information needed by the algorithm to determine when best to switch the power transistors that deliver energy to the motor. As the motor and related power transistors will operate at voltages of 400V, or even higher to take advantage of efficiency gains, the current-sensor signal delivered to the controller needs to be protected against surges and spikes.

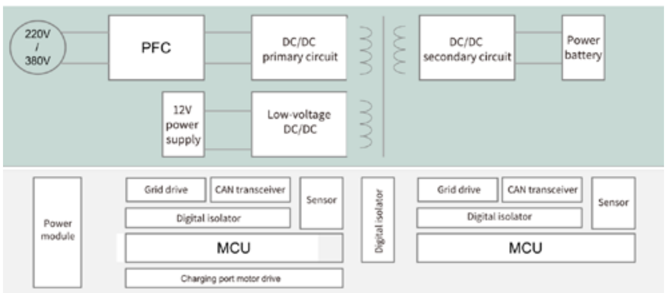

Figure 1: Power-factor corrected onboard charger and DC/DC converter modules in a typical EV (NEV WP – Fig 23)

Current sensors play a vital role in the onboard charger (OBC) together with the associated power-factor correction (PFC) circuit that is used to ensure that the EV complies with regulations for connecting high-voltage, high-current loads to the public electricity supply. In the OBC, sensors are often needed to measure the current flowing at the AC input as well as within the conversion circuitry and at the output to confirm that the charger is delivering AC power to the rest of the system correctly and that DC power is supplied at the correct level to the battery packs. To ensure safe operation of the microcontrollers that manage these systems, the current sensors in the high-voltage subsystems need to be isolated.

AC and DC choices

As well as considering attributes such as accuracy and isolation, another important factor in determining which current-sensor technology to use is whether the circuit uses AC or DC operation. Though the input and output from batteries will be DC-based, motor controllers and electric air conditioning and similar systems will typically operate on AC.

With DC, it is possible to employ shunt-based current sensors, which use high-resistance elements to generate a voltage signal from the current that passes through them. Shunt-based current sensors can offer high precision and strong protection from electromagnetic interference. However, their output needs external isolation as, despite the high resistance they present, they provide a direct path for current from the high-voltage subsystem to the control electronics.

Though magnetoresistive sensors are now beginning to appear, using a similar technology to that used in magnetic memories and hard disk-drive heads, the core technology for sensors used in either AC or DC circuits is the Hall effect. In a traditional Hall-effect sensor module, a magnetic core is wrapped around the conductor of the interface. This core surrounds the conductor except for a small air gap in which the Hall-sensor element sits.

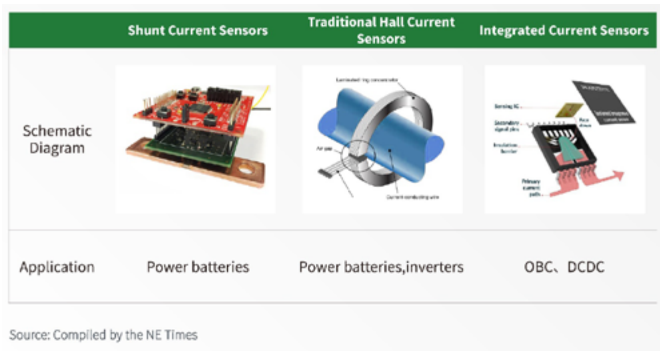

Figure 2: Different types of current sensor (Source: NEV WP - Fig 43)

A current passing through the core creates a magnetic field, which in turn generates an electric field. This electric field is detected by a Hall element placed in the air gap, resulting in an output voltage proportional to the field's strength. This voltage signal has a linear relationship with the current flowing through the primary conductor. Though the Hall-effect module is isolated from the primary conductor, a design that sees this type of module used widely in electricity distribution systems, it has the disadvantage of relatively large size. However, it is a design that can measure currents as high as 2000A safely.

Integrated Hall-effect sensors

Integrated-circuit current sensors using the Hall effect have the benefit of being much smaller and easier to deploy on PCBs. This type of Hall sensor does not use a separate magnetic core. Instead, current measurement is performed by sensing the magnetic field generated by the current flowing through a primary conductor that passes through the chip package.

Because of the smaller size of integrated devices, and the package constraints integration implies, the maximum current levels that can be measured are lower than with module-based sensors. The main reason for this lower limit is the resistance that the conductive path through the sensor may impose on the current flow, which leads to self-heating. However, manufacturers have succeeded in limiting this effect.

Integrated Hall-effect current sensors are often suitable for use in AC/DC converters and inverters that are used in onboard charging systems and in heating systems as well as some motors. Though overall isolation performance will be different to a module, because there is an insulating barrier between the primary conductor and the sensing element, the integrated Hall-effect current sensor will meet high isolation requirements.

One potential issue with direct sensing is that strong external magnetic fields can distort the signal, which could be problematic in the complex magnetic environment close to electric motors. One way to solve this problem is to employ two Hall-effect elements differentially. This placement cancels the effect of any common-mode magnetic fields.

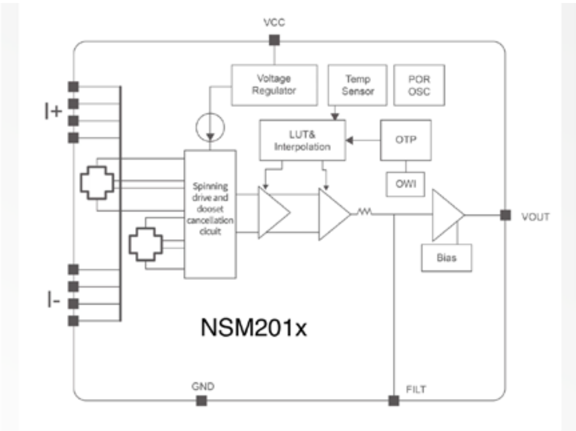

Figure 3: Block diagram showing use of differential Hall-effect sensing in the NSM201x series (Source: NEV WP - Fig 44)

Advantages of an IC-based implementation

The NSM2019 current sensor manufactured by NOVOSENSE Microelectronics provides an example of the benefits that result from an integrated design based on a differential architecture. The product's novel package design reduces self-heating by providing a primary conductor resistance of just 0.27Ω. This supports primary current levels as high as 100A.

Materials choices ensure the relatively small package achieves an operational isolation voltage of at least 1500V. On top of this, the insulation will survive 10kV of surge voltage and 13kA of surge current without additional protective devices. The dielectric withstand voltage reaches as high as 5000Vrms. The novel package design delivers a comparatively long creepage distance of 8.2mm. Creepage is an important parameter as it considers changes as the result of aging, such as environmental contamination, that could compromise isolation performance if the distance is inadequate. This combination of properties lets the devices easily meet the voltage and current surge protection requirements of today's EVs.

As well as handling the isolation needs of both today's EVs and future model designs, the NSM2019 has several features that are convenient for systems integration. The device supports both fixed and pseudo-differential output modes to improve signal integrity. Furthermore, the circuit is designed to ensure output voltage does not fluctuate with the supply voltage. This approach removes the need to employ a high-precision voltage regulator to supply power to the device, which simplifies the bill of materials.

The design of the NSM2019 takes into account the wide temperature variations that can be encountered in the automotive environment. Using a combination of offline calibration and thermal compensation algorithms, the output maintains high accuracy across the full temperature range of –40 to +150°C.

Summary

As vehicle makers continue to exploit the efficiency advantages of employing key subsystems with high-voltage circuitry, the importance of current-sensor technology in ensuring reliability, safety, and performance grows. Manufacturers are meeting this demand by developing sensors with intrinsic designs that guarantee safety and performance.

www.novosns.com

Tighter EU legal Limits on Standby Power Consumption: Could simple new Power ICs come to the Rescue?

In tune with the European Commission's (EC's) commitment for Europe to be a climate-neutral continent by 2050, new regulations coming into force in 2025 will clamp down on the amount of power that almost all types of domestic electronics equipment are allowed to dissipate when off or in standby mode.

By Vito Prezioso, Power Specialist Field Application Engineer (Southern Europe), Future Electronics

According to European Union (EU) research, annual energy consumption of household equipment in off mode or a standby mode was an estimated at 59.4 TWh in 2015. This power wastage was responsible for the emission of 23.8 million tonnes of CO2 equivalent greenhouse gases.

Now device manufacturers are to be compelled to design products to bring their standby power consumption within strict limits. But this will not always be a complicated and expensive effort: as this article explains, a simple IC added to an ac-dc power converter can on its own yield a substantial saving in power consumption whenever a device is plugged in.

Broad scope of new Ecodesign requirements

The EC's new regulation 2023/826 on standby power comes into effect from 9 May 2025: its goal is to cut annual energy consumption in Europe by 4 TWh. This is an ambitious target: it is to be achieved by regulating the power consumption of a very broad range of household products and of office equipment intended for use in a domestic setting.

The regulation applies to products with an integrated power supply. Products equipped with a low-voltage external power supply are not currently included in its scope, but manufacturers would be wise to expect to be required to comply sooner or later, as the EC is likely to want to provide a level playing field for competition between manufacturers.

The types of device which are listed in the regulation include kitchen equipment such as toasters and microwave ovens, white goods, IT equipment (except products such as laptop computers that are covered by specific Ecodesign regulations), audio-visual equipment, toys, sports equipment, and products which contain a motor, such as power-operated furniture and beds, and motorized blinds and shutters. A full list can be found at the EC's EUR-Lex law website.

The limits on energy consumption are tight: a maximum of 0.5 W in off mode, falling to 0.3 W after two years. Standby mode limits vary. If the device only maintains a reactivation function and indicator, the limit is 0.5 W. If a status or information display is active, the limit rises to 0.8 W for most products.

Still higher limits are applied to products which operate in networked standby. (Networked standby means a condition in which the equipment is able to resume a function by way of a remotely initiated trigger from a network connection.) Products that are classed as having HiNA (high network availability) capability, such as routers and gateways, must not use more than 8 W in networked standby. For non-HiNA products, networked standby power consumption is to be limited to 2 W.

A cheap and easy fix for high standby power consumption

A strategy for ensuring compliance with regulation 2023/826 should consider power consumption across the system as a whole, including in functions such as control, interfacing and sensing. But a fertile source of savings is sure to be the power supply circuit – and one of the quickest and easiest ways for many OEMs to cut standby power consumption is by eliminating the continuous power drain through the EMI filter's X-capacitor bleed resistors.

These resistors are found in the power supply of many household appliances and consumer devices to provide for compliance with IEC 60335-1, a safety standard for these products which specifies that the power supply's X-capacitor needs to be discharged below 34 V within one second after the device is powered off.

A typical EMI filter is shown in Figure 1. C1 and C2 represent the X-capacitors; R2 ensures that the X-capacitors are discharged after the input voltage is removed. The capacitance of the X-capacitors can vary from hundreds of nanofarads for low-power converters up to some microfarads in higher-power converters. To take an example, for a capacitor of 2.2 µF specified with a tolerance of ±20%, the maximum capacitance will be 2.64 µF. The mains input voltage is up to 264 V ac (240 V ac +10%). To discharge the capacitor to 34 V within one second, a resistor of 184 kΩ is required. This bleed resistor will dissipate 377 mW.

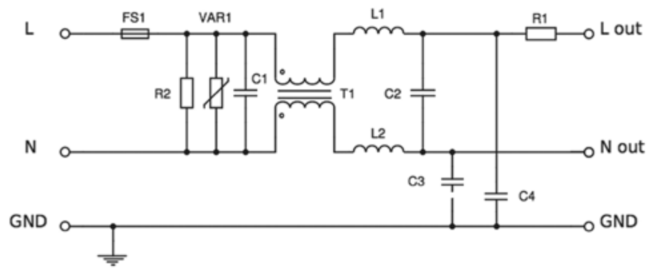

Figure 1: In this typical EMI filter, the bleed resistor R2 draws a continuous current as long as the device is plugged in

This circuit configuration makes it almost impossible to comply with the new standby power consumption regulation: the 377 mW dissipation continues all the time that the device is plugged into a mains power socket, whether the device is active, quiescent, or switched off.

Fortunately, it is easy to add a simple integrated circuit to stop power consumption through the bleed resistors except when the X-capacitors need to be discharged. Examples include the CAPZero-2 or CAPZero-3 from Power Integrations, the HF81 from Monolithic Power Systems, and the TEA1708T from NXP Semiconductors.

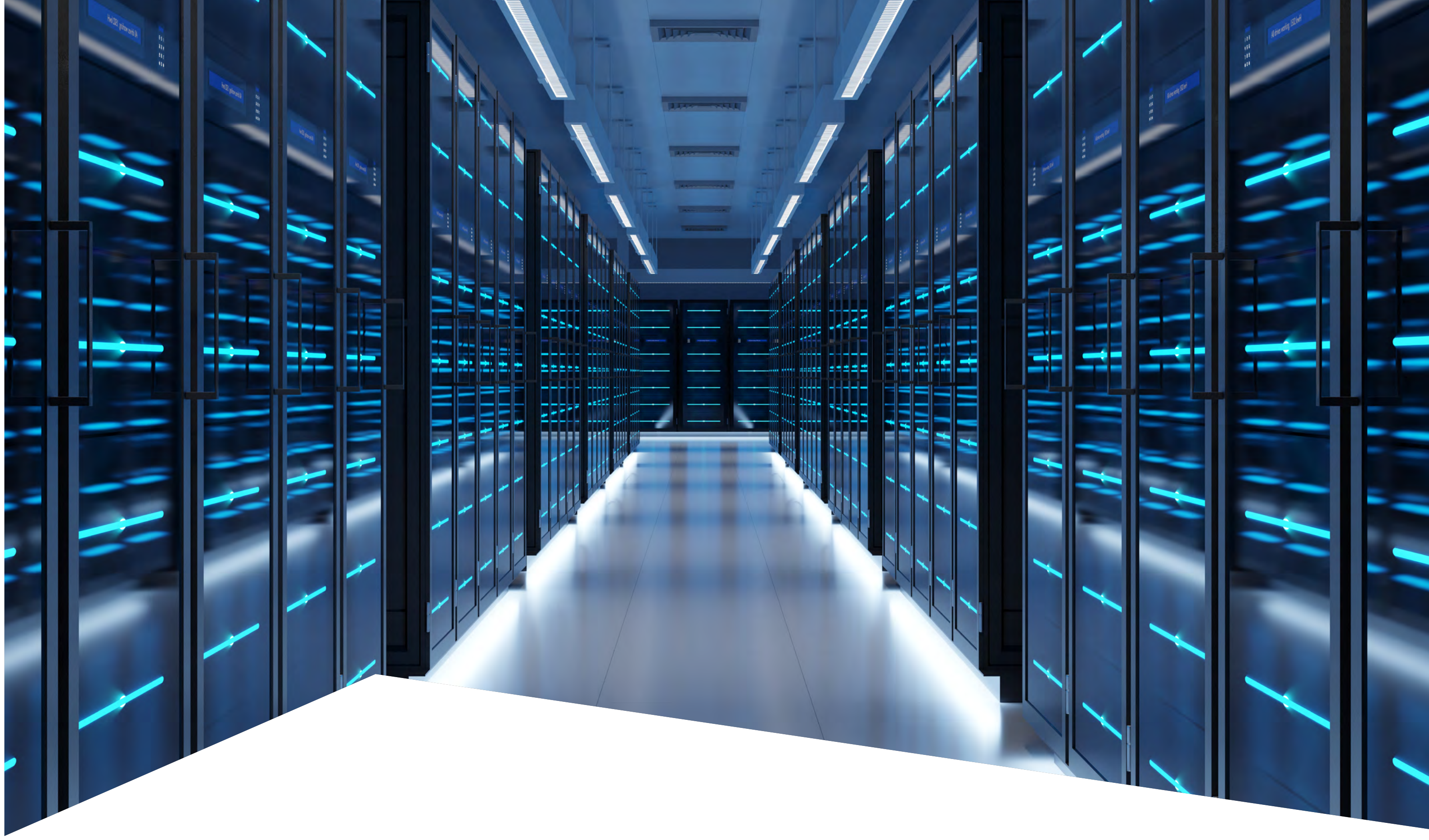

Power supply solutions for AI server racks

From 3 kW to 12 kW and beyond

- Best results through the targeted use of our Si, SiC, and GaN technologies
- Single-phase PSU system solutions from 3 kW up to 12 kW and more
- Exceptional efficiency: > 97.5%
- High power density: +100 W/in^3
- Extended hold up time
- Following specification ORv3

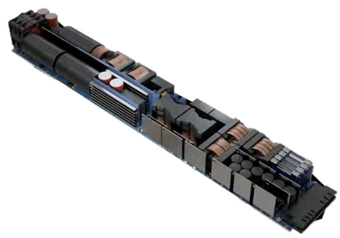

Si SiC GaN

For more details & registration - click here.

infineon

These parts are all of a similar design. They consist of MOSFETs with integrated drivers, plus voltage sensing and other circuits. They are placed in series with the bleed resistors. During normal operation (when an ac voltage is present), the MOSFETs are off, and so the resistors are disconnected and no current flows them through. When the device is unplugged and the ac voltage is removed, the MOSFETs turn on to bring the resistors into the circuit, which then discharge the X-capacitors.

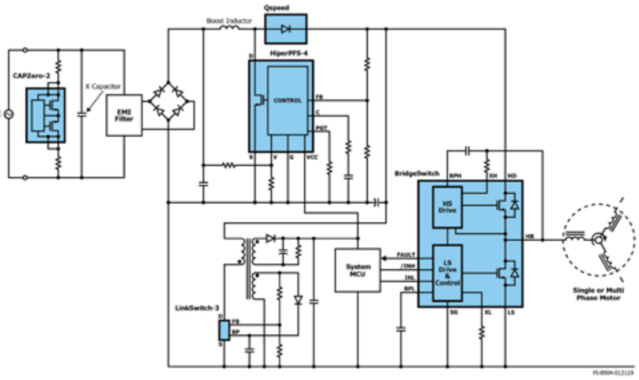

Figure 2: Typical high-voltage motor control board, showing the CAPZero-2 X-capacitor discharge circuit. (Image credit: Power Integrations)

Tests performed by Monolithic Power Systems reveal the huge power saving that can be made by using the HF81 in this way: the test results are published in the datasheet of the HF81 (see Figure 3). For our example above of an X-capacitor of 2.2 µF, the saving made by using the HF81 would bring power dissipation through the bleed resistors to below 200 mW – low enough to allow for compliance with the 2023/826 regulation. Separately, Power Integrations and NXP specify the power dissipation of their ICs at less than 5 mW.

X-capacitance	Total Series Resistance	Power Saving at an Input Voltage of 265 V ac
≤500 nF	1.5 MΩ	-
750 nF	1 MΩ	66 mW
1 µF	780 kΩ	86 mW
1.5 µF	480 kΩ	142 mW
2 µF	360 kΩ	191 mW
2.5 µF	300 kΩ	230 mW
3.5 µF	200 kΩ	347 mW
5 µF	150 kΩ	464 mW

Figure 3: Power savings made by replacing a conventional X-capacitor discharge circuit with one based on the HF81 from Monolithic Power Systems

The solution shown in Figure 2 provides a way to cut the power wasted through the bleed resistors: it can be implemented as a cheap and easy modification of an existing power supply design, with minimal change to the bill-of-materials or board layout.

For new designs, however, OEMs have the option to choose from a new generation of power controllers that include an integrated X-capacitor discharge circuit. Examples are:

- HR1275 from Monolithic Power Systems, a combination controller with multi-mode PFC and LLC power stages
- TEA2017 from NXP, a combination controller with multi-mode PFC and LLC power stages
- NCP1618 from onsemi, a multi-mode PFC controller
- HiperPFS-5 from Power Integrations, a quasi-resonant PFC controller with integrated gallium nitride (GaN) FET
- L4985 from STMicroelectronics, a PFC controller which operates in continuous conduction mode

These suppliers are innovating in their product designs to save even more power in standby mode. For instance, many work in burst mode when the load is below a certain threshold, allowing the power-supply control and switching circuits to be intermittently disabled.

The scale of the improvements that can be made are substantial: with its TEA2017, NXP has reduced low-load and quiescent mode power consumption compared to its predecessor part, the TEA2016 (see Figure 4).

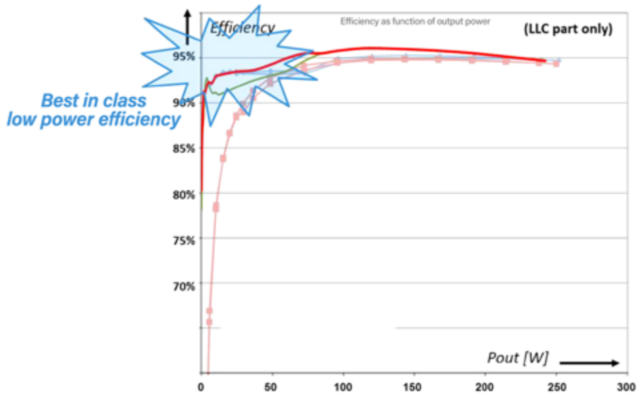

Figure 4: Efficiency graph showing the reduced power losses at low load in the latest TEA2017 power controller from NXP (red curve) compared to the TEA2016 (pink curve). (Image credit: NXP Semiconductors)

Implemented in an NXP evaluation board, the TEA2017DK1003, a 600 W offline ac–dc converter with a 12 V output, the TEA2017 enables the power supply to reduce no-load power consumption to 0.11 W with a 230 V ac input. The TEA2017 also provides the main power control functions in the new Lightning ac-dc converter board developed by Future Electronics' European Power Centre of Excellence. Technical information about the Lightning board, which provides a 42 V dc output and supports loads of up to 240 W, can be found at www.my-boardclub.com, where engineers can also apply to receive the board.

Power Integrations, onsemi and ST also supply evaluation boards which demonstrate the capability of controllers with integrated X-capacitor discharge to support compliance with regulation 2023/826.

Power Integrations provides the DER-672, a 220 W evaluation board which achieves no-load power consumption of 120 mW at 230 V ac thanks to its PFS5178F, a quasi-resonant PFC controller with GaN FET, operating in discontinuous conduction mode.

From onsemi comes the NCP13994MM360WGEVB, a 360 W evaluation board in which the NCP1618 multi-mode PFC controller is used in conjunction with the NCP13994, the latest current-mode LLC controller. At 230 V ac, the no-load power consumption of the NCP13994MM360WGEVB is 100 mW.

ST, on the other hand, supplies a 400 W evaluation board, the EVL400W-80PL, in which the L4985A PFC controller operating in continuous conduction mode achieves no-load power of less than 150 mW at 230 V ac.

Power semiconductor market responding to demand for lower standby power

The TEA2017 and the other new and improved products featured in this article show that the component market is ready to provide various solutions to power-supply designers who face the task of achieving compliance with the tight restrictions on standby and off mode power consumption specified in the EU's latest regulation.

www.futureelectronics.com


BASiC
Semiconductor
Visit us at PCIM EUROPE
Hall 9 Booth 118
11-13 June 2024
Compact & High Power Density
Pcore™6 Series - Automotive SiC MOSFET Module
Ideal for (Hybrid) Electric Mobility
Features
High power density
Low conducting and switching losses
Silver Sintering process for enhanced reliability
High operating temperature
Superior power cycling capability
Three Phase Full-Bridge topology
Low $R_{DS(on)}$ Trench Gate SiC-MOSFET
Voltage: 750V & 1200V
Current: 600A~950A
Qualified according to AQG-324
Double-Side Sintering &
Thick Copper Bonding Technology
SiC Schottky Diodes & MOSFETs, Automotive & Industrial Full-SiC Power Modules and Power Device Gate Driver Boards & ICs available.
www.basicsemi.com/en
autobu@basicsemi.com

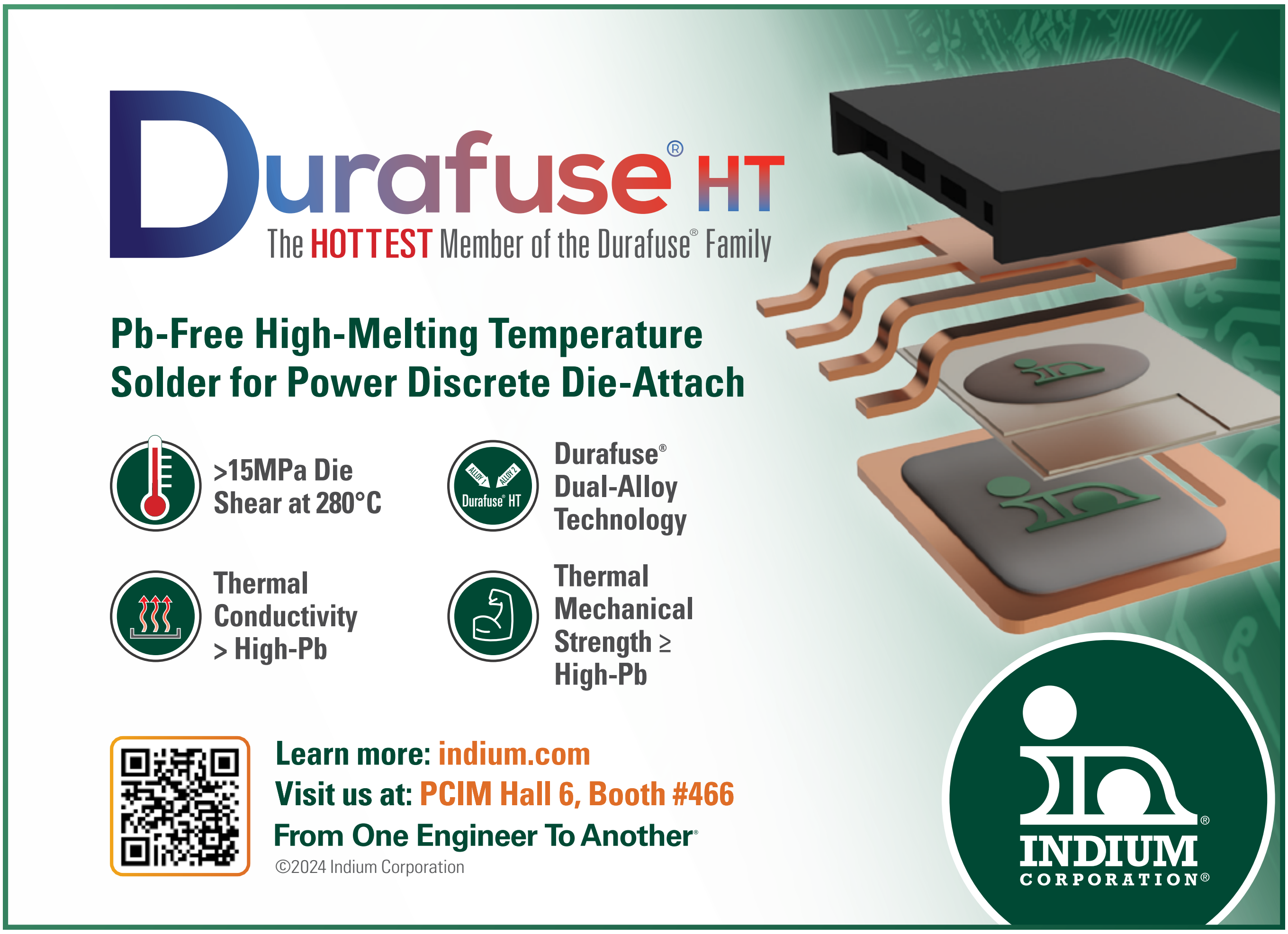
Durafuse® HT
The HOTTEST Member of the Durafuse® Family
Pb-Free High-Melting Temperature
Solder for Power Discrete Die-Attach
>15MPa Die Shear at 280°C
Durafuse® Dual-Alloy Technology
Thermal Conductivity > High-Pb
Thermal Mechanical Strength ≥ High-Pb
Learn more: indium.com
Visit us at: PCIM Hall 6, Booth #466
From One Engineer To Another®
©2024 Indium Corporation
INDIUM CORPORATION®

Digital Control for Isolated Bidirectional Power Converters

This article explores the implementation of isolated and bidirectional DC-to-DC power transfer by adapting a dedicated digital controller to work in reverse power transfer (RPT), in addition to its standard forward power transfer (FPT) function. System modeling, circuit design and simulation, and experimental work are presented to validate the theoretical concepts. The application demonstrates levels of conversion efficiency above 94% consistently in both energy transfer directions.

By Juan Carlos Rodriguez, Power Conversion Systems Engineer, Analog Devices

Introduction

Modular battery-based energy storage systems (ESSs) are key technologies for the construction of a green energy ecosystem, as they assist the effective utilization of renewable electricity. An increasingly popular application are second-life battery ESSs. In this submarket, up to 80% of the discarded batteries are expected to be repurposed into ESSs for stationary grid services, hence increasing the useful life of batteries from 5 years up to 15 years. These systems are expected to add up to 1 TWh to the grid capacity in 2030.[1] This emerging application is bound to gain more importance within the energy market in the near future.

A typical implementation consists of different stacks of battery modules transferring their energy to the centralized AC or DC buses (for some form of subsequent energy dispatchment to loads) via power converters. The challenge with this type of system is due to each module having different chemistries, capacities, and ageing profiles. In a traditional modular topology, the weakest module affects the total usable capacity of the full stack (Figure 1).

To tackle this limitation, in the architecture shown in Figure 2 the energy in the stack is transferred to a common, intermediate DC bus via individual DC-to-DC converters for each battery module. This energy is then used to support a centralized medium voltage (MV) AC or DC bus via a main power converter. The voltage and power levels in Figure 2 have been chosen based on typical figures from ESSs in the market: 48 V battery modules, 400 V (DC) intermediate DC buses, more than 20 kW (high power) main power converters, and up to 1500 V centralized buses.[2]

In Figure 2, because the ground references of each module in the stack are different, isolation is needed to implement the individual DC-to-DC converters for each battery module. In addition, for supporting hybrid systems like second-life battery ESSs, each of these converters must also be able to transfer power bidirectionally. In this way, independent charge/discharge of each module and charge balancing can be easily achieved. Therefore, the central blocks of the application herewith discussed are DC-to-DC converters that are at the same time isolated and bidirectional.

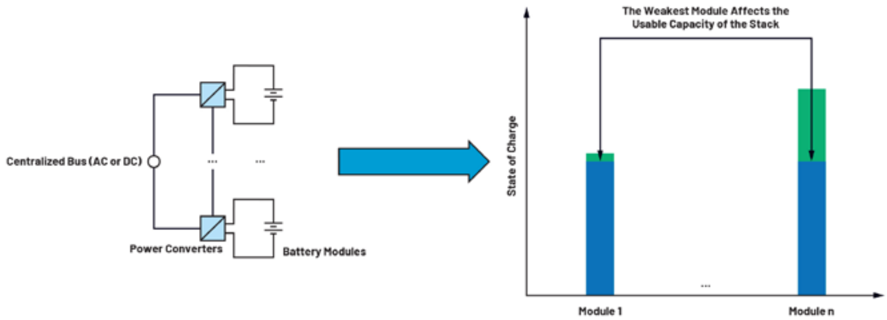

Figure 1: The challenge with modular ESSs.

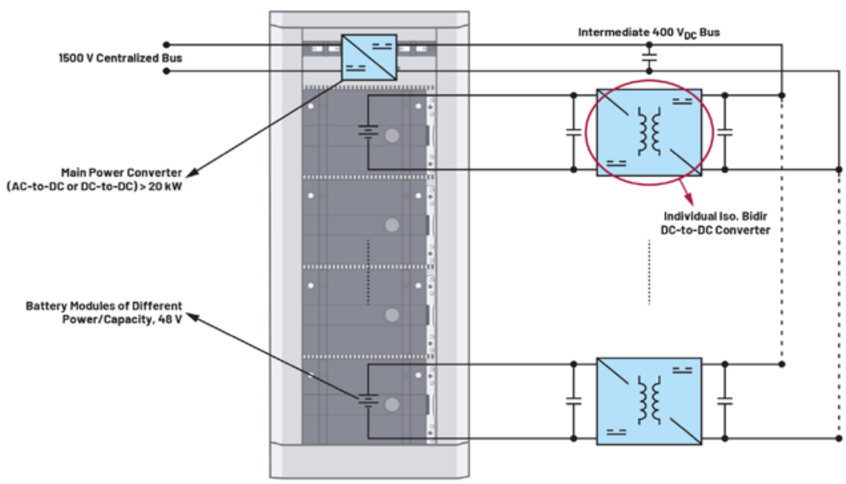

Figure 2: A modular battery-based ESS.

Over the following sections, dedicated digital controllers for power conversion are shown to be a good alternative for a safe and reliable implementation of the required type of DC-to-DC converter by adapting these controllers (usually built for unidirectional power transfer only) to bidirectional operation.

Dedicated Digital Controllers for Power Conversion Applications

For the control of the switching devices in high power DC-to-DC converters (larger than 1 kW), digital control is the current standard in industry, and it is typically based around microcontroller units (MCUs).[3] Despite this, an increased focus on functional safety (FS) across industrial applications could favor the case for using dedicated digital controllers instead. From the system design perspective, an easier FS certification is particularly beneficial in modular implementations as it facilitates the design process and, therefore, reduces the overall time to revenue. Some of the reasons that favor the case of dedicated digital controllers over MCUs are outlined next.[4]

- Microcontrollers depend on software, which up until the development of IEC 61508 was not allowed in a safety system due to it being considered unstable because of the number of states it contains.

Hence, a lot of the FS effort with an MCU goes into the process used to develop the software.

- The MCU itself would have to be certified in addition to the software.
- Although dedicated digital controllers (as configurable devices) are still data driven, their configuration process involves a limited variability language (LVL) as opposed to a full variability language (FVL), which is distinctive of MCUs.
- As a sequential digital machine, the functions of a dedicated digital controller can be completely verified by testing, which is generally not possible for the software in an MCU. As a result, the core safety functions are integrated by the device when using a dedicated controller.
- Added safety functions for MCU implementations might need considerable additional hardware compared to the integrated safety functions in a dedicated controller. This is prone to add more complexity to the system level, when using a failure modes, effects, and diagnostic analysis (FMEDA).
- When using a dedicated controller, additional safety (if needed) can be programmed in an external MCU, usually available at the system level.

The ADP1055 by Analog Devices is a digital controller especially built for isolated DC-to-DC high power conversion and offers a range of features for improved efficiency and safety. These functions include programmable overcurrent protection (OCP), overvoltage protection (OVP), undervoltage lockout (UVLO), and overtemperature (OTP). Like many equivalent off-the-shelf parts in the market, this controller is designed for energy transfer in one direction only—that is, FPT. To achieve a bidirectional operation, the application with the controller must be adapted to work also in RPT. The next section will explore one important aspect in both FPT and RPT modes, which is necessary to understand prior to the process of adaption. This is the efficiency of the target DC-to-DC converter.

Achieving Efficient Energy Conversion

Among the different technologies available for isolated and bidirectional power transfer in DC, the architecture in Figure 3a is one of the most used commercially due to its simplicity of implementation.[5]

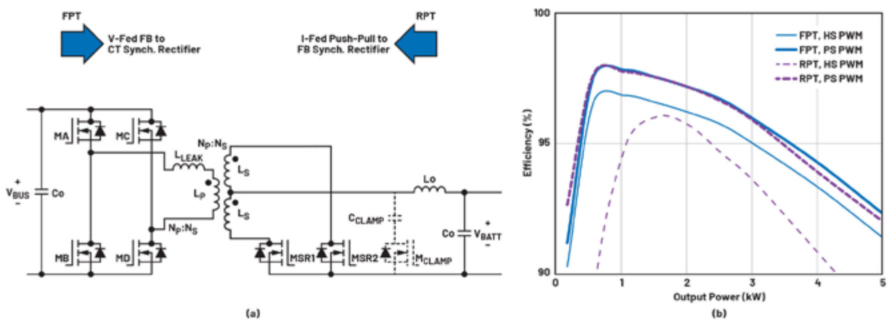

Figure 3: Power conversion topology simulation: (a) model and (b) efficiencies, in standard operation.

This topology can be seen either as a voltage-fed full-bridge to center-tap synchronous rectifier in FPT, or as a current-fed push-pull converter to full-bridge synchronous rectifier in RPT. A case study with 400 V (DC) in the primary (DC bus) and 48 V (DC) in the secondary (battery module), for high power levels larger than 1 kW, is depicted to illustrate the common challenges of the application. LTspice® was used to simulate the operation with typical wide band gap (WBG) power devices switching at 100 kHz. The parameters used in simulation are depicted in Table 1.

Circuit Parameter	Value
Rated DC Bus Voltage	V_{BUS} = 400 V (DC)
Rated Battery Voltage	V_{BATT} = 48 V (DC)
Switches MA, MB, MC, MD	SCT3017AL 650 V/18 A SiC MOSFETs
Switches MSR1, MSR2, M_{CLAMP}	IPB065N15N3 150 V/136 A MOSFETs
Transformer	Np/Ns = 6:1; Lm = 50 µH; L_{LEAK} =0.1 to 1 µH
Choke Inductor	Lo = 50 µH
Clamp Capacitor	C_{CLAMP} = 1 µF
Bus Capacitor	Co = 10 µF
Switching Frequency	100 kHz (effective 200 kHz)

Table 1: Simulation Study Parameters

The results in Figure 3b show a rapid decrease in efficiency for higher power levels when regular hard-switching (HS) PWM is used. This is accentuated when comparing RPT with FTP. To improve operation, two main loss mechanisms are identified, which can be mitigated with the corresponding switching techniques described next.

Soft switching: Figure 4a shows how in this low leakage inductance design, primary switches MA and MB do not turn off fast at the passive-to-active switching transitions when using regular PWM. This situation creates higher switching losses in the overall system. In this case, the use of phase-shifted (PS) PWM (aka, zero-voltage switching (ZVS), aka soft-switching) helps bring the drain-to-source voltages down to zero during these transitions. This can be done by providing appropriate, load-dependent dead times that allow the full discharge of the drain-to-source capacitances of the switches. The results of applying PS are shown in Figure 4b.

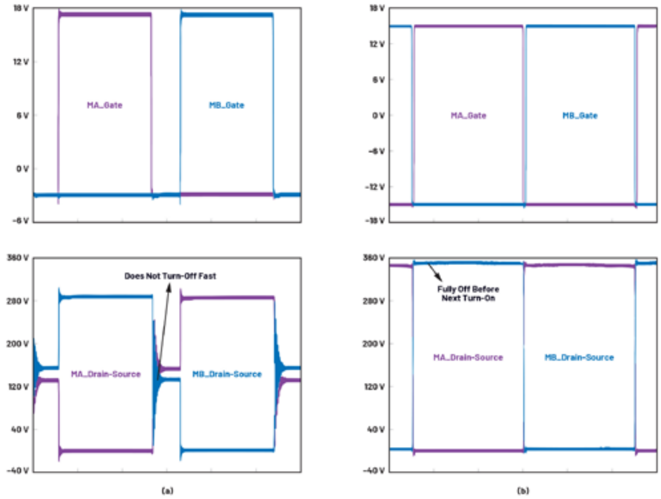

Figure 4: Primary switches passive-to-active transitions with (a) HS and (b) PS PWM.

Active clamping: Figure 5a shows how during the turn-off of the secondary switches MR1 and MR2, a large spike and ringing are observed on their drain-to-source voltages. These transient events endanger the integrity of the switch, waste energy, and contribute to electromagnetic interference (EMI). Digitally controlled active clamping using an additional switch (for example, with M_{CLAMP} in Figure 3) is the best alternative to alleviate the negative effects of this spike.[6] This can further increase the efficiency in this architecture. The results of applying a form of active clamping are shown in Figure 5b.

ECCE Europe

ENERGY CONVERSION CONGRESS & EXPO

2024

2-6 September, Darmstadt

ECPE

pels

IEEE POWER ELECTRONICS SOCIETY

TECHNISCHE UNIVERSITÄT DARMSTADT

Join the **European Flagship** Event for

Power Electronics

©Fotos darmstadtium.de

www.ecce-europe.org

ECCE Europe - Energy Conversion Congress & Expo
2-6 September 2024 in Darmstadt, Germany

Registration is open!

darmstadtium Science & Congress Centre

Scan for more Information available on the Conference Web Site including your Sponsorship & Exhibition Opportunities

Conference Focus Topics:

- Energy Transition
- Electrification of Heavy Duty Transportation
- Enabling Technologies for Sustainability

Conference Highlights:

- Cutting-edge Research Presentations
- Keynote Speakers for Focus Topics
- Industry Sessions
- Diverse Technical Tracks
- Tutorials on Monday
- Networking Opportunities
- Student Job Fairs

General Chairs: Prof. Gerd Griepentrog, Technical University Darmstadt
Prof. Oscar Lucia, University of Zaragoza

www.ecce-europe.org

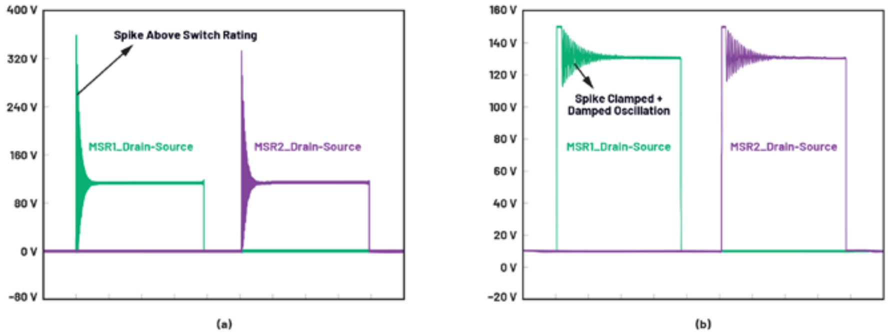

Figure 5: Primary switches passive-to-active transitions with (a) HS and (b) PS PWM.

The implementation of these strategies increased the efficiency of the converter from less than 80% to more than 90% at 5 kW in RPT. Similar efficiencies for both FPT and RPT are predicted by these simulation studies too, as shown in Figure 3b.

To implement these switching functions, the ADP1055 offers six programmable PWM outputs to form the timing of the switches and two GPIOs configurable as active clamp snubbers. Both functions are easily programmed within a user-friendly GUI. The benefits of these and other functions of this digital controller can be further studied in the ADP1055-EVALZ user guide, where the standard FPT application is considered.

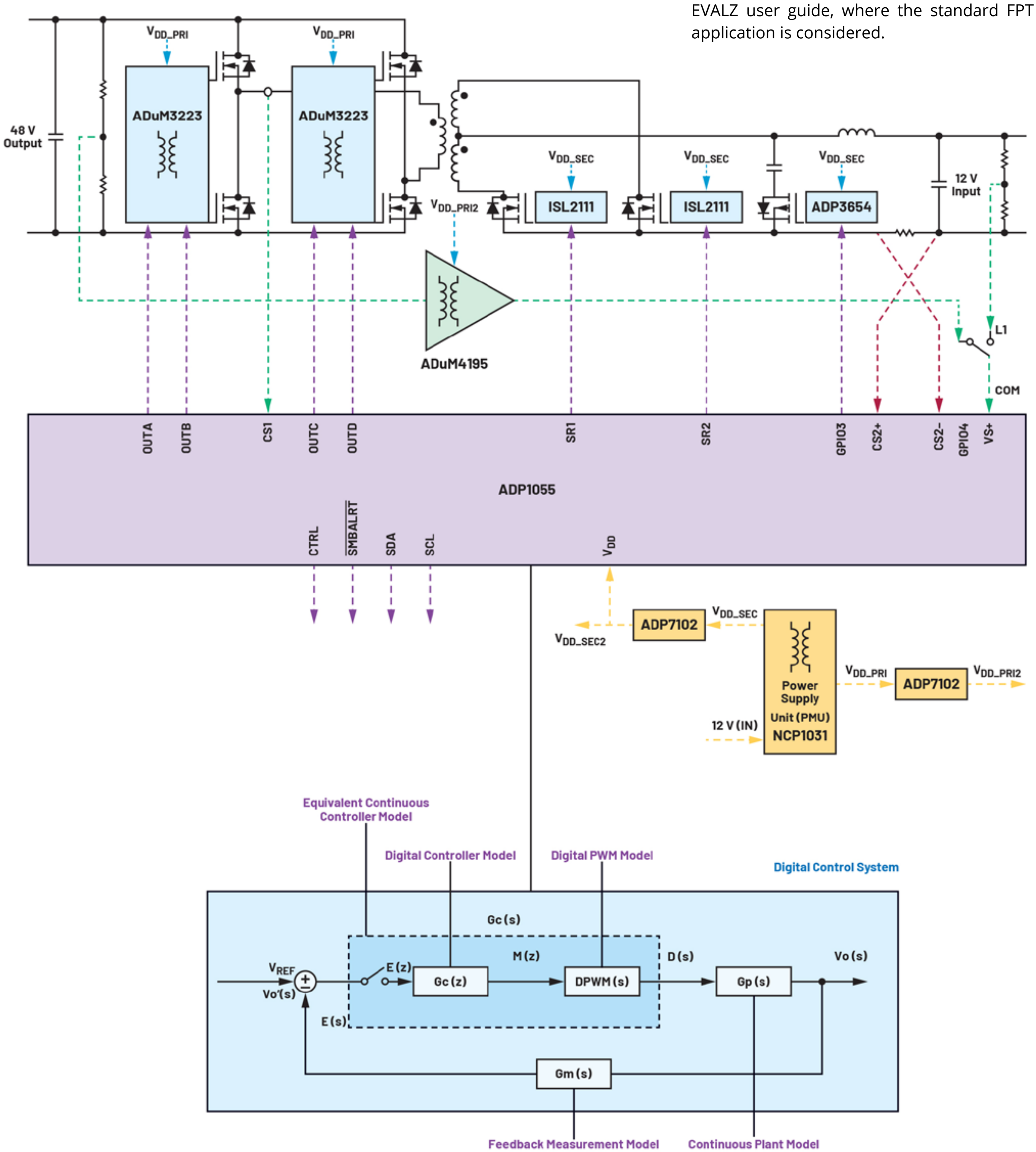

Figure 6: Signal chain to adapt RPT with a dedicated digital controller.

Once the mechanisms for achieving viable levels of efficiency have been identified, which are suitable for both FPT and RPT modes in this application, the adaption to RPT is finally explored next.

Reverse Power Transfer Adaption

In order to demonstrate the operation of the application under study in RPT, a low voltage (LV) experimental setup was created as a proof of concept. This setup was based on the hardware in the ADP1055-EVALZ user guide, originally designed for 48 V_{DC} to 12 V_{DC}/240 W FPT, using the ADP1055 as the main controller at switching frequency f_{SW} = 125 kHz, as a standard case. The RPT operation adaption then involved adequate hardware and software modifications. Figure 6 (top) shows the proposed signal chain on the hardware side for this task, with the following highlights:

- The four primary switches are turned on and off using two matching ADuM3223 isolated half-bridge gate drivers. The precise timing characteristics (54 ns max. isolator and driver propagation delay) of these drivers accurately reflect the control signals into the PWM.
- The isolated power supply unit in the ADP1055-EVALZ user guide is rewired and supplemented with an ancillary precision LDO (ADP1720) to account for the two ground references in the system and to energize all the different ICs of the application.
- On the measurement side, the terminals for current measurement on the shunt resistance are swapped so that the output current in the secondary of the transformer of the overall converter is measured in the right direction on terminals CS2+ and CS2– of the controller.
- Finally, the ADuM4195 isolated amplifier is used to provide a safe and accurate measurement of the DC bus voltage, which is the output variable in RPT mode, in contrast to FPT where the battery-side voltage was the controlled output.

The ADuM4195-based measurement scheme is one of the most important additions to the control loop hardware. Besides a safe 5 kV isolation voltage (from the high voltage primary to the LV control side), broad input range of up to 4.3 V, and around 0.5% accuracy at its reference voltage, the ADuM4195 features a high minimum bandwidth of 200 kHz. This allows faster loop operation for better transient response than the typical shunt regulator and optocoupler solutions, which is essential for the operation of the application at its 125 kHz switching frequency. Figure 7 shows the final experimental setup, with the hardware additions of Figure 6 implemented in an ADuM4195-based measurement daughter card, which was added to the original evaluation board in the ADP1055-EVALZ user guide.

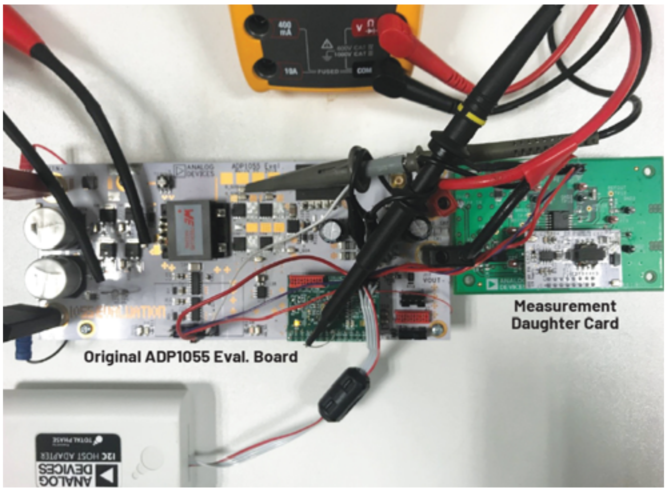

Figure 7: Experimental setup for the RPT proof of concept.

Figure 6 (bottom) also depicts the configuration performed on the software side for RPT adaption. The digital control system was studied in depth. The results are summarized in the descriptive blocks of the process, as follows:

- The right steady state response was achieved by changing the PWM settings to have duty cycle changes that are proportional to the secondary inductor charging. This is according to the boost-type operation that the architecture has in RPT mode.
- The transfer function of the plant in the Laplace domain, Gp(s), was identified with the AC small-signal equivalent circuit technique,[7] accounting for the LCL output filter of the design on the ADP1055-EVALZ user guide. Different from the FPT, the plant response in RPT is that of a second-order system with a righthand side zero (RHZ), typical of a boost converter in CCM. Note that a system of this type is intrinsically unstable and will need a reduction of bandwidth in the error amplifier.
- The feedback measurement Gm(s) was modeled upon the frequency response of the ADuM4195 working as an isolated follower (Figure 8), by using the MATLAB® System Identification Toolbox. A dominant pole around 200 kHz was confirmed, so that a fast response that remains above the target bandwidth of the control system (around 10% of the 250 kHz observable double frequency) is guaranteed.

- The option to add a pole in the standard digital compensator of the controller was taken, for a resulting reduced bandwidth in the overall control system, necessary in this nonminimum phase boost-like converter plant. Thus, the digital controller in Equation 1 was used (constants as defined in the ADP1055 user guide).

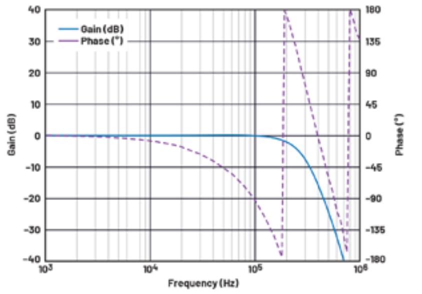

Figure 8: Frequency response of the ADuM4195.

In order to keep the analysis in the Laplace domain, a continuous-time model Gc(s) of Gc(z) was created, according to digital control theory.[9] Thus, a computational delay was added first (× z^{-1}), and the final representation in continuous time was achieved by using:
(a) the Tustin approximation and

$$\left(z = \frac{(4 f_{sw} + s)}{(4 f_{sw} - s)}\right)$$

(b) the Padé approximation to model the discrete PWM (DPWM) delay (of $T_{sa}/2=1/4f_{sw}$), so that:

- Finally, the open-loop transfer function Gol(s) = Gp(s) Gm(s) Gc(s) was studied for the design a stable response, using the MATLAB Control System Designer as a regular continuous-time control loop.

One of the main observations in this exercise is that if the same control constants as for FPT were used, the response in RPT would be unstable. Hence, a proper design of the final values of the constants in Gc(s) is vital for a reliable operation. Once a stable open-loop transfer function was achieved by design, the controller was transformed back into the digital domain. Figure 9 (left) shows the frequency response of the designed digital filter Gc(z), which can be easily configured graphically with the GUI of the ADP1055 on Figure 9 (right).

The functions for an increased efficiency studied in the previous section (PS PWM with adaptive dead times and active clamping) were also configured. Experimentally, it was observed that to achieve proper ZVS in the active-to-passive transitions for RPT, it was necessary to modify the dead times in the PWM sequence. Namely, the turn-on of the secondary switches was modified to happen before each transition from active to passive intervals to allow for current reversal.[9]

The adaption to RPT was tested successfully with 48 V obtained in the primary from an input of 12 V in the secondary. Outstanding output voltage regulation to load, and to input-voltage changes, respectively of 0.1% and 0.02% relative standard deviation (RSTDEV) were achieved, as shown in Figure 10a. Figure 10b and Figure 10c show the conversion efficiency and the step response to a 50% load change, respectively. The efficiency levels in RPT are similar to FPT mode, with a peak of 94% at midpower range, in both cases. The step response parameters (overshoot and settling time) are (1%; 1.5 ms) in RPT compared to (2%; 800 µs) with FPT. A lower overshoot with a slightly slower settling time are observed, composing a stable transient response. These results verify the validity and success of the design process for adapting the digital controller to work in bidirectional power transfer.

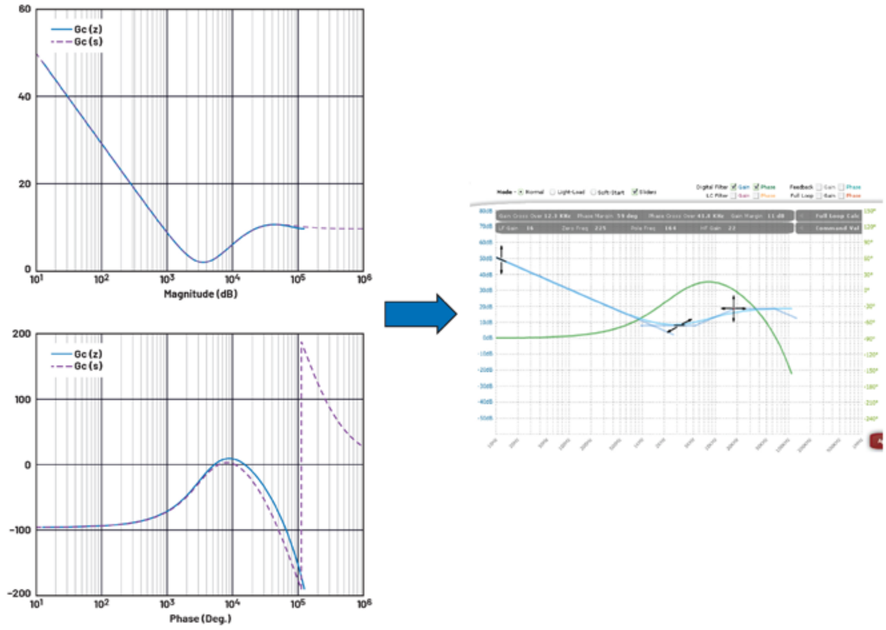

Figure 9: Digital filter response configured on the ADP1055.

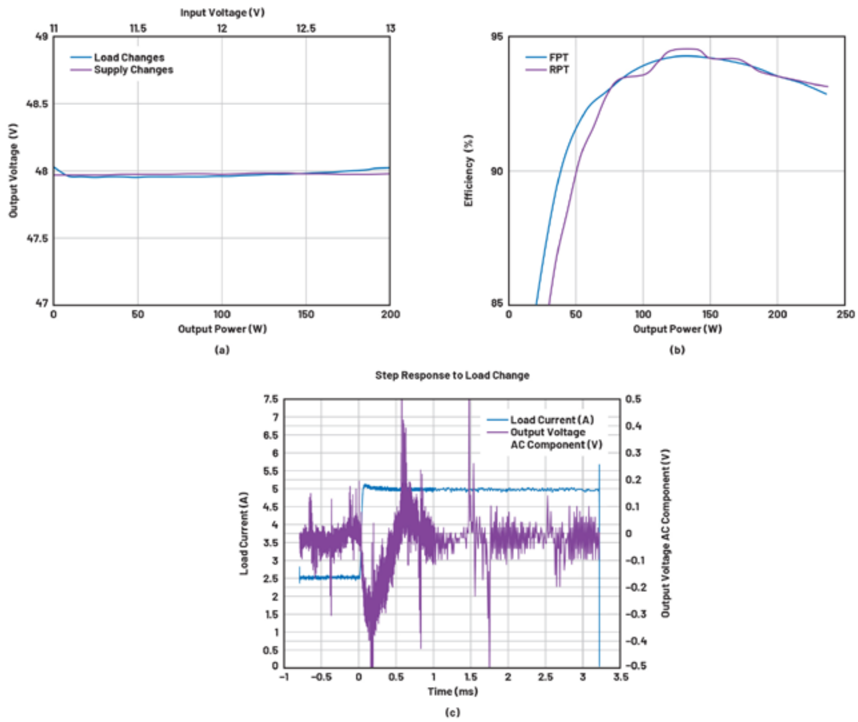

Figure 10: Resulting (a) output voltage regulation, (b) efficiency, and (c) 50% load-step response in RPT mode.

Conclusion

Dedicated digital controllers for power conversion are a good alternative for the implementation of safe and reliable applications within the energy market. This is because, compared to microcontroller devices, they can assist an easier FS certification, which reduces the time to revenue of system-level designs. Because these devices are usually built for unidirectional power transfer, this paper explores their adaption to bidirectional operation. Theoretical models, simulations, and experimental studies demonstrate the application of an isolated bidirectional DC-to-DC converter for battery-based ESSs. The results validate the feasibility of the application, with similar performances achieved for both energy transfer directions.

References

1 Venkata Anand Prabhala, Bhanu Prashant Baddipadiga, Poria Fajri, and Mehdi Ferdowsi. “An Overview of Direct Current Distribution System Architectures & Benefits.” Energies, Vol. 11, No. 9, September 2018.

2 Gerard Reid and Javier Julve. “Second Life-Batterien als flexible Speicher für Erneuerbare Energien.” Bundesverband Erneuerbare Energie e.V. (BEE), April 2016.

3 Hrishikesh Nene and Toshiyuki Zaitsu. “Bi-directional PSFB DC-DC Converter with Unique PWM Control.” IEEE Applied Power Electronics Conference and Exposition (APEC), 2017.

4 Tom Meany. “The Ideal Power Supply Monitor for Functional Safety.” EngineerZone, June 2020.

5 Yu Du, Srdjan Lukic, Boris Jacobson, and Alex Huang. “Review of High Power Isolated Bidirectional DC-DC Converters for PHEV/EV DC Charging Infrastructure.” IEEE Energy Conversion Congress and Exposition, 2011.

6 Subodh Madiwale. “Digital Control Enables High Reliability DC-to-DC Power Conversion with Active Snubbing.” Analog Devices, September 2016.

7 Robert W. Erickson and Dragan Maksimović. Fundamentals of Power Electronics, 2nd ed. Spring, January 2001.

8 Simone Buso and Paolo Mattavelli. Digital Control in Power Electronics, 2nd ed. Morgan & Claypool Publishers, May 2015.

9 Guipeng Chen, Yan Deng, Hao Peng, Xiangning He, and Yousheng Wang. “An Optimized Modulation Method tor Full-Bridge/Push-Pull Bi-Directional DC-DC Converter with Wide-Range ZVS and Reduced Spike Voltage.” ECON 2014—40th Annual Conference of the IEEE Industrial Electronics Society, 2014.

www.analog.com

Single-Board Plug-and-Play Gate Drivers

Power Integrations launched the SCALE-iFlex™ XLT family of dual-channel plug-and-play gate drivers for operation of single LV100 (Mitsubishi), XHP™ 2 (Infineon), HPnC (Fuji) and equivalent semiconductor modules up to 2300 V blocking voltage for wind, energy storage and solar renewable energy installations. This single-board driver enables active thermal management of inverter modules for improved system utilization and reduces the bill-of-material count for increased reliability. This compact new SCALE-iFlex XLT gate drivers fit inside the outline of the module, allowing the drivers to be mounted on the module, which gives converter system designers a high degree of mechanical design freedom.

SCALE-iFlex XLT dual-channel gate drivers feature Negative Temperature Coefficient (NTC) data reporting – an isolated temperature measurement of the power module – which allows accurate thermal management of converter systems. This enables system designers to optimize thermal design and obtain a 25 to 30 percent

Parameter	SCALE-iFlex XLT		Conventional Gate Driver	
Structure	Single PCBA		Stacked boards	
Size	Fits module outline	98 mm x 65.5 mm	Exceeds module outline	108 mm x 68 mm
Height	Low height (1 PCBA)	31.3 mm	High (multiple boards)	>50 mm
Part Count	Low	160	High	>250

converter power increase from the same hardware. The isolated NTC readout also reduces hardware complexity, eliminating multiple cables, connectors and additional isolation barrier crossing circuits. The gate drivers employ Power Integrations' SCALE-2 chip set which minimizes component count, enhancing reliability. The gate driver board also protects the power switches in the event of a short-circuit.

www.power.com

Maximum Isolation for Battery Management Systems

Würth Elektronik expands its WE-BMS transformer series for battery management systems with versions for an operating voltage of 1500 VDC. The component design features enhanced isolation in line with IEC 62368-1 with triple-insulated wire (primary and secondary side), as well as galvanic isolation and a test voltage of 6400 VDC. All this makes the new models in the series well-suited for use in large stationary energy storage systems from solar and wind farms, in intermediate storage systems in high-power charging stations to balance out peak loads, or for uninterruptible power supplies used in critical infrastructures.

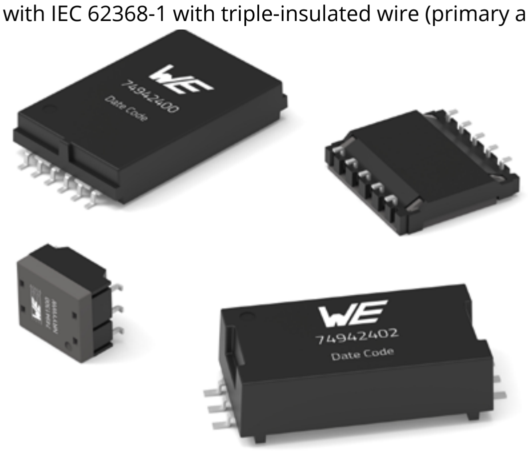

Battery management systems ensure safe operation of battery packs and provide information on battery and charge status. The downstream BMS controllers are connected in series, as are the battery cells. As voltage differences and electromagnetic interference can arise between the components connected in series, a BMS transformer helps isolate the components from each other and suppress interference. The latest members of Würth Elektronik's BMS transformer series guarantee this, even in systems with a high operating voltage of up to 1500 VDC. The longevity of the enhanced isolation of the modules as defined in IEC 62368-1 was tested using the partial discharge test in accordance with IEC 60664-1.

www.we-online.com

GaN FETs for High-Performance Class-D Audio Amplifiers

EPC has launched the EPC9192 reference design for efficient Class-D audio amplifiers. The EPC9192 showcases the capabilities of EPC's 200 V, EPC2307, eGaN FETs in a ground-referenced, split dual supply Single-Ended (SE) design, delivering 700 W per channel into a 4 Ω load. The EPC9192 features a modular design that allows for scalability and expandability. The motherboard hosts two PWM modulators and two half bridge power stage daughterboards, implementing a two-channel amplifier with 12 V housekeeping supplies and protections. Users are able to customize the PWM modulator and power stage, facilitating the evaluation and comparison of different devices and modulation techniques. The EPC9192 provides a dual split supply input, unregulated, ±42 V to ±85 V for power stage while its analog inputs may be balanced (XLR) or unbalanced (RCA). It is configurable for two independent SE channels or single channel BTL mode. Undervoltage, Overvoltage, Overcurrent, and Overtemperature protections are included in the device. Its switching frequency is beyond 600 kHz while the noise floor is 40 μV, and the frequency response in the range of 5 Hz - 20 kHz is +/- 0.5 dB, regardless of load.

www.epc-co.com

Two-Stage EMI Filters

EMIS now offers the MF410 series of single phase two stage EMI filters which are especially designed for applications with low impedance loads creating pulsed, continuous or intermittent interference noise and where high levels of mains borne interference may be present. The MF410 series provides high attenuation for both line-to-ground and line-to-line emissions and are available with power ratings from 1 A to 100 A. They are available in a number of termination options including Faston and screw connectors. Typical applications include industrial equipment and factory automation, servo drives and motor controllers, appliances, electronic data processing equipment, power supplies as well as medical equipment. The maximum continuous operating voltage is 250 VAC @ 50/60 Hz and DC while the operating frequency spans from DC – 400 Hz. The temperature range is specified -25 °C to +85 °C.

www.emisglobal.com

Automotive linear Regulators

STMicroelectronics' LDH40 and LDQ40 voltage regulators for automotive and industrial applications start-up from a 3.3V input and operate with up to 40 V applied. The LDH40 delivers up to 200 mA and is available in one version only, having adjustable output voltage from 1.2 V to 22 V. The 250 mA LDQ40 is available with a 1.2 V – 12 V adjustable output and a choice of 1.8 V, 2.5 V, 3.3 V, and 5.0 V fixed output voltages. The quiescent current of 2 µA at zero load and 300nA logic-controlled shutdown mode help preserve battery energy in always-on standby systems. The devices are stabilized with a small ceramic capacitor on the output. The automotive devices are AEC-Q100 qualified and packaged as 2 mm x 2 mm DFN6L devices with wettable flanks that ease PCB design and facilitate automated optical inspection. Their wide input-voltage range allows connection to a vehicle 12 V bus, that can reach up to 40 V transient, to power infotainment systems, instrument clusters, and ADAS. All the LDOs have system protection and management features including internal current limiting, thermal protection, soft-start, and output active discharge. There is an enable pin for shutdown control and a power-good pin for diagnostic monitoring. The LDQ40 devices also have short-circuit protection.

www.st.com

Power Factor Correction Chokes

ITG Electronics has introduced a line of power factor correction (PFC) chokes whose slim design enables engineers to incorporate them into tight spaces. The company's PFC282820B and PFC282822B series of PFC chokes are suitable for 500 - 1000 W continuous conduction mode PFC boost converter applications. ITG Electronics also offers a wider design (27.5 x 28.5 mm^3) compatible with power systems up to 2,000 W. These devices are part of ITG Electronics' broader Cubic Design PFC Choke series. Compared with traditional, toroidal-shaped PFC chokes, the series extension incorporates a flat wire and square core to save space and increase power density. ITG Electronics' range of PFC chokes are appropriate for AC to DC power conversion in industrial equipment and automative components manufacturing environments.

www.itg-electronics.com

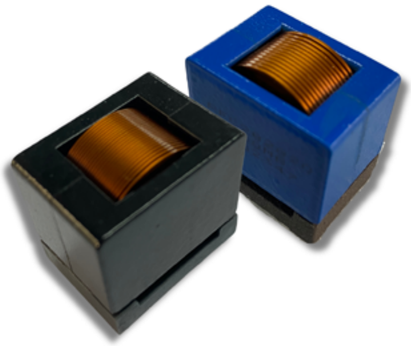

High-Capacity Regenerative Electronic Load

The PXZ series of efficient, reliable, high-capacity regenerative electronic loads from Kikusui has a rated power of 20 kW in 3U. In addition to the constant-current, constant-resistance, constant-voltage, and constant-power operating modes, this series has an I-V characteristic function that allows the user to set arbitrary I-V characteristics for each CC and CV operating mode. The series is also equipped with various functions, such as sequence, pre-charge, synchronous operation, pulse, sine, and VMCB functions. LAN, USB, and RS232C communication functions are included as standard, allowing direct integration into various evaluation systems. The PXZ series is scalable, and its capacity can be increased up to 200 kW when operating in parallel (up to 10 units).

www.kikusuiamerica.com

Integrated GaN System-in-Packages

Transphorm and Weltrend Semiconductor announced availability of two GaN System-in-Packages (SiPs). When combined with Weltrend's GaN SiP announced last year, the devices establish the first SiP product family based on Transphorm's SuperGaN® platform. The SiPs—WT7162RHUG24B and WT7162RHUG24C—integrate Weltrend's high frequency multi-mode (QR/Valley Switching) Flyback PWM controller with Transphorm's 150 mΩ and 480 mΩ SuperGaN FETs respectively. Like their 240 mΩ predecessor (WT7162RHUG24A), the devices pair with USB PD or programmable power adapter controllers to provide a total adapter solution. Other features include the UHV valley tracking charge mode, adaptive OCP compensation, and adaptive green mode control that allow engineers to design power supplies faster and with fewer components. Some key advantages of Transphorm's normally-off d-mode SuperGaN platform include its robustness (+/- 20 V gate margin with a 4 V noise immunity) and reliability (< 0.05 FIT) with the ability to increase power density by 50% over silicon. Weltrend's SiP designs complements this to create a near plug-and-play solution that speeds design while reducing form factor size.

240 mΩ, 150 mΩ, 480 mΩ SuperGaN SiPs

www.weltrend.com

USB Type-C Protection Switch for increased Efficiency and Safety

Alpha and Omega Semiconductor (AOS) has released the AOZ1377DI Type-C Protection Switch which is designed to enhance USB Type-C efficiency and safety. These protection Type-C switches have a current-limiting switch targeting applications that require comprehensive protections. AOZ1377DI supports up to 7 A with an input voltage of up to 20 V, making it usable for both sink and source applications. The AOZ1377DI offers features that significantly reduce voltage drop and power loss compared to back-to-back p-channel devices typically used in such applications. The device supports an input operating voltage range of 3.4 V to 23 V, with both VIN and VOUT terminals rated at a maximum of 28 V, and is capable of up to 7 A. These devices are suited for high-power applications requiring multi-port Type-C PD 3.0 current source supporting up to 100 W like in high-performance laptops, personal computers, monitors, docking stations, and other Type-C port applications. The AOZ1377DI has a True Reverse Current Blocking (TRCB) protection, which prevents undesired reverse current from VOUT to VIN. It also features an internal current-limiting and short-circuit current limit that protects the source device from large load current. The current limit threshold can be set externally with a resistor. Furthermore, the integrated back-to-back MOSFET is said to deliver "the industry's lowest ON resistance and highest SOA to safely handle high currents and a wide range of output capacitances on VOUT".

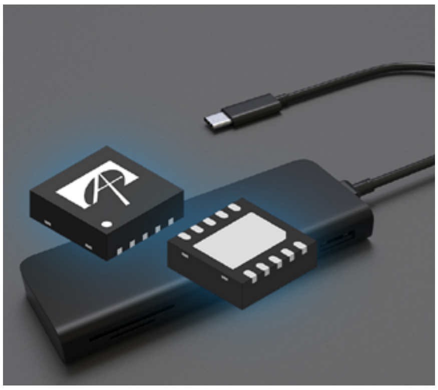

www.aosmd.com

Advertising Index

xEV power conversion tailored to your specific needs

Infineon is your trusted advisor, providing all three technologies and meeting any of your requirements:

- Cost-effectiveness
- Highest power density and efficiency
- Full design flexibility with reduced cooling efforts

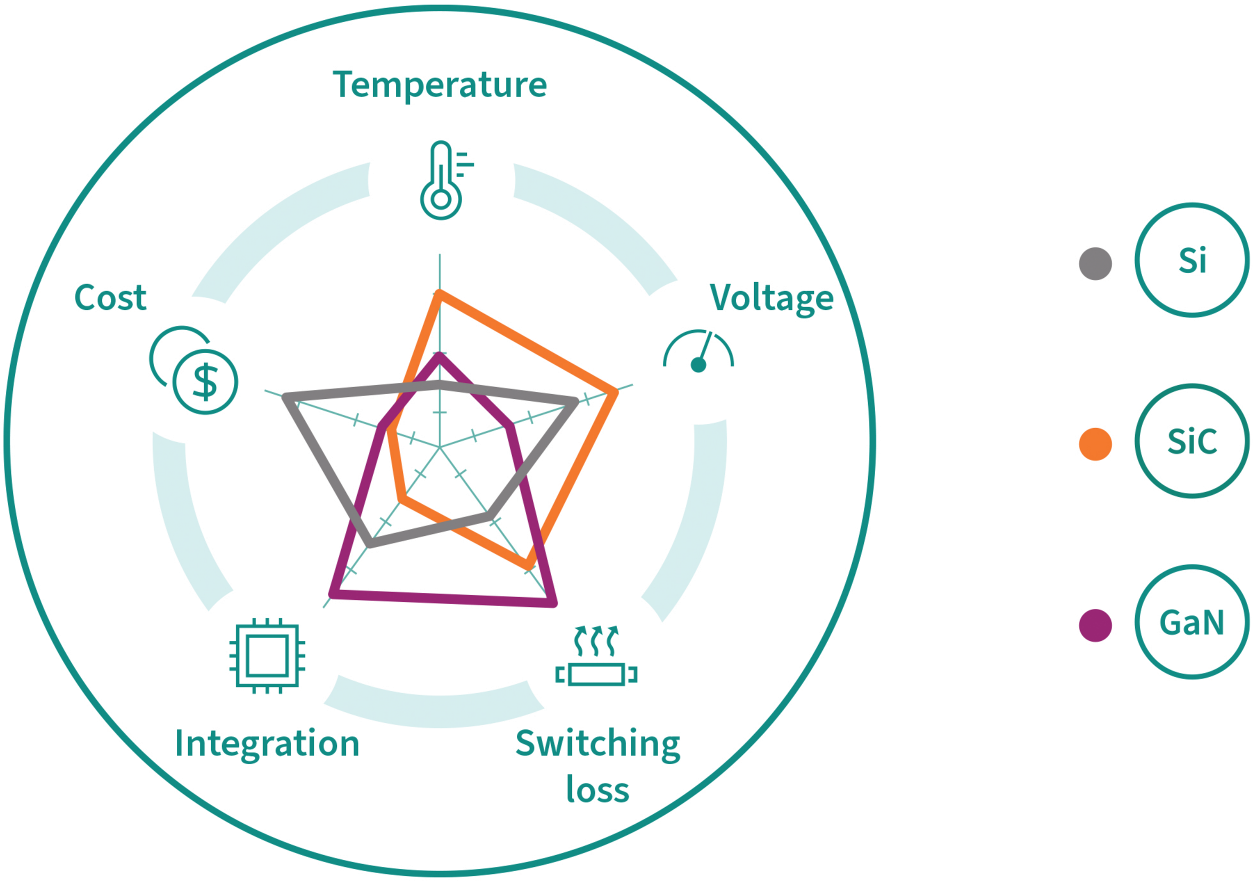

Discover our broad offering of automotive-qualified power switches:

Silicon MOSFETs	Silicon Carbide MOSFETs	Galium Nitride Transistors

For more details scan the QR codes

Efficient and sustainable power conversion enabled by wide-bandgap materials: SiC and GaN

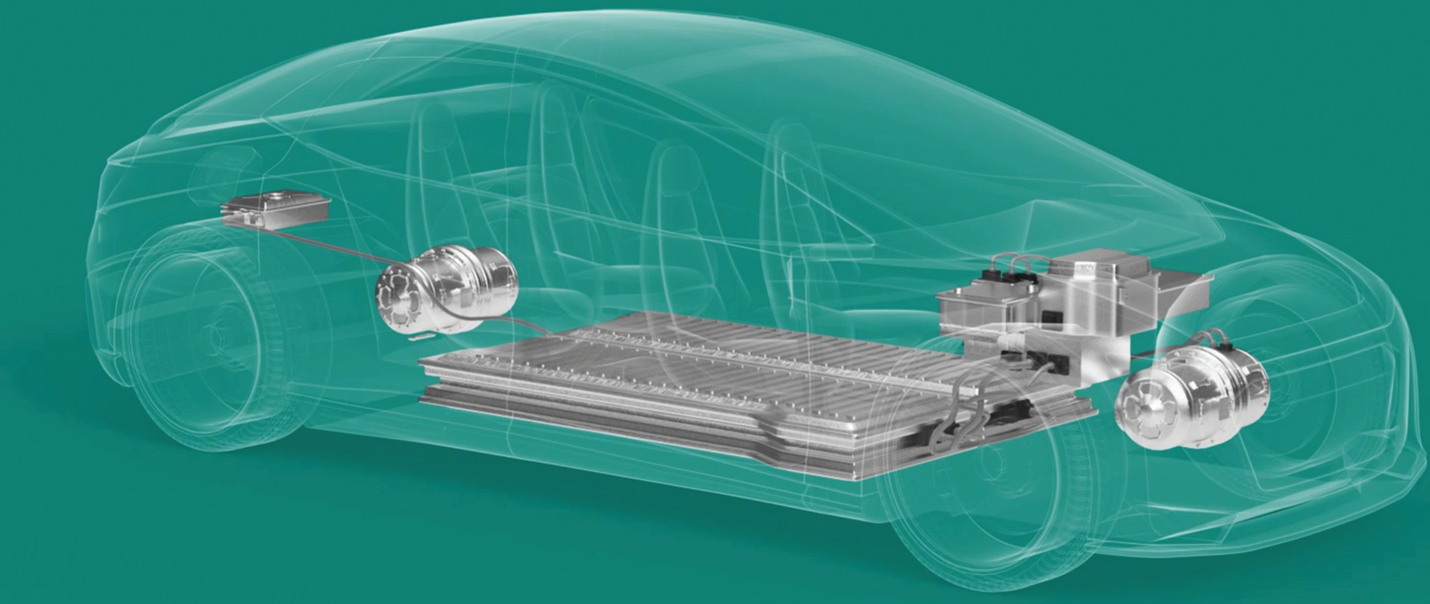

Higher performance
2x more power

Higher power density
2x smaller units

Higher efficiency
-50% power losses

Bidirectionality
2x longer lifetime

Scalable batteries
Faster charging

For more details scan the QR code.

infineon

fine power®

YOUR INNOVATION HUB

DISTRIBUTION HUB

Connectors & Switches

- Signal transmission (RJ45, USB, SFP, fiber-optical, ...)
  - RJ45 jacks with integrated magnetics
  - RJ45 cables
- Power transmission (Pin headers, board connectors, ...)
- Bus bars
- Micro switches
- All standard and customized

Your advantages

- Very cost effective
- High quality production
- Automotive BU with IATF-16949 production
- Full customization support

Visit us at
Hall 9, Booth 422

pcim
EUROPE

Nürnberg, 11. – 13.06.2024

www.finepower.com